2023

Investigation of dosing interval differences for nepafenac ophthalmic suspensions: A suspension-specific PBPK model with improved in vitro dissolution data

Xu Sun
Long Island University

INVESTIGATION OF DOSING INTERVAL DIFFERENCES FOR NEPAFENAC OPHTHALMIC SUSPENSIONS: A SUSPENSION-SPECIFIC PBPK MODEL WITH IMPROVED *IN VITRO* DISSOLUTION DATA

A DISSERTATION SUBMITTED IN PARTIAL FULFILLMENT OF THE REQUIREMENTS FOR THE DEGREE OF

DOCTOR OF PHILOSOPHY
WITH SPECIALIZATION IN PHARMACEUTICS

TO THE FACULTY OF THE ARNOLD & MARIE SCHWARTZ COLLEGE OF PHARMACY AND HEALTH SCIENCES

LONG ISLAND UNIVERSITY, BROOKLYN, NEW YORK

JANUARY 30, 2023

BY

XU SUN

SPONSORING COMMITTEE

David R. Taft, Ph.D. (Committee Chair, Division Chair)

Robert A. Bellantone, Ph.D. (Committee Co-Chair)

Rutesh H. Dave, Ph.D.

Kevin R. Sweeney, Ph.D.

Joseph J. Bova (Vice Dean for Academic Affairs)

ABSTRACT

Nepafenac is a nonsteroidal anti-inflammatory drug (NSAID) for the treatment of inflammation associated with cataract surgery. It is marketed as two ophthalmic suspensions—NEVANAC® (0.1% administered three times a day) and ILEVRO® (0.3% administered once a day). The primary mediator of pain relief is amfenac, which is a metabolite of nepafenac. The primary goal of this project was to explain how was the dosing interval affected by changes in formulation properties. The approach incorporated three novel elements. 1) A physiologically based pharmacokinetic (PBPK) model that is specific to this application for nepafenac and amfenac was constructed, which allowed tracking the specific pharmacokinetics while minimizing the use of unnecessary compartments and variables. 2) A precorneal model was constructed to allow the modeling of interactions between formulations and the tear layer and other components on the ocular surface, which allowed assessing differences in formulation properties on the resulting pharmacokinetics. 3) A novel dissolution test (IVDT) was performed on NEVANAC® and ILEVRO® separately to determine the specific drug dissolution and distribution in each formulation and allow improved modeling of the *in vivo* nepafenac drug delivery. The model was written in the programming language "R" and was used for *in silico* simulations to assess the reasons for the dosing interval change in terms of formulation properties. This approach aligned with current FDA initiatives in quantitative modeling methods (QMM). This work facilitated explaining the dosing interval question, created increased knowledge of how to construct and evaluate ocular PBPK models, and contributed to advancing the art of ocular PBPK modeling.

DEDICATION

This dissertation in dedicated to my family, my advisors, and many of my friends.

My parents have granted me lots of financial and emotional support during these five and half years. I wish my grandparents who left us during the tough time of the pandemic could share my happiness at this great moment in heaven. My cousin is always proud of me for choosing this rough, maybe lonely but worthful way of my life.

This is for my teacher and friend Dr.Robert A.Bellantone. He is the most wise person I have ever met in my life. I enjoyed each time of our discussion and all of the work we have been doing together. He always came up with inspiring ideas and gave me encouragement whenever I was struggling or frustrated in my real life. He affected everyone around him with his optimistic and active mind which will keep benefiting a lot of us in the future.

I also want to dedicate this thesis to my many friends and church family who have cared and loved me so much for not who I will become but who I am right now. Their warm kindness has always been my harbor of refuge during the sailing to the unknown future.

There are so many friends or even strangers who ever brought me power in different moments of my life. I want to dedicate this thesis to all of the people who I love and people who delivered their love to me.

ACKNOWLEDGEMENTS

During my time of study for the Ph.D. degree at Long Island University, many people provided me with priceless support, encouragement, and motivation.

I would like to thank Dr. David Taft for being the major advisor of my thesis project. He is an amazing professor who made the interaction of teaching and learning full of pleasure and fun. He also initiated my interest in PK/PD studies and modeling works. I want to express my deepest appreciation to Dr. Robert Bellantone for being my co-advisor and project leader. He came up with the initial idea of the whole project and he led the way in exploring and thinking from which knowledge and experience I gained were countless. He has the mind of a great educator, and he played the role of both teacher and friend in my research and life. I will never forget the support from Dr. Rutesh Dave and Dr. Kenneth Morris who gave their hands and helped me out of the financial predicament during the first three years of my Ph.D. program. I also thank Dr. Kevin Sweeney for bringing precious knowledge and rich industrial experience to my dissertation project as a responsible committee member and a respectable advisor on my career path. Of course, I want to thank Dr. Adam Feng for introducing me to Dr. Bellantone's lab and building a connection with those great minds.

I will always remember the help from my seniors Vamshikrishna Jogiraju and Harshith Neeli for their life-changing suggestions and selfless directions. I want to thank my lab-mates Qing Cai and Armita Azarpanah for their valuable advice and kind help. I would also like to expression my appreciation to my classmate Ehsan Abdordideh and his wife Yu June Lee for the great happiness they shared with me during our time together.

Lastly, I want to appreciate the support from my family, especially my loving parents. They trusted my choice to pursue the Ph.D., degree and they always stand with me no matter if I am happy or sad during this long way. Their love formed my shield of fearless and carried me through all of the difficulties in my limited but wonderful life experience.

TABLE OF CONTENTS

LIST OF FIGURES

LIST OF TABLES

CHAPTER 1. INTRODUCTION

This is a PBPK modeling study intended to investigate the dosing interval difference of two nepafenac ophthalmic suspensions NEVANAC® (nepafenac 0.1% ophthalmic suspension, apply for every 8 hours) and ILEVRO® (nepafenac 0.3% ophthalmic suspension, apply for every 24 hours).

Nepafenac (2-amino-3-benzoylphenyl acetamide) is a nonsteroidal, anti-inflammatory prodrug indicated for the treatment of pain and inflammation associated with cataract surgery (NDA 21-862/S-008; NDA 21862/S-017). The molecular weight of nepafenac is 254.28 g/Mol (PubChem) and its nominal solubility in water is 21.5 μg/mL calculated from pulsatile microdialysis test results. Amfenac (2-amino-3-benzoylphenyl acetic acid) is an active metabolite of nepafenac. It is a typical NSAID (non-steroidal anti-inflammatory) compound that is primarily responsible for the analgesic effect (Ke et al., 2000). The molecular weight of amfenac is 255.27 g/Mol (PubChem)

The structures of nepafenac and amfenac are shown in **Figure 1-1:**

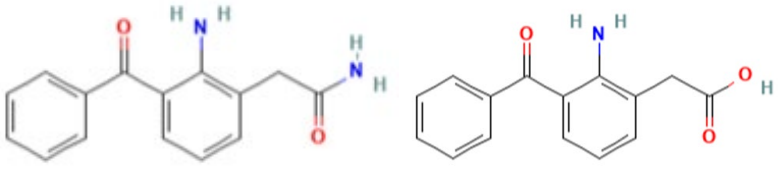

Nepafenac **Amfenac**

Figure 1-1. Molecule structures of nepafenac and amfenac

NEVANAC® and ILEVRO® are two nepafenac ophthalmic suspensions marketed in the US. The major differences between these two formulations lie in their doses and viscosities. Other properties such as particle size and polymer matrix also vary and that might affect the apparent solubility and dissolution rate of drugs in the formulation. The indicated dosing interval of ILEVRO® (once a day) is triple that of NEVANAC® (three times a day).

In a clinical study of the anti-inflammatory efficacy of NEVANAC®, Gamache et al. (2000) reported a prostaglandin reduction of 85–95% and 55% in the iris/ciliary body and the retina /choroid area, respectively. Inhibition of local cyclooxygenase (COX-1 and COX-2) was sustained for 6 h in the iris/ ciliary body site and 4 h in the retina/choroid site. A longer inflammatory clearing effect is expected for ILEVRO® (nepafenac ophthalmic suspension, 0.3%), as implied by its extended dosing interval. The long-lasting therapeutic effect makes nepafenac a preferred agent over other ocular NSAIDs such as diclofenac and bromfenac (Sheppard et al., 2018) (Walters et al., 2007). A hypothesis was proposed that this advantage of longer therapeutic effect results from the superior permeability of nepafenac through ocular tissues and a potent local enzyme inhibition effect of amfenac at therapeutic sites (Chastain et al., 2016). However, the pharmacokinetic properties of nepafenac and amfenac after the instillation of nepafenac ophthalmic suspension have not been explicitly illustrated in the literature.

The pharmacokinetic processes governing the fates of nepafenac and its active metabolite amfenac in the ocular tissues after the absorption of nepafenac should be independent of differences in formulation properties. Thus, one of the primary goals of this study was to identify and characterize potential formulation properties that, when changed, affect the

absorption of nepafenac and the resulting fates of the nepafenac and amfenac in the ocular tissues, including accounting for the drug and metabolite accumulation at therapeutic sites and changes in the dosing interval or frequency. A novel pulsatile microdialysis (PMD) based *in vitro* dissolution tests method (Bellantone et al., 2022) was incorporated with an ocular physiologically based pharmacokinetic (PBPK) model for the first time in this study to figure out how the dosing interval change related to the formulation properties.

Pulsatile microdialysis (PMD) is an advanced method for *in vitro* drug release testing that is specifically optimized for drug dissolution or release from a formulation into an aqueous medium with a small volume that cannot dissolve all of the nepafenac in the administered formulation, such as the tear layer on the ocular surface. PMD was performed on NEVANAC® and ILEVRO® and the results were used to simulate formulation-specific *in vivo* dissolution profiles of nepafenac into tears. PMD was also used to determine the fraction of nepafenac that is initially dissolved in the aqueous phase of the ophthalmic suspension, which is assumed to almost instantly provide dissolved nepafenac to the tears. This is important because only the dissolved nepafenac is available for the drug disposition processes *in vivo*. mixed with the tear layer. initial fraction of the nepafenac that formulation specific properties such as the drug's dissolution rate and the fraction of the total drug in the suspension that was dissolved in the aqueous phase before it is applied to the eye.

The ocular PBPK model was established using the R programming language. The compartmental design was based on both a physical and physiological understanding of drug molecule characters and ocular tissue properties. A precorneal model is included to

monitor the drug release and absorption at the ocular surface under dynamic biological processes including tear turnover, drug drainage, and drug absorption. An oily layer secreted by Meibomian glands serves as a chemical depot on the ocular surface and interacts with lipophilic drug molecules. such as nepafenac, via partitioning effect and prevent them from being washed down to the nasal-lacrimal duct by tear.

Although available modeling tools and published results are neither sufficient nor explicit regarding drug-tear interaction at the precorneal layer, we managed to adjust parameter values in the precorneal model based on basic physical understanding (e.g. octanol/water partitioning factor) and knowledge from PMD test results.

The tissue compartments model was built to characterize drug distribution and metabolism in ocular tissues. Nepafenac is a prodrug that is converted to active metabolite amfenac in ocular tissues. Amfenac is a potent enzyme inhibitor that works to reduce vessel destruction related to prostaglandins at the therapeutic site of action in both the anterior and posterior segments of the eye (Yanni et al., 2010). The local concentrations of nepafenac and amfenac directly affect the duration of the therapeutic effect. Evaluation of local drug concentration and other pharmacokinetic properties requires the implementation of a drug-specific ocular compartmental PBPK model. Existing ocular PBPK models include an excessive number of compartments and parameters that are not numerically relevant to the drug's bioavailability evaluation (Le Merdy et al., 2020). A vital drawback of such kind of model is the overuse of parameters that can be adjusted to fit the clinical data. Statistically, each parameter must be controlled to stay in a reasonable range. It is not practical to do so when so many parameters are included in the model. This shortage certainly weakens the power of the

existing models despite they can be easily fitted to different clinical data. To solve this problem an ocular PBPK model is being developed that includes only relevant compartments and an associated number of parameters that can be easily controlled based on data from literature and exploratory simulations.

The novelty of this study includes, but is not limited to PMD-based IVDTs experiments that are performed under physiologically relevant conditions (dissolution into thin layer; low volume receiver; non-sink condition and not well-stirred environment); a suspension-specific precorneal model that helps to access transient volume change, tear turnover, drug drainage, and potential drug depot effect; and an innovative ocular PBPK model developed and evaluated by R programming language using the built-in ordinary differential equation (ODE) solver to avoid using of "universal" models in commercial packages such as GastroPlus® (Le Merdy., 2019).

The research project provides an accurate *in vivo* dissolution model for the PBPK study taking advantage of in-house PMD-based IVDT instruments. The suspension-specific precorneal compartment, as the connection of *in vitro* dissolution test and ocular PBPK modeling analysis, was utilized to evaluate the impact of formulation properties on drug release and residence time at the tear layer. The ocular PBPK model incorporated with different ocular tissue compartments enabled the calculation of local concentrations of prodrug and active metabolite. Such information is essential for access to postulated physiological and physiochemical processes that might prolong the dosing interval.

From a long-term perspective, this study provided the first case of ophthalmic suspension bioavailability access incorporated with an improved *in vitro* releasing test method and

formulation-specifically designed ocular PBPK model. Moreover, the proposed PBPK model developed by the R programming language could offer an easy access platform to researchers for further PBPK studies on different drugs and formulations.

CHAPTER 2. BACKGROUND AND LITERATURE SURVEY

2.1 Model-based Drug Development (MBDD) for PBPK and Clinical Simulations

The quantitative assessment of therapeutical efficacy and risk is one of the most pivotal and challenging issues during the progress of clinical drug development. Model-based drug development has been started by regulatory agencies, academia, and pharmaceutical companies as a modernized quantitative method to address those costly challenges during clinical drug development and to help with decision-making by properly leveraging data collected from different stages of a project (Kimiko and Pinheiro, 2015). Among them, pharmacokinetics (PK) and pharmacodynamic (PD) models have proved to be very successful in the prediction of drug availability, drug-drug interaction, and therapeutic effect. The current application of model-based drug development is not limited to non-compartmental analysis (NCA), or simple compartmental analysis (such as central and peripheral) based on the traditional PK/PD model approach.

More sophisticated quantitative modeling methods are being developed to better represent the interaction between drugs and the human body with the incorporation of the drug's physicochemical characteristics as well as the physiological properties of the body environment. Regarding ocular drug delivery and disposition, physiologically-based pharmacokinetic (PBPK) modeling has been used in various drug development studies as a powerful tool that accounts for the physiological structure and characteristics of the eye to represent each step of the drug molecule's movement after administration to the ocular surface. The advantage particularly lies in drug development studies where direct

measurement of local drug concentration or sampling method for quantitative analysis could become the major challenge.

PBPK models help to simulate a drug's absorption across membranes, distribution, local metabolism at specific locations with enzyme activity, blood vessel elimination, and potential drug-drug interaction before the drug molecules reach the therapeutic site of action. The application of PBPK models enables scientists to simultaneously track the drug at each physiological section as it travels through the body. The model can also be used as an *in silico* platform for clinical simulations with a set of hypothetical parameter values, such as demographic characteristics of a patient population, the sample size of each study arm, dosing regimens, or physiological characteristics of individuals. In industrial drug development, PBPK modeling helps to provide instructive information for clinal trial design. Collaborated with other quantitative analysis methods, it sets the standard of best-in-class/ or best-in-market candidates for target indications.

2.2 Significance of ocular PBPK modeling

2.2.1 Ophthalmic suspension formulations and physiological interactions

A suspension is a commonly used dosage form when an active pharmaceutical ingredient is poorly soluble in water under physiological conditions. It typically contains polymers and other excipients to engineer the physical properties of formulations. The drug is distributed in the different phases of the formulation—undissolved drug particles could either suspend in the matrix formed by polymer materials or bind with a carrier or solubilizer in the oil phase, while only a small portion of the drug is dissolved in the aqueous phase of the formulation.

Of interest in this project are ophthalmic suspensions for drugs with poor aqueous solubility. These contain the drug in both its dissolved and undissolved forms, typically with more than 90%, and often 95-99%, of the drug as undissolved, suspended particles. In this project, the formulation of interest contains the drug nepafenac, which is marketed as NEVANAC® (0.1% nepafenac suspension) and ILEVRO® (0.3% nepafenac suspension). Nepafenac is poorly soluble in water (nominally 14 µg/mL in water) (FDA, 2012). Based on that solubility in water, the nominal dissolved fraction of the nepafenac is approximately 14 µg/mL /1000 µg/mL or 1.4% in the NEVANAC® (0.1% nepafenac suspension), and about 14 µg/mL /3000 µg/mL or 0.47% in the ILEVRO® (0.3% nepafenac suspension). It is important to note, however, that these dissolved fraction estimates are based on the nepafenac solubility in water and may be different in the actual formulation due to the presence of excipients in the formulations.

Once a drug formulation is administrated to the ocular surface, the volume of the administered liquid usually exceeds the capacity of the conjunctival sac and will spill out immediately. Since the conjunctival sac has a maximum capacity of approximately 40 µL (microliters) while the undisturbed tear reservoir volume is around 7.5 µL (Missel and Sarangapani, 2019), the remaining drug formulation was removed rapidly by nasal-lacrimal drainage. Depending on the viscosity of the formulation, the drug can remain at the ocular surface for a short period, ranging from ~12 minutes for low-viscosity formulations to ~30 minutes for higher-viscosity formulations (Le Merdy et al., 2019). During that residence time, solid particles in the formulation dissolve into the aqueous phase and interact with chemical or physiological components in the tear layer. For instance, the protective oily layer secreted by Meibomian glands in eyelids works to slow

the evaporation of the tear film. The oily layer itself, when encountering lipophilic drug molecules such as nepafenac, could act as a potential drug depot given the high tendency to partition into oils. This oily depot on the ocular surface could rapidly absorb lipophilic drug molecules and hold them from nasal-lacrimal drainage. Subsequently, the drug accumulated in the oily layer releases into the tear film at a relatively slow rate (that might be represented as a zero-order process). This chemical depot-caused 'sustained-release' might be a significant factor that explains the drug's extended therapeutic effect in both of anterior chamber and posterior chamber of the eye. Therefore, it is postulated that an ocular PBPK model with a unique pre-corneal drug-tear interaction compartment is needed to accurately represent this drug depot effect that happens on the ocular surface.

Despite the existence of a potential chemical drug depot such as an oily layer, which might significantly increase the drug's availability in the eye, only a very limited portion of the drug will likely get absorbed from the corneal epithelium or conjunctiva, at least in part because most of the drug will not dissolve before being cleared from the ocular surface. Once absorbed, drug molecules will distribute into ocular tissues from the anterior segment of the eye to the posterior segment of the eye. Both local metabolism and systemic absorption are involved during the process. Meanwhile, certain physiological components might also reduce availability at therapeutic sites. One of the critical factors is melanin which is a pigment-protein present in the pigmented ocular tissues such as the iris and ciliary body. The binding of drug molecules with melanin may lead to drug accumulation in pigmented tissues and retain drugs in the melanin-containing cells (Le Merdy et al., 2022).

An ocular PBPK model is also highly favorable to accounting for tear protein binding that affects the drug's absorption and intra-ocular bioavailability. Previous studies have indicated that even before the drug is absorbed, binding to tear proteins also accounts for reducing the drug's availability in the eye (Agrahari et al., 2016). There are approximately 0.7% of body proteins in the tear liquid including lysozyme, lactoferrin, secretory immunoglobin A, serum albumin, lipocalin, and lipophilin (Lehrer et al., 1998). Drug molecules bound to those proteins are constrained from getting absorbed by the eye, resulting in a lower concentration of free drug at the therapeutic site.

Given the limited residence time, whether the dissolution of solid particles in the formulation is fast enough to promote the ocular bioavailability of solid particles in the formulation is another crucial question addressed in this dissertation research. Considering the poor intrinsic solubility of nepafenac in water and the very low volume of the aqueous receiver (for instance, the volume of tears), it is likely that only a very small fraction of the drug in the solid particles will dissolve and be absorbed within the short ocular residence time. In this scenario, it would be anticipated that the drug already dissolved in the aqueous phase of the suspension would dominate what is available in the eye. It is also possible that any drug molecules that are bound to formulation excipients, such as polymers, might release quickly enough to have some bioavailability. Thus, with the development of the formulation, the inclusion of solubilizers along with reducing the drug particle size (such as nanosuspensions) might do the following: 1) increase the fraction of the drug in the formulation that is dissolved, or 2) increase the dissolution rate in the eye. Veiga et al. designed and evaluated novel cyclodextrin-based aggregate formulations to efficiently deliver nepafenac topically to the eye structure (Veiga et al.,

2020). Compared to the commercially available nepafenac suspension, the investigational formulations showed a high permeation through the bovine sclera with greater anti-inflammatory activity. To further assess drug dissolution characteristics and availability in the eye, it is important to account for the impact of formulation variables in the development of an ocular PBPK model.

2.2.2 Physiological constraints

The USFDA recommended *in vivo* testing to establish the bioequivalence of specific ocular drug products. Accurate, sensitive, and reproducible clinical endpoints are required for bioequivalence testing (Agrahari et al., 2016). However, in the study of ophthalmic drug products, acquiring samples from ocular tissues for quantitative analysis or direct measurement of local drug exposure could be the major challenge due to the inaccessibility of internal compartments of the eye. Other than the sampling issue, large inter-subject variability that reduces study sensitivity, patient safety issues, and the prohibitively high costs of clinical studies are also factors that hinder the proof of bioequivalence in generic ophthalmic products (Chockalingam et al., 2019). In ophthalmic studies, the drug is thought to reach therapeutic sites before getting absorbed into the systemic circulation. Even though a large portion of the drug delivered to the eye would be systemically absorbed through nasal-lacrimal drainage, it is neither practical (the system concentration of the drug is lower than the limit of quantitation, or LOQ) nor of our interest to measure drug concentration in blood.

Besides, given the delicate structure of the human eyes, *in vitro* measurements of physiological parameters such as tissue membrane volume, thickness, and permeability

are costly and complicated. Ocular PBPK models can be developed and verified using data from pre-clinical studies and extrapolated to humans by optimizing parameter estimates based on clinical trial data. For example, New Zealand rabbits have been shown to share similar ocular anatomic characteristics with humans. They have been widely adopted as an ideal platform for pre-clinical studies to develop ocular quantitative models that can be used to predict drug exposure and metabolism in human eyes. The utilization of ocular PBPK models might eventually replace or significantly reduce the need for extensive, expensive preclinical and clinical testing.

Ocular PBPK models can provide insight into drug partitioning in eye tissues and serve as an alternative methodology to study the PK/PD relationship for ophthalmic drugs (Le Merdy et al., 2022). For instance, the partition coefficient of a drug might not be easy to assess or measure directly through *in vivo* tests, but the value of certain parameters related to the partitioning effect could be roughly determined as a range through less costly *in vitro* permeability tests. The range of parameter values could help with the data fitting when verifying the ocular PBPK model against a set of clinical trial data. This is another example of the successful collaboration of *in vitro* test results with statistical optimization as a solid alternative to *in vivo* experimental data.

2.2.3. Formulation factors affecting drug delivery

The use of PBPK modeling improves the sensitivity to detect the specific effects of certain formulation differences on drug delivery or physiological performance. It provides a less expensive and risk-controlled alternative to clinical testing for assessing the manufacturing factors affecting the bioavailability (BA) and bioequivalence (BE) of

drug products. This has especially great potential application for so-called complex dosage forms and modified-release formulations. For instance, PBPK modeling was applied as an alternative BE approach that avoids the comparative clinical endpoint BE study of topical diclofenac gel (Tsakalozou et al., 2021).

With improved manufacturing techniques, ophthalmic suspensions can be developed as complex formulations containing a polymer matrix that interacts with drug particles under different chemical/physiological conditions. Drug release and delivery from the original ophthalmic suspensions can be affected by the physical properties of the original formulation.

Particle size is one of the physicochemical factors that can affect the dissolution rate of a drug on the ocular surface. Assuming perfectly spherical particles, particle size is inversely proportional to the total surface area per amount of nepafenac (the standard surface area). The higher the standard surface area, the faster the drug dissolves in response to concentration loss due to dilution or drug absorption.

Viscosity is another important factor as it affects the residence time when the drug stays in contact with the tear layer before being washed out via the nasal-lacrimal duct. Formulations with a higher viscosity tend to have a longer residence time which allows a higher drug absorption at the ocular surface given a constant corneal or conjunctival absorption rate.

Some polymers in the ophthalmic suspension can bind to the drug particle and facilitate the drug dissolution process in the tear or water phase. Certain solubilizing effects might be pH or salt sensitive. The apparent dissolution rate of particles in the ophthalmic

suspension could either be parameterized in the PBPK model or be determined by the *in vitro* dissolution test of the original formulation (instead of particles of the pure drug) into a biologically relevant media. Then the *in vitro* dissolution data can be used to extrapolate the *in vivo* drug release as input of the ocular PBPK model.

Drug distribution in the original formulations could be the dominant factor that affects the drug's absorption and availability in the eye. Considering that nepafenac is a poorly soluble prodrug in water and the dissolution of solid drug particles in water is slow, the drug in the oil phase of formulation might not get a chance to dissolve and permeate through the ocular surface during the 10-15 minutes of residence time before being drained by the nasal-lacrimal duct. In this case, there would be almost no ocular bioavailability of drug particles suspended in the original formulations. If the solid particles cannot dissolve during the residence time, drug absorption will highly depend on the amount of free drug in the aqueous phase of the initial formulation. Increasing the dose strength of the formulation would not change the drug's availability in the eye.

The formulation factors mentioned above must be thoroughly considered and correctly modeled in the ocular PBPK model to obtain the convincible simulation result of drug exposure.

2.3 Statement of the Problem

Nepafenac ophthalmic suspension is prescribed for the treatment of cataract surgery-related ocular inflammation. Currently, there are two nepafenac ophthalmic suspensions available in the US market: NEVANAC® (0.1% nepafenac suspension) and ILEVRO®

(0.3% nepafenac suspension). The two formulations are different not only in dose strength but also in the excipients of the formulations.

Of particular interest is that the label claimed dosing intervals of the two formulations are inversely proportional to their dose strength. Tripling the total drug concentration of the suspension from 0.1% to 0.3% results in a proportional prolongation of its dosing interval from every 8 hours to every 24 hours. While neither product is formulated as sustained release, this observation of dosing interval change cannot be simply explained by the elevation of dose strength. In other words, when drug release is not expected to be zero order which is common in the case of sustained release formulations, tripling of the dose strength does not directly lead to a tripled dosing interval based on the pharmacokinetic understanding. To explain the reason behind this unique observation, two hypotheses are proposed on the potential factors that might lead to this dosing interval change.

First, given that the two formulations share the same active pharmaceutical ingredients, once the drug is absorbed in ocular tissues, the pharmacokinetics and pharmacodynamics of the formulations should not exhibit any difference other than drug efficacy change resulting from the local drug exposure gap. Therefore, it is expected that the physical properties of the formulation should account for a major part of this observed dosing interval change.

Second, considering that the therapeutic period of nepafenac suspension goes far beyond its residence time on the ocular surface leads to speculation that there could be chemical or drug depots on the ocular surface that facilitate drug absorption via partitioning effects, protecting the drug from the tear drainage, and consistently releasing the accumulated

drug to the tear film at a slower rate. These depots may exist physiologically in the form of the meibomian layer (a thin layer of oil on the tear surface that is produced by the meibomian glands) and the presence of mucin (which has been shown to complex with some drugs) as a component of the tear layer. This depot effect, if proven to be significant, could partially explain the extended therapeutic period of nepafenac ophthalmic suspensions.

Potential reasons for the change in dosing interval can also be postulated based on physiological considerations. For instance, drug binding to melanin at pigmented ocular tissues could affect the drug's distribution and drug exposure at therapeutic sites. The chemical drug depot effect and the enzymatic metabolism were incorporated into the developed ocular PBPK model to address the major goal of this study, which is to explore possible physical or physiological factors that can mathematically account for the increase in dosing intervals occurring in response to differences in the nepafenac ophthalmic suspension formulations.

2.4 Literature Survey

2.4.1 Ocular Pharmacokinetics and Ophthalmic Suspension Pharmacokinetics

The eye is a delicate organ that has a three-layer structure consisting of connective tissues, vascular tissues, and neural tissue. It is sensitive and protected from foreign materials by anatomical and physiological barriers (Agrahari et al., 2016). The bioavailability of topical applied ophthalmic drugs is primarily limited by the precorneal loss resulting from nasal-lacrimal drainage, drug binding to tear proteins, and systemic absorption from the vascularized tissue surface. Other factors that reduce a drug's

intraocular availability include a melanin binding effect (Hu, 2008) in pigmented tissues such as the iris and ciliary body and local drug metabolism by tissue enzymes. Oily layers that are secreted by ocular glands to protect the tear film (Butovich, 2011) can also shift the intraocular bioavailability of ophthalmic drugs (Davidson and Kuonen, 2004). Any drug in the systemic circulation is hindered and largely prevented from entering the ocular environment by different anatomical barriers such as the blood-aqueous-barrier (BAB) at the anterior chamber and the blood-retina-barrier (BRB) at the posterior chamber (Coca, 2014).

Ocular pharmacokinetics is the assessment of a drug's absorption, distribution, metabolism, and excretion within the intraocular environment. Drug concentrations differ at different ocular sites, such as tear film conjunctival sac, anterior chamber, vitreous cavity, and periocular space, which are major targets of ocular pharmacokinetics studies. The ocular pharmacokinetics has been frequently described by multi-compartmental models which assume a homogenous drug distribution in each ocular tissue. Tissue compartments such as tear film, cornea, aqueous humor, iris and ciliary body, lens, vitreous humor, sclera, choroid, and retina are commonly represented in the ocular physiologically-based pharmacokinetic models (Goel et al., 2010; Smith et al., 2020). Depending on the therapeutic site, the distribution pathway of the drug to the anterior chamber or posterior chamber of the eye is highlighted in different published ocular PBPK models. Drug delivery to the posterior chamber has always been a challenge and it has been the focus of different ophthalmic studies (Geroski and Edelhauser, 2001; Maurice, 2002; Varela et al., 2020). Major parameters considered in the ocular PBPK models are tissue or liquid volumes, membrane permeability, enzyme metabolism rate,

and systemic absorption rate (Ramsay et al., 2018). Animal data from pre-clinical studies are routinely used for the development and verification of ocular PBPK models (Schoenwald and Stewart, 1980; Chockalingam et al., 2019).

Ophthalmic suspensions are usually designed when a drug is poorly soluble in water. The pharmacokinetics of ophthalmic suspension is much more complicated than ophthalmic solution given the involvement of drug dissolution before the drug can be absorbed into the ocular surface. Formulation factors such as viscosity and particle size can have a significant impact on the drug's dissolution properties (Hui and Robinson, 1985; Siepmann and Siepmann, 2013). The effect of drug distribution in the original formulation on drug absorption and intraocular bioavailability has not been assessed in research published to date.

2.4.2 Previous work

Le Merdy introduced a state-of-art ocular PBPK model in recent publications using the software platform GastroPlus® (Le Merdy et al., 2019; Le Merdy et al., 2020). The ocular compartmental absorption and transit (OCAT) model developed was designed as a one-size-fits-all model that included all the tissue compartments based on the anatomic structure of the eye. The model incorporated q specific pre-corneal compartment to simulate the drug-tear interactions on the ocular surface. Published *in vitro* dissolution data were used to model the *in vivo* drug release as input in this ocular PBPK model. The model was verified using in-house rabbit ocular PK data generated from preclinical testing in rabbits. The overall approach and methodology used in these studies are novel

and significant from different perspectives. However, the proposed OCAT model can be further improved for several reasons.

First, while it was designed to be a one-size-fits-all model, the OCAT model is not formulation-specific, and it cannot be used to assess the drug performance difference caused by formulation changes (instead of drug molecule change). The preferred model being pursued in this investigation would be able to consider variables such as viscosity, particle size, and drug distribution (oil phase, aqueous phase, polymer phase, etc.) in the original formulations. The model should also be expected to reflect the effects (when applicable) of adding solubilizers, changing pH, adding salts, etc. when they are included in the ophthalmic suspensions.

Second, it was well-intended to include all relevant tissue compartments to predict ocular drug disposition. Meanwhile, efforts should be made to reduce the number of parameters in the model to avoid the impact of local versus global optimization when fitting the model to a set of clinical data (especially when there are just a few data points). Moreover, increasing the number of parameters in the model decreased the power of each parameter. Even if each has an estimated value, it is easy to explain the physiological meaning of certain parameters but hard to explain the impact of that parameter on the overall prediction. Consequently, the OCAT model can be improved by keeping parameters only if they are numerically relevant to the simulation results.

Third, the pre-corneal model proposed in the published literature should consider dynamic processes such as drug dissolution and tear turnover in the drug-tear interaction compartment, but they do not account for the partition effect of drug molecules into the

chemical depot on the ocular surface. The chemical depot is particularly important in the case of lipophilic prodrugs such as nepafenac and it might help to explain the dosing interval changes caused by formulation factors.

Fourth, the *in vitro* dissolution data used to model the *in vivo* drug delivery were obtained based on particles of pure drugs dissolved in bulk media (Lu et al., 1993). Those data do not apply to ophthalmic suspension studies because the physiological conditions of the ocular surface are completely different from those of the GI tract. That is why it is critical that *in vitro* dissolution data based on biorelevant conditions be measured and used to inform the ocular PBPK model.

2.5 Unanswered Questions from Previous Studies

2.5.1 Existing ocular PBPK models do not mechanistically address the precorneal structure and function

The precorneal surface, or conjunctival sac, is the first physiological location the ophthalmic formulation interacts with after administration. Serving as the outermost protective barrier of the eye, the precorneal environment consists of the corneal surface and sclera surface which allows limited permeation of the drug to enter the intra-ocular environment. Conjunctivas (bulbar conjunctiva and palpebral conjunctiva) are vascularized tissues that perform a supportive function at the ocular surface. Drug molecules exposed to conjunctivas are subjected to systemic absorption, which is a partial cause of the drug loss from the precorneal surface region. Other than solid tissues, the precorneal surface also contains mucosa as part of the mucosal immune system which applies adaptive effector mechanisms present in the tissue and tears to protect eyes from invading antigens or pathogens (Knop and Knop, 2007). This mucosal layer together with

proteins in the tear film might interact with dissolved drug molecules and change the drug's intra-ocular availability. Moreover, an oily layer secreted by meibomian glands covers the tear film and prevents it from rapid evaporation. Given the lipophilic properties of ophthalmic drugs such as nepafenac, the existence of the oily layer on the top of the tear film can affect the drug's residence time and consequently vary the drug absorption through corneal epithelium or sclera.

This complicated physiological structure of the precorneal surface and its potential effect on drug dissolution/absorption has not been explicitly represented in existing ocular models. For example, the OCAT model only programs tear turnover and drainage to the nasal-lacrimal duct without any involvement of chemical and physiological components that might significantly affect the drug's availability to the ocular tissues.

2.5.2 Existing PBPK models do not appropriately account for mechanistic interactions of the formulation with ocular tissues

The precorneal surface consists of complicated physiological structures that have different interactions with ophthalmic formulations. The oily layer and mucosa have the potential to serve as a chemical drug depot that keeps the drug molecules from being washed out by tears or drained via the nasal-lacrimal duct. The depot facilitates the absorption of the lipophilic drug by a partitioning effect and can significantly increase the residence time of drug molecules on the ocular surface. The tear film contains proteins that could bind with drug molecules and potentially reduce the drug's absorption through the cornea or sclera. Neither of those effects was considered in previous pre-corneal models.

2.5.3 There is a lack of biorelevant in vitro dissolution data to support ocular PBPK model development in previous work

Performing *in vitro* dissolution or release testing is a standard part of evaluating dosage forms containing any undissolved drug content. This is a nearly-universal practice with solid oral dosage forms (tablets and capsules) and oral suspensions, which typically employ setups such as the USP Type II apparatus with dissolution media volumes of 500 to 900 mL. These setups and receiver medium volumes can be useful for quality control and maybe the prediction of *in vivo* oral absorption in some cases because the nominal volume of GI fluids is 100-200 mL. However, they are not relevant to the *in vivo* dissolution of ophthalmic suspensions because ophthalmic suspensions contain drugs with poor aqueous solubility, and the *in vivo* receiver medium primarily of tears is a very low-volume receiver with extremely limited ability to dissolve the drug particles in the suspension.

The tear film is a thin layer (volume of ~ 7.5 µL) and the volume of the reservoir that can hold the tear layer plus the administered ophthalmic formulation is ~ 42.5 µL (Missel et al., 2019; Le Merdy., 2019) which is thousands of times smaller than the volume of GI fluids, which is nominally 100-200 mL (Mudie et al., 2014). Given the very small tear volume, the dissolution of a drug in general, and one with poor aqueous solubility in particular, is anticipated to be very slow and extremely limited. Even if the drug dissolution happens with dynamic tear turnover, the reservoir itself is under more of an unstirred physical condition which is not at all comparable to the GI tract. Therefore, given the completely different physiological environment, traditional or previously established *in vitro* drug release tests, which were more appropriate for evaluating factors

relevant to physiological conditions relevant to GI absorption (volumes, pH, stirring rate, etc.) are not suitable for ophthalmic formulations. *In vitro* drug release or dissolution data acquired from traditional setups, when being applied to model the *in vivo* drug release process at the precorneal surface, will cause mechanistic biases on the data fit and simulation results.

To construct experiments that are more relevant to liquid ophthalmic formulations, *in vitro* drug release tests must be performed under biorelevant conditions reflective of the precorneal surface. This critical consideration was not properly addressed in previous ocular model development studies, thus providing inaccurate drug-release data as input to the physiological region and rendering the calculated results of the model questionable. One way to correct this limitation is to base the *in vivo* drug-delivery modeling on data that are obtained from physiologically relevant *in vitro* release experiments, which ideally would reflect small reservoir volumes and non-sink conditions and the short ocular residence times. In this investigation, these *in vitro* data were obtained using pulsatile microdialysis (PMD). Such *in vitro* drug dissolution data is used to model *in vivo* delivery by performing calculations using a model that appropriately accounts for the precorneal components and processes.

CHAPTER 3. OBJECTIVES OF THIS RESEARCH

3.1 This dissertation moves the state-of-the-art ocular PBPK modeling forward in several ways

3.1.1 The precorneal model includes partitioning and depot effects

Drug molecules partitioning in the chemical drug depots on the precorneal surface can significantly change intra-ocular drug availability. This crucial effect was not captured by published precorneal models. The proposed model developed in this research not only includes dynamic processes such as drug dissolution, tear turnover, nasal-lacrimal drainage, and drug absorption but also reflected the interaction between drug molecules with a potential chemical depot on the top of the tear film. Incorporating this special drug depot effect on the precorneal surface into the model is innovative and critically important for identifying formulation factors that might significantly impact the dosing interval.

3.1.2 Improved ocular PBPK model

Nepafenac is a unique prodrug with lipophilic properties that allow the drug to penetrate the biological membrane and to distribute rapidly across different ocular tissues (Jones and Neville, 2013). The proposed distribution pathway of nepafenac (Chastain et al., 2016) is different from conventional topically applied ocular NSAIDs and therefore the PBPK model needs to be adjusted to represent this concentration gradient across multi-directions among different ocular tissues.

The prodrug nepafenac is metabolized by hydrolysis that is catalyzed by local amidase enzymes to produce the active metabolite amfenac. Amfenac is a potent inhibitor of

cyclooxygenase (COX-1 and COX2). It reduces the downstream generation of prostaglandin and consequently suppresses the inflammation at target sites (Ke et al., 2000). This enzyme metabolism mechanism was not included in a published ocular PBPK model that was established for dexamethasone ophthalmic suspension, a topical steroidal anti-inflammatory drug that does not undergo metabolism to produce its active form (Le Merdy et al., 2019). The enzyme kinetics are incorporated into the nepafenac-amfenac ocular PBPK model, and thus represents an update of existing knowledge of ocular pharmacokinetics.

The ocular PBPK model established in this dissertation applied a transport formalism to describe drug exchanges between adjacent compartments. A major advantage of "transport" formalism is the introduction of the partitioning coefficient in the model equation. It replaced one of the rate constants in the traditional pharmacokinetic formalism with a ratio relationship between the rate constant and the partition coefficient. Since the partition coefficient (or reasonable ranges of values) can be estimated from laboratory data, the rate constants (*k's*) in the transport formalism would be the only remaining parameters needing to be estimated. Using a measured partition coefficient and fitting for a single rate constant is numerically advantageous compared to the traditional pharmacokinetic formalism in which both rate constants must be estimated together. This dissertation document will follow the notation that a partition coefficient between materials *X* and *Y* is denoted as K_{XY} = concentration in X divided by the concentration in *Y*. (As used here, *X* will typically denote the more lipophilic compartment and *Y* will denote the more aqueous-like compartment.)

3.1.3 PBPK model simulations were used to identify mechanisms that affect the dosing interval changes observed due to formulation differences

The established ocular PBPK model can be used as an *in silico* platform of exploratory simulation design to identify potential factors or mechanisms that affect optimal doing intervals. For example, the particle size of ophthalmic suspension might be expected to affect the drug's *in vivo* dissolution rate given that smaller drug particles have a larger specific surface area (surface area per gram of particles).

On the other hand, it is very possible that in nepafenac formulations, which contain a drug with poor aqueous solubility, the ocular residence time may be too short to allow for significant dissolution before the drug is cleared from the ocular region. In that case, the initial drug distribution may be more important, specifically the fraction of the nepafenac dissolved in the aqueous portion of the formulation or complexed with excipients that allow for rapid release into the aqueous phase. This is because it is assumed that only dissolved drug molecules can partition into oily depots or be absorbed into physiological tissues. Thus, if undissolved drug particles cannot further dissolve, knowing the fraction rapidly available to the aqueous phase was critical for assessing how much drug in the formulation might be bioavailable.

The ocular PBPK model enables ones to run a set of simulations with a hypothetical drug particle radius to check whether there is a significant impact of this formulation factor on the drug release and absorption, especially during the estimated residence period. Similarly, simulations can be carried out to evaluate the impact of other factors on ocular bioavailability such as viscosity, initial drug distribution, partitioning effect, the permeability of drug molecules, and enzyme kinetics. Those simulations help to identify

the factor(s) or mechanism(s) that might be decisive to the overall drug availability at the therapeutic sites of action. Moreover, running experimental simulations using the established ocular PBPK model serves as a powerful tool to answer the major question of this study: How was the dosing frequency of a nepafenac suspension impacted by formulation factors?

3.2 Statement of the problem

Nepafenac is marketed as two aqueous-based ophthalmic suspensions— NEVANAC® and ILEVRO®. While neither formulation is sustained release, and neither is thought to have an extended ocular residence time, tripling the total drug concentration of the suspension from 0.1% to 0.3% causes a change in the required dosing frequency of the nepafenac suspensions.

3.3 Specific aims and how will they facilitate achieving the main goals

The overall question to answer is why two ophthalmic suspension formulations, neither of which is thought to exhibit prolonged ocular residence times nor sustained release characteristics, exhibit a difference in dosing frequency from every 8 hours to every 24 hours. To answer this question, it is important to investigate two considerations—what factors are responsible for the prolonged dosing intervals (even every 8 hours is much longer than the anticipated ocular residence time), and what factors account for tripling the dosing interval when the administered dose of the nepafenac is tripled.

The first consideration suggests physiological reasons and motivates building a suitable ocular PBPK model that incorporates the pharmacokinetic characteristics of nepafenac

and amfenac to trace the local drug concentration and the potential depot effect caused by the reversible enzyme binding mechanism.

The second consideration suggests investigating differences in the formulations themselves in addition to the pharmacokinetics. This involved characterization of the formulations, including factors affecting the delivery of nepafenac to the ocular tissues that differ between NEVANAC® and ILEVRO®. These factors include the dissolution of nepafenac from the formulations, drug distribution in the formulations when administered, and viscosity differences, among others, all of which would be expected to influence the *in vivo* dissolution and drug delivery by potentially interacting differently with the ocular precorneal layer.

Four specific aims were identified to test the potential reasons for prolonged dosing intervals associated with the nepafenac ophthalmic suspension products.

1. To identify the factors of formulation properties affecting the absorption of two nepafenac ophthalmic suspensions: NEVANAC® and ILEVRO®.
2. To simulate the *in vivo* drug dissolution based on data from a PMD-based *in vitro* drug release test.
3. To investigate the impact of lipidic drug depot on drug absorption on the ocular surface.
4. To characterize the distribution of nepafenac pro-drug and its metabolism behavior in the different ocular tissues especially the iris/ciliary body in the anterior segment and retina/choroid area in the posterior segment.

3.3.1 Physical properties identification (Specific Aim #1)

At the formulation stage, two physical properties of NEVANAC® and ILEVRO® were the particle size distribution and the formulation viscosity.

As a starting point, if perfectly spherical particles are assumed, particle size is inversely proportional to the total surface area per amount of nepafenac (the standard surface area). The higher the standard surface area, the faster the drug dissolves in response to concentration loss due to dilution or drug absorption. Viscosity is another important factor as it affects the residence time when the drug stays in touch with the tear layer before being washed down to the nasal-lacrimal duct or diluted by tear turnover. Formulations with higher viscosity are expected to have a longer residence time and that allows higher drug absorption at the ocular surface. On the other hand, higher viscosity may result in slower particle dissolution. Test results were compared to the theoretical calculation to provide experimental support for our primary assumption.

3.3.2 In vitro drug dissolution characterization (specific aim #2)

At the releasing stage, a goal is to determine or model the nepafenac concentration vs. time profile in the precorneal layer over a period exceeding anticipated ocular residence time. To do this, the following dissolution properties were experimentally determined for the NEVANAC® and ILEVRO® formulations:

- *In vivo* dissolution rate of the drug
- Apparent solubility of the drug
- Initial drug distribution in diluted and undiluted formulations
- Potential drug-polymer interactions if applicable

Data for the dissolution rates and initial drug distributions from the PMD-based IVDTs are required for the understanding of formulation differences between NEVANAC® and ILEVRO®. Concentration-time profiles obtained from the PMD test were input into in-house physiologically relevant models describing dissolution into non-sink, low-volume, thin-layer receivers with limited agitation and tear exchange.

3.3.3 Depot effect on the ocular surface (specific aim #3)

After the drug is instilled on the ocular surface, drug particles start to dissolve into the mixture of the aqueous phase and tear. Physiological processes including tear turnover and nasal-lacrimal drainage start simultaneously. The goal was to incorporate a suspension-specific pre-corneal compartment into the ocular PBPK model that can reflect these mechanisms applied to the interaction between tear and drug. Physical and physiological processes include drug dissolution, tear turnover, nasal-lacrimal drainage, tear evaporation, drug absorption, and partitioning of the drug into the depot. This model considered the impact of formulation properties on drug release and absorption at the ocular surface. For example, a formulation with a higher viscosity should have a longer residence time and that might result in greater drug absorption through the corneal epithelium and conjunctiva surfaces.

In addition, mucin and the oily layer secreted by meibomian glands could work as potential physiological drug depots. This is postulated because drugs are known to bind to mucin, and the lipophilic nature of the nepafenac molecule makes it likely to partition into an oily layer as well as lipophilic tissue membranes due to its less polar molecular structure. This partitioning effect might serve as an important factor that helps to explain

the long last therapeutic effect of nepafenac ophthalmic suspensions. Therefore, the precorneal model should be able to reflect the difference in drug absorption in the simulation results of the different formulations.

3.3.4 Enzyme binding and metabolism kinetics

Once the drug gets absorbed through corneal epithelium or palpebral/bulbar conjunctivas, it can be assumed that the drug's bioavailability would no longer depend on the formulation properties discussed above. At this stage, it is desirable to characterize the drug distribution and metabolism behavior in ocular tissues. That requires the information about the following:

- Nepafenac and amfenac distribution paths from the anterior to posterior segments
- Amidase abundance and activities in different ocular tissues
- Mechanism of the enzyme kinetics
- Local concentration of nepafenac and amfenac at therapeutic sites such as the iris/ciliary body and retina/choroid area over the dosing intervals

Published data were used to establish ranges for the parameter values in the proposed model. Parameter sensitivity analysis was carried out to identify predominant factors and corresponding parameters in the model. Compartments and parameters that were not significantly relevant to or necessary components of the simulations were ruled out to enhance the power of the final ocular PBPK model.

CHAPTER 4. THE OCULAR PBPK MODEL

4.1 Brief description and summary

4.1.1 Ocular component of the PBPK model

The established ocular PBPK model represents the eye as a collection of the following compartments: pre-cornea surface, cornea, palpebral conjunctiva, bulbar conjunctiva, aqueous humor, iris-ciliary body (ICB), vitreous humor, sclera, choroid, and retina. The sclera, choroid, and retina are separated into three different segments: the limbus to the ore serrata segment (L-OS), the ora serrata to the equator segment (OS-E), and the equator to the posterior pole segment (E-PP). The L-OS segment only applies to the sclera while OS-E and E-PP segments apply to all three tissues. The different segments within the same tissue (from L-OS to OS-E to E-PP) are designed to track the drug concentration gradient of nepafenac and amfenac towards the periocular direction and the different tissues (from the sclera to choroid to retina) of the same segment are designed to track the drug concentration gradient of nepafenac and amfenac towards the perpendicular direction (from outside to inside) of the eye. The lens is not permeable to the drug molecules, nor does it serve as any therapeutic target in the treatment of inflammation associated with cataract surgery. Therefore, it is not considered an additional compartment in this proposed model. A central-system compartment is included in the model to represent part of drug loss due to systemic absorption of the drug from vascularized tissues such as conjunctivas and the choroid. The basic structure of the human eye is shown in Figure 4-1

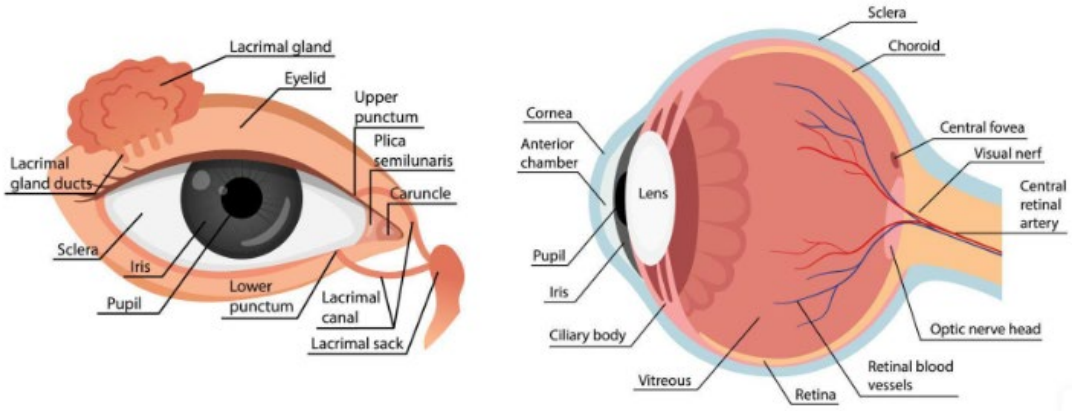

Figure 4-1. Human eye structure

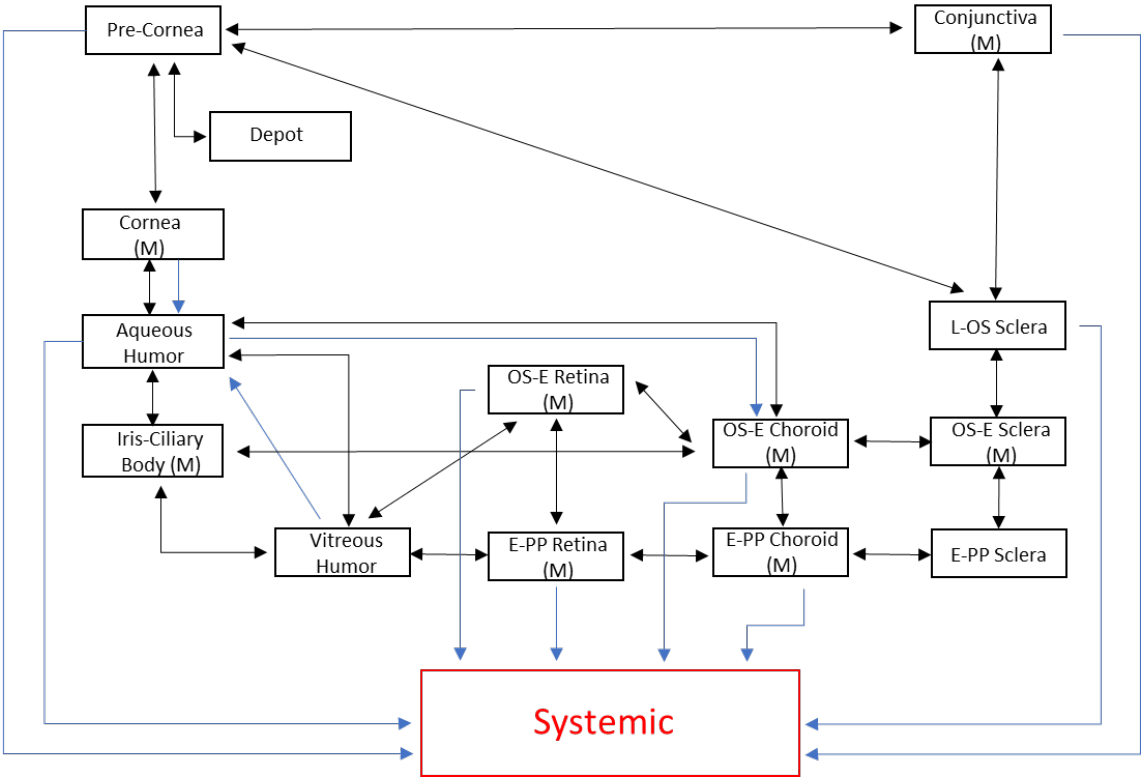

Figure 4-2. Diagram of Proposed Ocular PBPK Model with tissue and site compartments.

4.1.2 Precorneal model

The pre-corneal drug-tear interaction model is designed to represent a variety of mechanisms resulting in drug dissolution, drug loss due to drainage, drug partitioning into a chemical depot on the top of the tear film, and productive drug absorption through cornea and sclera. Those mechanisms are subjected to topical ophthalmic suspension once it is dropped on the precorneal surface. The total volume of the precorneal compartment (consisting of the tear film and conjunctival sac) drastically increases due to the instillation of the drug formulation and the tear production caused by irritation. The maximum load of the precorneal space is set to 40 μl for the reference of a normal human eye. The total volume of instilled drug and tear film gradually returns to the base volume which is set to 7 μl based on the volume of the tear film at static or steady state status [Jarvinen et al., 1995]. The drug loss is accounted for by both dissolved drug molecules and undissolved drug particles in the formulation. The dissolution rate of drug particles was described using *in vitro* dissolution data obtained using pulsatile microdialysis (PMD). In addition, the drug's initial (just before administration) distribution in the ophthalmic suspension was also described based on *in vitro* data obtained using PMD. These were determined because only dissolved drug is subjected to productive absorption through the corneal epithelium and sclera surface, and *in vitro* data based on PMD experiments provide more biorelevant data than other experimental methods, thus improving the bases on which the *in vivo* drug disposition is based. Tear production is assumed to equal the sum of the evaporation and base drainage rates. The tear production, evaporation, and base drainage rates are assumed to be constant. The transient drainage rate is modeled as declining in a first-order manner from a maximum (immediately after

instilling a drop) to zero after a short period depending on the drug's residence time affected by formulation viscosity (signifying a return to the base drainage rate). The partitioning effect of the drug molecules into chemical drug depots is included as a crucial factor in the precorneal model. Simulations based on values of partition coefficients elucidate how quickly the drug accumulated in the depot and the resulting impact on drug absorption.

4.1.3 PMD-based *in vitro* drug-releasing data

The *in vivo* drug release can be calculated in theory from the drug particle geometry, drug solubility, and *in vitro* experimental dissolution rate data, but these would assume ideal conditions and be highly simplified to make the calculations tractable. In reality, each formulation has different proprieties and components, and all must be quantitatively considered when modeling the *in vivo* drug release to facilitate simulations that account for the impact of formulation differences on the dosing frequency. For instance, there might be a solubilizer or other factors that affect the apparent solubility or dissolution rate of the drug.

Given the considerations discussed above, it is more accurate to model the *in vivo* drug dissolution profile based on a set of *in vitro* dissolution data acquired from a biorelevant experimental setup. For the proposed model, a novel PMD-based method was initially applied to test the *in vitro* dissolution behavior of both formulations (NEVANAC® 0.1% and ILEVRO® 0.3%), using experimental factors that were selected to represent the physiological condition of the precorneal surface. Data acquired from the PMD-based *in vitro* drug release test were used to calculate two important parameters: initial drug

distribution in the formulation and the apparent drug dissolution rate into the reservoir. With the support of a set of *in vitro* dissolution data based on the PMD method, *in vivo* drug release as input of the precorneal model was modeled and the simulation results demonstrated the validity of the approach.

4.1.4 The mechanics of the model

The proposed ocular PBPK model is constructed to represent passive diffusion between adjacent tissue compartments and convective fluid between aqueous compartments. Tissue compartments where the distribution and metabolism of nepafenac and amfenac happen to occur were identified and connected based on ocular physiology. Compartment characteristics such as volume and permeability, which affect the diffusion coefficients in the model equations, were obtained from the literature. Drug exchange through passive diffusion between neighbor compartments (compartment "1" and compartment "2" in the example equation below) was described in the following "transport" formalism shown by Eq. 1:

$$\frac{dM_2}{dt} = k\left(\frac{M_1}{V_1} - \frac{M_2}{KV_2}\right) \qquad \textbf{(Eq. 1)}$$

Partition properties determined by organ-specific hydrophilicity and lipophilicity are considered within the equation where k is a kinetic constant (units of volume per time), and K is a unitless parameter that reflects the partitioning effect between lipidic and aqueous compartments. Compared to the pharmacokinetic formalism (for instance, $dM_2/dt = k_1C_1 - k_2C_2$ in which k_1 and k_2 must be fitted together), this "transport" formalism allows an evaluation of the partitioning constant K by reference to the tissue or

compartment hydrophilicity/lipophilicity rather than by fitting for it. Thus, only the value of the kinetic rate constant k is obtained by parameter estimation (i.e., model fitting), which reduces the fitted parameter set and helps to mitigate errors caused by fitting for two parameters (k_1 and k_2) that may compensate for each other.

Enzyme kinetics for the conversion of the prodrug (nepafenac) to the active compound (amfenac) is also included in the proposed model. The conversion rate described by Equation 2:

$$\frac{Exp_i \times V_{max} \times \frac{M_i}{V_i \times MW_{nep}}}{K_{mi} + \frac{M_i}{V_i \times MW_{nep}}} \quad \textbf{(Eq. 2)}$$

In Eq. 2, Exp_i describes the level of enzyme expression (μM) at certain ocular tissue compartments, V_{max} represents the maximum velocity (μg/min/ug) of nepafenac metabolism reaction mediated by amidase, MW_{nep} represents the molecular weight of nepafenac, K_{mi} represents the nepafenac substrate concentration (μM) when the amidase-mediated metabolism reaction is half of the maximum velocity V_{max}, M_i describes the mass of nepafenac (μg) prodrug in the respective ocular tissue compartments, and V_i (μl) is the volume of the respective ocular tissue compartment. It is worth noting that the conversion rate only depends on the amidase and the nepafenac substrate, but not the amfenac product generated during the process.

4.1.5 Summary of how the model was used

The established ocular PBPK model was used as the platform for *in silico* simulations using a set of exploratory parameter values to assess potential mechanisms that explain the dosing interval differences between the drug products. One of the examples would be

changing the dissolution rate and the solubility (to represent initial drug distribution in the aqueous phase of the formulations) to determine which factor has a higher impact on the drug's availability into the cornea. Also, a sensitivity analysis of parameters was performed to identify parameters that were not relevant to the overall simulation results.

Overall, the model was used for the following purposes:

- Identify major formulation factors (particle size, viscosity, drug distribution, etc.) that affect the drug availability and dosing frequency
- Test the effect of proposed mechanisms such as chemical drug depot on the precorneal surface and protein binding at pigmented ocular tissues on the drug ocular absorption and distribution
- Determine time-dependent drug concentrations in different ocular tissues to explore different distribution pathways (i.e., anterior to posterior versus periocular) of nepafenac and amfenac
- Provide an open-source platform for ocular PBPK and quantitative pharmacology studies

4.2 The ocular component of the PBPK model

4.2.1 Overview of relevant physiological compartments for nepafenac and amfenac

The cornea compartment

The cornea is a transparent tissue layer located at the anterior part of the eye (in front of the iris and aqueous humor). The cornea of adult humans has an average size of 11.5mm horizontal diameter and 10mm vertical diameter. The corneal route is the main route for

the delivery of drugs to the anterior chamber. Permeation of hydrophilic drugs and macromolecules through the corneal epithelium is limited by the presence of tight junctions between adjacent outer superficial epithelial cells. The abundant presence of hydrated collagen in the stroma may hamper the diffusion of highly lipophilic agents (Willoughby et al., 2010).

In the proposed model for this research, the corneal epithelium and corneal stroma were combined into a single cornea compartment with a total volume of 50 μL, given that the thickness of corneal epithelium (45.7 ± 5.9 μm) is less than 1/9 that of the corneal stroma (426.4 ± 38.5 μm) (Reinstein et al., 2010). Moreover, the diffusion process of lipophilic prodrugs such as nepafenac was mainly determined by corneal stroma in which the presence of hydrated collagen will slow down the movement of the drug.

The drug diffusion rate (mass of drug that can be absorbed into the cornea per time) is determined by the permeability of nepafenac in the corneal stroma (the rate-limiting step). Drug molecules dissolved in the tear film are absorbed into the cornea compartment and the drug accumulated in the cornea will interact with the tear film and aqueous humor through passive diffusion. Outward liquid convection exists from the corneal stroma to the aqueous humor. Partitioning effects are considered between tear film and corneal as well as corneal and aqueous humor.

The change in the mass of nepafenac in the corneal compartment with time is described by Equation 3:

$$\frac{dM_c}{dt} = k_{tc}\left(\frac{M}{V} - \frac{M_c}{V_c \times K_{ptc}}\right) - k_{cah}\left(\frac{M_c}{V_c \times K_{pcah}} - \frac{M_{ah}}{V_{ah}}\right) - Q_{cah}\left(\frac{M_c}{V_c}\right) -$$

$$\left(\frac{Exp_c \times V_{max} \times \frac{M_c}{V_c \times MW_{nep}}}{K_{mi} + \frac{M_c}{V_c \times MW_{nep}}}\right) \times \frac{MW_{nep}}{1000000} \qquad \textbf{(Eq. 3)}$$

The change in the mass of amfenac in the corneal compartment with time is described by Equation 4:

$$\frac{dMA_c}{dt} = \left(\frac{Exp_c \times V_{max} \times \frac{M_c}{V_c \times MW_{nep}}}{K_{mi} + \frac{M_c}{V_c \times MW_{nep}}}\right) \times \frac{MW_{amf}}{1000000} - kA_{cah}\left(\frac{MA_c}{V_c \times K_{pcah}} - \frac{MA_{ah}}{V_{ah}}\right) - Q_{cah}\left(\frac{MA_c}{V_c}\right)$$

(Eq. 4)

M_c: Mass of nepafenac accumulated in the cornea compartment

MA_c: Mass of amfenac accumulated in the cornea compartment

M: Mass of nepafenac dissolved in the tear film compartment

M_{ah}: Mass of nepafenac accumulated in the aqueous humor compartment

MA_{ah}: Mass of amfenac accumulated in the aqueous humor compartment

V: Volume of the tear film compartment

V_c: Volume of the corneal compartment

V_{ah}: Volume of the aqueous humor compartment

k_{tc}: Rate constant of nepafenac transport from the tear film to the cornea

k_{cah}: Rate constant of nepafenac transport from the cornea to the aqueous humor

kA_{cah}: Rate constant of amfenac transport from the cornea to the aqueous humor

K_{ptc}: Partition coefficient of nepafenac between the tear film and the cornea (concentration in the tear film divided by the concentration in the cornea)

K_{pcah}: Partition coefficient of nepafenac between the cornea and the aqueous humor (concentration in the cornea divided by the concentration in the aqueous humor)

Exp_{con}: Expression of amidase at the conjunctiva

KA_{ptc} : Partition coefficient of amfenac between the tear film and the cornea (concentration in the tear film divided by the concentration in the cornea)

KA_{pcah}: Partition coefficient of amfenac between the cornea and the aqueous humor (concentration in the cornea divided by the concentration in the aqueous humor)

Q_{cah}: Rate of liquid convection from the cornea to the aqueous humor

V_{max}: Maximum velocity of amidase metabolism (generation of amfenac product)

K_{mi}: Nepafenac concentration at which velocity of amidase metabolism reaches half of the maximum velocity

Exp_c: Expression of amidase at the cornea

The conjunctiva compartment

The conjunctiva lines the lids and then bends back over the surface of the eyeball, constituting an outer covering to the forward part of the eyeball, and terminating at the transparent region of the eye, the cornea. The portion that lines the lids is called the palpebral portion of the conjunctiva; the portion covering the white of the eyeball is called the bulbar conjunctiva (Davson and Perkins, 2022). The conjunctiva is vascularized tissue and drugs absorbed into the conjunctiva are subjected to system absorption. This pathway was considered to contribute to drug loss in the case of intra-ocular targeting ophthalmic formulations. Drug accumulated in the bulbar conjunctiva will transport into the sclera (limbus to ora serrata section) which is more permeable than the cornea but less permeable than the conjunctiva by passive diffusion. In this model, the palpebral conjunctiva and the bulbar conjunctiva were combined into a whole conjunctiva compartment.

The change in the mass of nepafenac in the conjunctiva compartment with time is described by Equation 5:

$$\frac{dM_{con}}{dt} = k_{tcon}\left(\frac{M}{V} - \frac{M_{con}}{V_{con}\times K_{ptcon}}\right) - k_{conlossc}\left(\frac{M_{con}}{V_{con}} - \frac{M_{lossc}}{V_{lossc}}\right) - Q_{cons}\left(\frac{M_{con}}{V_{con}}\right) - \left(\frac{Exp_{con}\times V_{max}\times\frac{M_{con}}{V_{con}\times MW_{nep}}}{K_{mi}+\frac{M_{con}}{V_{con}\times MW_{nep}}}\right)\times\frac{MW_{nep}}{1000000} \quad \textbf{(Eq. 5)}$$

The change in the mass of amfenac in the conjunctiva compartment with time is described by Equation 6:

$$\frac{dMA_{con}}{dt} = \left(\frac{Exp_{con}\times V_{max}\times\frac{M_{con}}{V_{con}\times MW_{nep}}}{K_{mi}+\frac{M_{con}}{V_{con}\times MW_{nep}}}\right)\times\frac{MW_{amf}}{1000000} - kA_{conlossc}\left(\frac{MA_{con}}{V_{con}} - \frac{MA_{lossc}}{V_{lossc}}\right) - QA_{cons}\left(\frac{MA_{con}}{V_{con}}\right) \quad \textbf{(Eq. 6)}$$

M_{con}: Mass of nepafenac accumulated in the conjunctiva compartment

MA_{con}: Mass of amfenac accumulated in the conjunctiva compartment

M: Mass of nepafenac dissolved in the tear film compartment

M_{lossc}: Mass of nepafenac accumulated in the sclera (limbus to ora serrata section) compartment

MA_{lossc}: Mass of amfenac accumulated in the sclera (limbus to ora serrata section) compartment

V: Volume of the tear film compartment

V_{con}: Volume of the conjunctiva compartment

V_{lossc}: Volume of the sclera (limbus to ora serrata section) compartment

k_{tcon}: Rate constant of nepafenac transport from the tear film to the conjunctiva compartment

$k_{conlossc}$: Rate constant of nepafenac transport from the conjunctiva compartment to the sclera (ora serrata section)

$kA_{conlossc}$: Rate constant of amfenac transport from the conjunctiva compartment to the sclera (ora serrata section)

K_{ptcon}: Partition coefficient of nepafenac between the tear film and the conjunctiva (concentration in the tear film divided by the concentration in the conjunctiva)

KA_{ptcon}: Partition coefficient of amfenac between the tear film and the conjunctiva (concentration in the tear film divided by the concentration in the conjunctiva)

Q_{cons}: Rate of nepafenac systemic absorption from the conjunctiva compartment

QA_{cons}: Rate of amfenac systemic absorption from the conjunctiva compartment

Exp_{con}: Expression of amidase at the conjunctiva

The aqueous humor compartment

The aqueous humor is a clear transparent liquid that fills the anterior chamber of the eye (the region between the cornea and iris) and posterior chamber of the eye (the region behind the iris), and it functions to nourish the cornea and lens. Aqueous humor is generated by the ciliary processes (a specific region of the ciliary body) into the posterior chamber and flows through the pupil into the anterior chamber (Davson and Perkins, 2022) before being drained to the aqueous vein through the trabecular meshwork, or the uveoscleral pathway (Goel et al., 2010). Ocular compartments that interact with aqueous humor include the corneal stroma, iris, ciliary body (ICB), sclera (limbus to ora serrata section), and vitreous humor. Inward liquid convection exists from vitreous humor to aqueous humor while outward liquid convection happens from aqueous humor to the sclera (limbus to ora serrata section). Meanwhile, drugs accumulated in the aqueous humor are subjected to systemic absorption through vein drainage.

The change in the mass of nepafenac in the aqueous humor compartment with time is described by Equation 7:

$$\frac{dM_{ah}}{dt} = k_{cah}\left(\frac{M_c}{V_{c\times}K_{pcah}} - \frac{M_{ah}}{V_{ah}}\right) + Q_{cah}\left(\frac{M_c}{V_c}\right) + Q_{vhah}\left(\frac{M_{vh}}{V_{vh}}\right) - k_{ahicb}\left(\frac{M_{ah}}{V_{ah}} - \frac{M_{icb}}{V_{icb}\times K_{pahicb}}\right) -$$

$$k_{ahvh}\left(\frac{M_{ah}}{V_{ah}} - \frac{M_{vh}}{V_{vh}}\right) - k_{ahosecho}\left(\frac{M_{ah}}{V_{ah}} - \frac{M_{osecho}}{V_{osecho}\times K_{pahosecho}}\right) - Q_{ahosecho}\left(\frac{M_{ah}}{V_{ah}}\right) - Q_{ahs}\left(\frac{M_{ah}}{V_{ah}}\right)$$

(Eq. 7)

The change in the mass of amfenac in the aqueous humor compartment with time is described by Equation 8:

$$\frac{dMA_{ah}}{dt} = k_{Acah}\left(\frac{MA_c}{V_c\times KA_{pcah}} - \frac{MA_{ah}}{V_{ah}}\right) + Q_{cah}\left(\frac{MA_c}{V_c}\right) + Q_{vhah}\left(\frac{MA_{vh}}{V_{vh}}\right) - kA_{ahicb}\left(\frac{MA_{ah}}{V_{ah}} - \frac{MA_{icb}}{V_{icb}\times KA_{pahicb}}\right) -$$

$$kA_{ahvh}\left(\frac{MA_{ah}}{V_{ah}} - \frac{MA_{vh}}{V_{vh}}\right) - kA_{ahosecho}\left(\frac{MA_{ah}}{V_{ah}} - \frac{MA_{osecho}}{V_{osecho}\times KA_{pahosecho}}\right) - Q_{ahosecho}\left(\frac{MA_{ah}}{V_{ah}}\right) - QA_{ahs}\left(\frac{MA_{ah}}{V_{ah}}\right)$$

(Eq. 8)

M_c: Mass of nepafenac accumulated in the cornea compartment

MA_c: Mass of amfenac accumulated in the cornea compartment

M_{ah}: Mass of nepafenac accumulated in the aqueous humor compartment

MA_{ah}: Mass of amfenac accumulated in the aqueous humor compartment

M_{vh}: Mass of nepafenac accumulated in the vitreous humor compartment

MA_{vh}: Mass of amfenac accumulated in the vitreous humor compartment

M_{icb}: Mass of nepafenac accumulated in the iris and ciliary body compartment

MA_{icb}: Mass of amfenac accumulated in the iris and ciliary body compartment

M_{osecho}: Mass of nepafenac accumulated in the choroid (ora serrata to equator section)

MA_{osecho}: Mass of amfenac accumulated in the choroid (ora serrata to equator section)

V_c: Volume of the cornea compartment

V_{ah}: Volume of the aqueous humor compartment

V_{vh}: Volume of the vitreous humor compartment

V_{icb}: Volume of the iris and ciliary body compartment

V_{lossc}: Volume of the choroid (ora serrata to equator section) compartment

k_{cah}: Rate constant of nepafenac transport from the cornea to the aqueous humor

kA_{cah}: Rate constant of amfenac transport from the cornea to the aqueous humor

k_{ahicb}: Rate constant of nepafenac transport from the aqueous humor to the iris and ciliary

kA_{ahicb}: Rate constant of amfenac transport from the aqueous humor to the iris and ciliary

k_{ahvh}: Rate constant of nepafenac transport from the aqueous humor to the vitreous humor

kA_{ahvh}: Rate constant of amfenac transport from the aqueous humor to the vitreous humor

$k_{ahosecho}$: Rate constant of nepafenac transport from the aqueous humor to the choroid (ora serrata to equator section)

$kA_{ahosecho}$: Rate constant of amfenac transport from the aqueous humor to the choroid (ora serrata to equator section)

K_{pcah}: Partition of nepafenac coefficient of nepafenac between the cornea and the aqueous humor (concentration in the cornea divided by the concentration in the aqueous humor)

KA_{pcah}: Partition coefficient of amfenac between the cornea and the aqueous humor (concentration in the cornea divided by the concentration in the aqueous humor)

K_{pahicb}: Partition of nepafenac coefficient of nepafenac between the aqueous humor and the iris and ciliary body compartment (concentration in the aqueous humor divided by the concentration in the iris and ciliary body compartment)

KA_{pahicb}: Partition coefficient of amfenac between the aqueous humor and the iris and ciliary body compartment (concentration in the aqueous humor divided by the concentration in the iris and ciliary body compartment)

$K_{pahosecho}$: Partition coefficient of nepafenac between the aqueous humor and the choroid (ora serrata to equator section) which is the concentration in the aqueous humor divided by the concentration in the choroid (ora serrata to equator section)

$KA_{pahosecho}$: Partition coefficient of amfenac between the aqueous humor and the choroid (ora serrata to equator section) which is the concentration in the

aqueous humor divided by the concentration in the choroid (ora serrata to equator section)

Q_{cah}: Rate of liquid convection from the cornea to the aqueous humor

Q_{vhah}: Rate of liquid convection from the vitreous humor to the aqueous humor

Q_{ahs}: Rate of nepafenac systemic absorption from the aqueous humor compartment

QA_{ahs}: Rate of amfenac systemic absorption from the aqueous humor compartment

The iris and ciliary body (ICB) compartment

The iris, ciliary body, and part of the choroid (ora serrata to equator section) comprise the forward portion of the uvea, which is the middle layer of the eye. The iris is a pigmented tissue that gives the color of the eye and controls the amount of light entering the eye by adjusting the diameter of the pupil. The ciliary body is a muscular ring under the surface of the eyeball that helps to control the power and shapes of the lens and is also the site of aqueous humor production (Davson and Perkins, 2022). The iris and the ciliary body are the sites of prostaglandin production and, therefore, are targeted as the major therapeutic sites of ocular NSAIDs at the anterior section of the eye (Perkins, 1975; Ke et al., 2000). Also, studies have shown that nepafenac is converted by amidase to amfenac primarily in the iris and ciliary body at the anterior section of the eye (Ke et al., 2000; Chastain et al., 2016). The ocular compartments that interact with the iris and ciliary body (ICB) are the aqueous humor, choroid (ora serrata to equator section), and vitreous humor. An outward liquid convection exists from the iris and ciliary body compartment to the vitreous humor compartment. Bioactivation (hydrolysis reaction carried on by amidase) of nepafenac prodrug occurs in the ICB compartment.

The change in the mass of nepafenac in the ICB compartment with time is described by Equation 9:

$$\frac{dM_{icb}}{dt} = k_{ahicb}\left(\frac{M_{ah}}{V_{ah}} - \frac{M_{icb}}{V_{icb}\times K_{pahicb}}\right) - k_{icbosecho}\left(\frac{M_{icb}}{V_{icb}} - \frac{M_{osecho}}{V_{osecho}}\right) - k_{icbvh}\left(\frac{M_{icb}}{V_{icb}\times K_{pvhicb}} - \frac{M_{vh}}{V_{vh}}\right) - \left(\frac{Exp_{icb}\times V_{max}\times\frac{M_{icb}}{V_{icb}\times MW_{nep}}}{K_{mi}+\frac{M_{icb}}{V_{icb}\times MW_{nep}}}\right)\times\frac{MW_{nep}}{1000000}$$

(Eq. 9)

The change in the mass of amfenac in the ICB compartment with time is described by Equation 10:

$$\frac{dMA_{icb}}{dt} = \left(\frac{Exp_{icb}\times V_{max}\times\frac{M_{icb}}{V_{icb}\times MW_{nep}}}{K_{mi}+\frac{M_{icb}}{V_{icb}\times MW_{nep}}}\right)\times\frac{MW_{amf}}{1000000} + kA_{ahicb}\left(\frac{MA_{ah}}{V_{ah}} - \frac{MA_{icb}}{V_{icb}\times KA_{pahicb}}\right) - kA_{icbosecho}\left(\frac{MA_{icb}}{V_{icb}} - \frac{MA_{osecho}}{V_{osecho}}\right) - kA_{icbvh}\left(\frac{MA_{icb}}{V_{icb}\times KA_{pvhicb}} - \frac{MA_{vh}}{V_{vh}}\right)$$

(Eq. 10)

M_{ah}: Mass of nepafenac accumulated in the aqueous humor compartment

MA_{ah}: Mass of amfenac accumulated in the aqueous humor compartment

M_{icb}: Mass of nepafenac accumulated in the iris and ciliary body compartment

MA_{icb}: Mass of amfenac accumulated in the iris and ciliary body compartment

M_{osecho}: Mass of nepafenac accumulated in the choroid (ora serrata to equator section)

MA_{osecho}: Mass of amfenac accumulated in the choroid (ora serrata to equator section)

V_{ah}: Volume of the aqueous humor compartment

V_{icb}: Volume of the iris and ciliary body compartment

V_{osecho}: Volume of the choroid (ora serrata to equator section) compartment

$k_{icbosecho}$: Rate constant of nepafenac transport from the iris and ciliary to the choroid (ora serrata to equator section)

k_{icbvh}: Rate constant of nepafenac transport from the iris and ciliary to the vitreous humor

$kA_{icbosecho}$: Rate constant of amfenac transport from the iris and ciliary to the choroid (ora serrata to equator section)

kA_{icbvh}: Rate constant of amfenac transport from the iris and ciliary to the vitreous humor

K_{pahicb}: Partition coefficient of nepafenac between the aqueous humor and the iris and ciliary body compartment (concentration in the aqueous humor divided by the concentration in the iris and ciliary body compartment)

K_{picbvh}: Partition coefficient of nepafenac between the iris and ciliary body and the vitreous humor (concentration in iris and ciliary body divided by the concentration in the vitreous humor)

KA_{pahicb}: Partition coefficient of amfenac between the aqueous humor and the iris and ciliary body compartment (concentration in the aqueous humor divided by the concentration in the iris and ciliary body compartment)

KA_{picbvh}: Partition coefficient of amfenac between the iris and ciliary body and the vitreous humor (concentration in iris and ciliary body divided by the concentration in the vitreous humor)

Q_{icbvh}: Rate of liquid convection from the iris and ciliary body to the vitreous humor

V_{max}: Maximum velocity of amidase metabolism (generation of amfenac product)

K_{mi}: Nepafenac concentration at which velocity of amidase metabolism reaches half of the maximum velocity

Exp_{icb}: Expression of amidase at the iris and ciliary body

The sclera compartment

The sclera is the white outer cover of the eye that protects the eye from external force and antagonists. The sclera consists of the same collagen fibers as the cornea, and it is connected to the cornea at the limbus (Davson and Perkins, 2022). The sclera is a vascularized layer that expands from the anterior section of the eyeball forward to the posterior pole. Passive diffusion happens in both the periocular direction (from anterior section to posterior section) and the perpendicular direction (from outer tissues to inner tissues). In the proposed ocular model, the sclera is separated into three compartments: the sclera limbus to ora serrata section (lossc), the sclera ora serrata to equator section (osesc), and the sclera equator to posterior pole section (eppsc). The ocular compartments that interact with the sclera are the tear film and the conjunctiva. Any drug that accumulates in the sclera is subjected to systemic absorption.

The change in the mass of nepafenac in the sclera compartment with time is described by Equations 11-13:

$$\frac{dM_{lossc}}{dt} = k_{tlossc}\left(\frac{M}{V} - \frac{M_{lossc}}{V_{lossc}\times K_{ptlossc}}\right) + k_{conlossc}\left(\frac{M_{con}}{V_{con}} - \frac{M_{lossc}}{V_{lossc}}\right) - k_{losscosesc}\left(\frac{M_{lossc}}{V_{lossc}} - \frac{M_{osesc}}{V_{osesc}}\right) - Q_{losscs}\left(\frac{M_{lossc}}{V_{lossc}}\right) \quad \textbf{(Eq. 11)}$$

M: Mass of nepafenac dissolved in the tear film compartment

M_{con}: Mass of nepafenac accumulated in the conjunctiva compartment

M_{lossc}: Mass of nepafenac accumulated in the sclera (limbus to ora serrata section)

M_{loscho}: Mass of nepafenac accumulated in the choroid (limbus to ora serrata section)

M_{osesc}: Mass of nepafenac accumulated in the sclera (ora serrata to equator section)

V: Volume of the tear film compartment

V_{con}: Volume of the conjunctiva compartment

V_{lossc}: Volume of the sclera (limbus to ora serrata section) compartment

V_{loscho}: Volume of the choroid (limbus to ora serrata section) compartment

V_{osesc}: Volume of the sclera (ora serrata to equator section) compartment

k_{tlossc}: Rate constant of nepafenac transport from the tear film to the sclera (limbus to ora serrata section)

$k_{conlossc}$: Rate constant of nepafenac transport from the conjunctiva compartment to the sclera (ora serrata section)

$k_{losscloscho}$: Rate constant of nepafenac transport from the sclera (limbus to ora serrata section) to the choroid (limbus to ora serrata section)

$k_{losscosesc}$: Rate constant of nepafenac transport from the sclera (limbus to ora serrata section) to the sclera (ora serrata to equator section)

$K_{ptlossc}$: Partition coefficient of nepafenac between the tear film and sclera (limbus to ora serrata section) which is the concentration in the cornea divided by the concentration in the sclera (limbus to ora serrata section)

Q_{losscs}: Rate of nepafenac systemic absorption from the sclera (limbus to ora serrata section) compartment

$$\frac{dM_{osesc}}{dt} = k_{losscosesc}\left(\frac{M_{lossc}}{V_{lossc}} - \frac{M_{osesc}}{V_{osesc}}\right) - k_{osescosecho}\left(\frac{M_{osesc}}{V_{osesc}} - \frac{M_{osecho}}{V_{osecho}}\right) - k_{osesceppsc}\left(\frac{M_{osesc}}{V_{osesc}} - \frac{M_{eppsc}}{V_{eppsc}}\right) - \left(\frac{Exp_{osesc} \times V_{max} \times \frac{M_{osesc}}{V_{osesc} \times MW_{nep}}}{K_{mi} + \frac{M_{osesc}}{V_{osesc} \times MW_{nep}}}\right) \times \frac{MW_{nep}}{1000000}$$

(**Eq. 12**)

M_{lossc}: Mass of nepafenac accumulated in the sclera (limbus to ora serrata section)

M_{osesc}: Mass of nepafenac accumulated in the sclera (ora serrata to equator section)

M_{eppsc}: Mass of nepafenac accumulated in the sclera (equator to posterior pole section)

M_{osecho}: Mass of nepafenac accumulated in the choroid (ora serrata to equator section)

V_{lossc}: Volume of the sclera (limbus to ora serrata section) compartment

V_{osesc}: Volume of the sclera (ora serrata to equator section) compartment

V_{eppsc}: Volume of the sclera (equator to posterior pole section) compartment

V_{osecho}: Volume of the choroid (ora serrata to equator section) compartment

$k_{losscosesc}$: Rate constant of nepafenac transport from the sclera (limbus to ora serrata section) to the sclera (ora serrata to equator section)

$k_{osesceppsc}$: Rate constant of nepafenac transport from the sclera (ora serrata to equator section) to the sclera (equator to posterior pole section)

$k_{osescosecho}$: Rate constant of nepafenac transport from the sclera (ora serrata to equator section) to the choroid (equator to posterior pole section)

Exp_{osesc}: Expression of amidase at the sclera (ora serrata to equator section) to the choroid (equator to posterior pole section)

$$\frac{dM_{eppsc}}{dt} = k_{osesceppsc}\left(\frac{M_{osesc}}{V_{osesc}} - \frac{M_{eppsc}}{V_{eppsc}}\right) - k_{eppsceppcho}\left(\frac{M_{eppsc}}{V_{eppsc}} - \frac{M_{eppcho}}{V_{eppcho}}\right)$$

(**Eq. 13**)

M_{osesc}: Mass of drug accumulated in the sclera (ora serrata to equator section)

M_{eppsc}: Mass of drug accumulated in the sclera (equator to posterior pole section)

M_{eppcho}: Mass of drug accumulated in the choroid (equator to posterior pole section)

V_{osesc}: Volume of the sclera (ora serrata to equator section) compartment

V_{eppsc}: Volume of the sclera (equator to posterior pole section) compartment

V_{eppcho}: Volume of the choroid (equator to posterior pole section) compartment

$k_{osesceppsc}$: Rate constant of drug transport from the sclera (ora serrata to equator section) to the sclera (equator to posterior pole section)

$k_{eppsceppcho}$: Rate constant of drug transport from the sclera (equator to posterior pole section) to the choroid (equator to posterior pole section)

The change in the mass of amfenac in the sclera compartment with time is described by Equations 14-16:

$$\frac{dMA_{lossc}}{dt} = kA_{conlossc}\left(\frac{MA_{con}}{V_{con}} - \frac{MA_{lossc}}{V_{lossc}}\right) - kA_{losscosesc}\left(\frac{MA_{lossc}}{V_{lossc}} - \frac{MA_{osesc}}{V_{osesc}}\right) - QA_{losscs}\left(\frac{MA_{lossc}}{V_{lossc}}\right)$$

(Eq. 14)

MA_{con}: Mass of amfenac accumulated in the conjunctiva compartment

MA_{lossc}: Mass of amfenac accumulated in the sclera (limbus to ora serrata section)

MA_{loscho}: Mass of amfenac accumulated in the choroid (limbus to ora serrata section)

MA_{osesc}: Mass of amfenac accumulated in the sclera (ora serrata to equator section)

V_{diss}: Volume of the tear film compartment

V_{con}: Volume of the conjunctiva compartment

V_{lossc}: Volume of the sclera (limbus to ora serrata section) compartment

V_{loscho}: Volume of the choroid (limbus to ora serrata section) compartment

V_{osesc}: Volume of the sclera (ora serrata to equator section) compartment

$kA_{conlossc}$: Rate constant of amfenac transport from the conjunctiva compartment to the sclera (ora serrata section)

$kA_{losscloscho}$: Rate constant of amfenac transport from the sclera (limbus to ora serrata section) to the choroid (limbus to ora serrata section)

$kA_{losscosesc}$: Rate constant of amfenac transport from the sclera (limbus to ora serrata section) to the sclera (ora serrata to equator section)

QA_{losscs}: Rate of amfenac systemic absorption from the sclera (limbus to ora serrata section) compartment

$$\frac{dMA_{osesc}}{dt} = \left(\frac{Exp_{osesc} \times V_{max} \times \frac{M_{osesc}}{V_{osesc} \times MW_{nep}}}{K_{mi} + \frac{M_{osesc}}{V_{osesc} \times MW_{nep}}}\right) \times \frac{MW_{amf}}{1000000} + kA_{losscosesc}\left(\frac{MA_{lossc}}{V_{lossc}} - \frac{MA_{osesc}}{V_{osesc}}\right) -$$

$$k_{Aosescosecho}\left(\frac{MA_{osesc}}{V_{osesc}} - \frac{MA_{osecho}}{V_{osecho}}\right) - kA_{osesceppsc}\left(\frac{M_{Aosesc}}{V_{osesc}} - \frac{MA_{eppsc}}{V_{eppsc}}\right)$$

(Eq. 15)

MA_{lossc}: Mass of amfenac accumulated in the sclera (limbus to ora serrata section)

MA_{osesc}: Mass of amfenac accumulated in the sclera (ora serrata to equator section)

MA_{eppsc}: Mass of amfenac accumulated in the sclera (equator to posterior pole section)

MA_{osecho}: Mass of amfenac accumulated in the choroid (ora serrata to equator section)

V_{lossc}: Volume of the sclera (limbus to ora serrata section) compartment

V_{osesc}: Volume of the sclera (ora serrata to equator section) compartment

V_{eppsc}: Volume of the sclera (equator to posterior pole section) compartment

V_{osecho}: Volume of the choroid (ora serrata to equator section) compartment

$kA_{losscosesc}$: Rate constant of amfenac transport from the sclera (limbus to ora serrata section) to the sclera (ora serrata to equator section)

$kA_{osesceppsc}$: Rate constant of amfenac transport from the sclera (ora serrata to equator section) to the sclera (equator to posterior pole section)

$kA_{osescosecho}$: Rate constant of amfenac transport from the sclera (ora serrata to equator section) to the choroid (equator to posterior pole section)

Exp_{osesc}: Expression of amidase at the sclera (ora serrata to equator section) to the choroid (equator to posterior pole section)

$$\frac{dMA_{eppsc}}{dt} = kA_{osesceppsc}\left(\frac{MA_{osesc}}{V_{osesc}} - \frac{MA_{eppsc}}{V_{eppsc}}\right) - kA_{eppsceppcho}\left(\frac{MA_{eppsc}}{V_{eppsc}} - \frac{MA_{eppcho}}{V_{eppcho}}\right)$$

(**Eq. 16**)

MA_{osesc}: Mass of amfenac accumulated in the sclera (ora serrata to equator section)

MA_{eppsc}: Mass of amfenac accumulated in the sclera (equator to posterior pole section)

MA_{eppcho}: Mass of amfenac accumulated in the choroid (equator to posterior pole section)

V_{osesc}: Volume of the sclera (ora serrata to equator section) compartment

V_{eppsc}: Volume of the sclera (equator to posterior pole section) compartment

V_{eppcho}: Volume of the choroid (equator to posterior pole section) compartment

$kA_{osesceppsc}$: Rate constant of amfenac transport from the sclera (ora serrata to equator section) to the sclera (equator to posterior pole section)

$kA_{eppsceppcho}$: Rate constant of amfenac transport from the sclera (equator to posterior pole section) to the choroid (equator to posterior pole section)

The choroid compartment

The choroid is a layer of blood vessels and connective tissue that is located between the sclera and the retina and is mainly responsible for the blood supply that provides nutrition to the innermost layer of the retina (Davson and Perkins, 2022). It expands from the ora serrata at the anterior section to the posterior pole. The choroid causes the breakdown of vessels and affects the light reflection of the retina. In addition, it produces prostaglandins and, thus, is a target site for ocular NSAIDs. The choroid is also a compartment in which the conversion of nepafenac prodrug to the active metabolite amfenac occurs (Gamache, et al., 2000). In this proposed model, the choroid is separated into two compartments: the choroid ora serrata to equator section (osecho) and the choroid equator to posterior pole section (eppcho). The ocular compartments that interact with the sclera include the aqueous humor, sclera, iris and ciliary body, and retina. Inward liquid convection exists from aqueous humor to the iris and ciliary body compartment, and the drug that accumulates in the choroid is subjected to systemic absorption.

The change in the mass of nepafenac in mass in the choroid compartment with time is described by Equations 17 -18:

$$\frac{dM_{osecho}}{dt} = k_{osescosecho}\left(\frac{M_{osesc}}{V_{osesc}} - \frac{M_{osecho}}{V_{osecho}}\right) + k_{ahosecho}\left(\frac{M_{ah}}{V_{ah}} - \frac{M_{osecho}}{V_{osecho}\times K_{pahosecho}}\right) +$$

$$k_{icbosecho}\left(\frac{M_{icb}}{V_{icb}} - \frac{M_{osecho}}{V_{osecho}}\right) - k_{osechooseret}\left(\frac{M_{osecho}}{V_{osecho}} - \frac{M_{oseret}}{V_{oseret}}\right) -$$

$$k_{osechoeppcho}\left(\frac{M_{osecho}}{V_{osecho}}-\frac{M_{eppcho}}{V_{eppcho}}\right)+Q_{ahosecho}\left(\frac{M_{ah}}{V_{ah}}\right)-Q_{osechos}\left(\frac{M_{osecho}}{V_{osecho}}\right)-$$

$$\left(\frac{Exp_{osecho}\times V_{max}\times\frac{M_{osecho}}{V_{osecho}\times MW_{nep}}}{K_{mi}+\frac{M_{osecho}}{V_{osecho}\times MW_{nep}}}\right)\times\frac{MW_{nep}}{1000000} \qquad \textbf{(Eq. 17)}$$

M_{ah}: Mass of nepafenac accumulated in the aqueous humor compartment

M_{icb}: Mass of nepafenac accumulated in the iris and ciliary body compartment

M_{osesc}: Mass of nepafenac accumulated in the sclera (ora serrata to equator section)

M_{osecho}: Mass of nepafenac accumulated in the choroid (ora serrata to equator section)

M_{eppcho}: Mass of nepafenac accumulated in the sclera (equator to posterior pole section)

M_{oseret}: Mass of nepafenac accumulated in the retina (equator to posterior pole section)

V_{ah}: Volume of the aqueous humor compartment

V_{icb}: Volume of the iris and ciliary body compartment

V_{osesc}: Volume of the sclera (ora serrata to equator section)

V_{osecho}: Volume of the choroid (ora serrata to equator section)

V_{eppcho}: Volume of the choroid (equator to posterior pole section)

V_{oseret}: Volume of the retina (ora serrata to equator section)

$k_{osescosecho}$: Rate constant of nepafenac transport from the tear film to the sclera (ora serrata to equator section) and the choroid (ora serrata to equator section)

$k_{ahosecho}$: Rate constant of nepafenac transport from the aqueous humor to the choroid (ora serrata to equator section)

$k_{icbosecho}$: Rate constant of nepafenac transport from the iris and ciliary body to the choroid (ora serrata to equator section)

$k_{osechooseret}$: Rate constant of nepafenac transport from the choroid (ora serrata to equator section) to the retina (ora serrata to equator section)

$k_{osechoeppcho}$: Rate constant of nepafenac transport from the choroid (ora serrata to equator section)

to the choroid (equator to posterior pole section)

$K_{pahosecho}$: Partition coefficient of nepafenac between the aqueous humor and the choroid (ora serrata to equator section) which is the concentration in the cornea divided by the concentration in the choroid (ora serrata to equator section)

$Q_{ahosecho}$: Rate of liquid convection from the aqueous humor to the choroid (ora serrata to equator section)

$Q_{osechos}$: Rate of nepafenac systemic absorption from the choroid (ora serrata to equator section)

V_{max}: Maximum velocity of amidase metabolism (generation of amfenac product)

K_{mi}: Nepafenac concentration at which velocity of amidase metabolism reaches half of the maximum velocity

Exp_{osecho}: Expression of amidase at the choroid (ora serrata to equator section)

$$\frac{dM_{eppcho}}{dt} = k_{eppsceppcho}\left(\frac{M_{eppsc}}{V_{eppsc}} - \frac{M_{eppcho}}{V_{eppcho}}\right) + k_{osechoeppcho}\left(\frac{M_{osecho}}{V_{osecho}} - \frac{M_{eppcho}}{V_{eppcho}}\right) - k_{eppchoeppret}\left(\frac{M_{eppcho}}{V_{eppcho}} - \frac{M_{eppret}}{V_{eppret}}\right) - Q_{eppchos}\left(\frac{M_{eppcho}}{V_{eppcho}}\right) - \left(\frac{Exp_{eppcho} \times V_{max} \times \frac{M_{eppcho}}{V_{eppcho} \times MW_{nep}}}{K_{mi} + \frac{M_{eppcho}}{V_{eppcho} \times MW_{nep}}}\right) \times \frac{MW_{nep}}{1000000} \quad \textbf{(Eq. 18)}$$

M_{eppsc}: Mass of nepafenac accumulated in the sclera (equator to posterior pole section)

M_{eppcho}: Mass of nepafenac accumulated in the choroid (equator to posterior pole section)

M_{osecho}: Mass of nepafenac accumulated in the choroid (ora serrata to equator section)

M_{eppret}: Mass of nepafenac accumulated in the retina (equator to posterior pole section)

V_{eppsc}: Volume of the sclera (equator to posterior pole section) compartment

V_{eppcho}: Volume of the choroid (equator to posterior pole section) compartment

V_{osecho}: Volume of the choroid (ora serrata to equator section) compartment

V_{eppret}: Volume of the retina (equator to posterior pole section) compartment

$Q_{eppchos}$: Rate of nepafenac systemic absorption from the choroid (equator to posterior pole section)

$k_{eppsceppcho}$: Rate constant of nepafenac transport from the sclera (equator to posterior pole section) to the choroid (equator to posterior pole section)

$k_{osechoeppcho}$: Rate constant of nepafenac transport from the choroid (ora serrata to equator section) to the choroid (equator to posterior pole section)

$k_{eppchoeppret}$: Rate constant of nepafenac transport from the choroid (equator to posterior pole section) to the retina (equator to posterior pole section)

V_{max}: Maximum velocity of amidase metabolism (generation of amfenac product)

K_{mi}: Nepafenac concentration at which velocity of amidase metabolism reaches half of the maximum velocity

Exp_{osecho}: Expression of amidase at the choroid (equator to posterior pole section)

The change in the masts of amfenac in mass in the choroid compartment with time is described by Equations 19 and 20:

$$\frac{dMA_{osecho}}{dt} = \left(\frac{Exp_{osecho} \times V_{max} \times \frac{M_{osecho}}{V_{osecho} \times MW_{nep}}}{K_{mi} + \frac{M_{osecho}}{V_{osecho} \times MW_{nep}}} \right) \times \frac{MW_{amf}}{1000000} + kA_{osescosecho} \left(\frac{MA_{osesc}}{V_{osesc}} - \frac{MA_{osecho}}{V_{osecho}} \right) + kA_{ahosecho} \left(\frac{MA_{ah}}{V_{ah}} - \frac{MA_{osecho}}{V_{osecho} \times KA_{pahosecho}} \right) + kA_{icbosecho} \left(\frac{MA_{icb}}{V_{icb}} - \frac{MA_{osecho}}{V_{osecho}} \right) - kA_{osechooseret} \left(\frac{MA_{osecho}}{V_{osecho}} - \frac{MA_{oseret}}{V_{oseret}} \right) - kA_{osechoeppcho} \left(\frac{MA_{osecho}}{V_{osecho}} - \frac{MA_{eppcho}}{V_{eppcho}} \right) + Q_{ahosecho} \left(\frac{MA_{ah}}{V_{ah}} \right) - QA_{osechos} \left(\frac{MA_{osecho}}{V_{osecho}} \right) \quad \textbf{(Eq. 19)}$$

MA_{ah}: Mass of amfenac accumulated in the aqueous humor compartment

MA_{icb}: Mass of amfenac accumulated in the iris and ciliary body compartment

MA_{osesc}: Mass of amfenac accumulated in the sclera (ora serrata to equator section)

MA_{osecho}: Mass of amfenac accumulated in the choroid (ora serrata to equator section)

MA_{eppcho}: Mass of amfenac accumulated in the sclera (equator to posterior pole section)

MA_{oseret}: Mass of amfenac accumulated in the retina (equator to posterior pole section)

V_{ah}: Volume of the aqueous humor compartment

V_{icb}: Volume of the iris and ciliary body compartment

V_{osesc}: Volume of the sclera (ora serrata to equator section)

V_{osecho}: Volume of the choroid (ora serrata to equator section)

V_{eppcho}: Volume of the choroid (equator to posterior pole section)

V_{oseret}: Volume of the retina (ora serrata to equator section)

$kA_{osescosecho}$: Rate constant of amfenac transport from the tear film to the sclera (ora serrata to equator section) and the choroid (ora serrata to equator section)

$kA_{ahosecho}$: Rate constant of amfenac transport from the aqueous humor to the choroid (ora serrata to equator section)

$kA_{icbosecho}$: Rate constant of amfenac transport from the iris and ciliary body to the choroid (ora serrata to equator section)

$kA_{osechooseret}$: Rate constant of amfenac transport from the choroid (ora serrata to equator section) to the retina (ora serrata to equator section)

$kA_{osechoeppcho}$: Rate constant of amfenac transport from the choroid (ora serrata to equator section) to the choroid (equator to posterior pole section)

$KA_{pahosecho}$: Partition coefficient of amfenac between the aqueous humor and the choroid (ora serrata to equator section) which is the concentration in the cornea divided by the concentration in the choroid (ora serrata to equator section)

$Q_{ahosecho}$: Rate of liquid convection from the aqueous humor to the choroid (ora serrata to equator section)

$QA_{osechos}$: Rate of amfenac systemic absorption from the choroid (ora serrata to equator section)

V_{max}: Maximum velocity of amidase metabolism (generation of amfenac product)

K_{mi}: Nepafenac concentration at which velocity of amidase metabolism reaches half of the maximum velocity

Exp_{osecho}: Expression of amidase at the choroid (ora serrata to equator section)

$$\frac{dMA_{eppcho}}{dt} = \left(\frac{Exp_{eppcho} \times V_{max} \times \frac{M_{eppcho}}{V_{eppcho} \times MW_{nep}}}{K_{mi} + \frac{M_{eppcho}}{V_{eppcho} \times MW_{nep}}} \right) \times \frac{MW_{amf}}{1000000} + kA_{eppsceppcho} \left(\frac{MA_{eppsc}}{V_{eppsc}} - \frac{MA_{eppcho}}{V_{eppcho}} \right) + kA_{osechoeppcho} \left(\frac{MA_{osecho}}{V_{osecho}} - \frac{MA_{eppcho}}{V_{eppcho}} \right) - kA_{eppchoeppret} \left(\frac{MA_{eppcho}}{V_{eppcho}} - \frac{MA_{eppret}}{V_{eppret}} \right) - QA_{eppchos} \left(\frac{MA_{eppcho}}{V_{eppcho}} \right)$$ **(Eq. 20)**

MA_{eppsc}: Mass of amfenac accumulated in the sclera (equator to posterior pole section)

MA_{eppcho}: Mass of amfenac accumulated in the choroid (equator to posterior pole section)

MA_{osecho}: Mass of amfenac accumulated in the choroid (ora serrata to equator section)

MA_{eppret}: Mass of amfenac accumulated in the retina (equator to posterior pole section)

V_{eppsc}: Volume of the sclera (equator to posterior pole section) compartment

V_{eppcho}: Volume of the choroid (equator to posterior pole section) compartment

V_{osecho}: Volume of the choroid (ora serrata to equator section) compartment

V_{eppret}: Volume of the retina (equator to posterior pole section) compartment

$QA_{eppchos}$: Rate of amfenac systemic absorption from the choroid (equator to posterior pole section)

$kA_{eppsceppcho}$: Rate constant of amfenac transport from the sclera (equator to posterior pole section) to the choroid (equator to posterior pole section)

$kA_{osechoeppcho}$: Rate constant of amfenac transport from the choroid (ora serrata to equator section) to the choroid (equator to posterior pole section)

$kA_{eppchoeppret}$: Rate constant of amfenac transport from the choroid (equator to posterior pole section) to the retina (equator to posterior pole section)

V_{max}: Maximum velocity of amidase metabolism (generation of amfenac product)

K_{mi}: Nepafenac concentration at which velocity of amidase metabolism reaches half of the maximum velocity

Exp_{osecho}: Expression of amidase at the choroid (equator to posterior pole section)

The retina compartment

The retina is the innermost layer of the eye that receives light and converts it into signals that are sent to the optic nerves. There is a monolayer of pigmented cells located at the outmost part of the retina is called retinal pigmented epithelium (RPE), which plays an important role in maintaining visual function (Yang et al., 2021). The RPE cells form tight junctions and act as the outer part of the blood-retinal barrier (BRB) which regulate the movement of solutes and nutrients from the choroid to the sub-retinal space (Campbell and Humphries, 2012). In contrast, the inner part of the blood-retinal barrier (BRB) is in the inner retinal microvasculature that mediates the highly selective diffusion of molecules from the blood to the retina (Campbell and Humphries, 2012). The retina expands from the ora serrata at the anterior section to the posterior pole and is the major posterior therapeutic site of ocular NSAIDs for the treatment of ocular inflammation associated with cataract surgery. Studies have shown that the retina is also responsible for the conversion of nepafenac prodrug to the active metabolite amfenac (Gamache, et al., 2000). In the proposed ocular PBPK model, the retina is separated into two compartments: the retina ora serrata to equator section (oseret) and the retina equator to posterior pole section (eppret). The ocular compartments that interact with the sclera include the choroid and the vitreous humor. Any drug that is accumulated in the choroid is subjected to systemic absorption.

The change of nepafenac mass with time in the retina compartment is described by equations 21-22:

$$\frac{dM_{oseret}}{dt} = k_{osechooseret}\left(\frac{M_{osecho}}{V_{osecho}} - \frac{M_{oseret}}{V_{oseret}}\right) - k_{oseretvh}\left(\frac{M_{oseret}}{V_{oseret}\times K_{poseretvh}} - \frac{M_{vh}}{V_{vh}}\right) - k_{osereteppret}\left(\frac{M_{oseret}}{V_{oseret}} - \frac{M_{eppret}}{V_{eppret}}\right) - Q_{oserets}\left(\frac{M_{oseret}}{V_{oseret}}\right) - \left(\frac{Exp_{oseret}\times V_{max}\times\frac{M_{oseret}}{V_{oseret}\times MW_{nep}}}{K_{mi}+\frac{M_{oseret}}{V_{oseret}\times MW_{nep}}}\right)\times\frac{MW_{nep}}{1000000}$$ (**Eq. 21**)

M_{osecho}: Mass of nepafenac accumulated in the choroid (ora serrata to equator section)

M_{oseret}: Mass of nepafenac accumulated in the retina (ora serrata to equator section)

M_{eppret}: Mass of nepafenac accumulated in the retina (equator to posterior pole section)

M_{vh}: Mass of nepafenac accumulated in the vitreous humor compartment

V_{osecho}: Volume of the choroid (ora serrata to equator section) compartment

V_{oseret}: Volume of the retina (ora serrata to equator section) compartment

V_{eppret}: Volume of the retina (equator to posterior pole section) compartment

V_{vh}: Volume of the vitreous humor compartment

$k_{osechooseret}$: Rate constant of nepafenac transport from the choroid ora serrata to equator section) to the retina (ora serrata to equator section)

$k_{osereteppret}$: Rate constant of nepafenac transport from the retina (ora serrata to equator section) to the retina (equator to posterior pole section)

$k_{oseretvh}$: Rate constant of nepafenac transport from the retina (ora serrata to equator section) to the vitreous humor

$K_{poseretvh}$: Partition coefficient of nepafenac between the retina (ora serrata to equator section) and the vitreous humor which is concentration in the retina (ora serrata to equator section) divided by the concentration in the vitreous humor

$Q_{oserets}$: Rate of nepafenac systemic absorption from the retina (ora serrata to equator section)

V_{max}: Maximum velocity of amidase metabolism (generation of amfenac product)

K_{mi}: Nepafenac concentration at which velocity of amidase metabolism reaches half of the maximum velocity

Exp_{oseret}: Expression of amidase at the retina (ora serrata to equator section)

$$\frac{dM_{eppret}}{dt} = k_{eppchoeppret}\left(\frac{M_{eppcho}}{V_{eppcho}} - \frac{M_{eppret}}{V_{eppret}}\right) + k_{oseretteppret}\left(\frac{M_{oseret}}{V_{oseret}} - \frac{M_{eppret}}{V_{eppret}}\right) - k_{eppretvh}\left(\frac{M_{eppret}}{V_{eppret}\times K_{peppretvh}} - \frac{M_{vh}}{V_{vh}}\right) - Q_{epprets}\left(\frac{M_{eppret}}{V_{eppret}}\right) - \left(\frac{Exp_{eppret}\times V_{max}\times\frac{M_{eppret}}{V_{eppret}\times MW_{nep}}}{K_{mi}+\frac{M_{eppret}}{V_{eppret}\times MW_{nep}}}\right)\times\frac{MW_{nep}}{1000000} \quad \textbf{(Eq. 22)}$$

M_{eppcho}: Mass of nepafenac accumulated in the choroid (equator to posterior pole section)

M_{oseret}: Mass of nepafenac accumulated in the retina (ora serrata to equator section)

M_{eppret}: Mass of nepafenac accumulated in the retina (equator to posterior pole section)

M_{vh}: Mass of nepafenac accumulated in the vitreous humor compartment

V_{eppcho}: Volume of the choroid (equator to posterior pole section) compartment

V_{oseret}: Volume of the retina (ora serrata to equator section) compartment

V_{eppret}: Volume of the retina (equator to posterior pole section) compartment

V_{vh}: Volume of the vitreous humor compartment

$k_{eppchoeppret}$: Rate constant of nepafenac transport from the choroid (equator to posterior pole section) to the retina (ora serrata to equator section)

$k_{oseretteppret}$: Rate constant of nepafenac transport from the retina (ora serrata to equator section) to the retina (equator to posterior pole section)

$k_{eppretvh}$: Rate constant of nepafenac transport from the retina (equator to posterior pole section) to the vitreous humor

$K_{peppretvh}$: Partition coefficient of nepafenac between the retina (equator to posterior pole section) and the vitreous humor which is concentration in the retina

(equator to posterior pole section) divided by the concentration in the vitreous humor

$Q_{epprets}$: Rate of nepafenac systemic absorption from the retina (equator to posterior pole section)

V_{max}: Maximum velocity of amidase metabolism (generation of amfenac product)

K_{mi}: Nepafenac concentration at which velocity of amidase metabolism reaches half of the maximum velocity

Exp_{eppret}: Expression of amidase at the retina (equator to posterior pole section)

The change of amfenac mass in the retina compartment with time is described by equations 23-24:

$$\frac{dMA_{oseret}}{dt} = \left(\frac{Exp_{oseret} \times V_{max} \times \frac{M_{oseret}}{V_{oseret} \times MW_{nep}}}{K_{mi} + \frac{M_{oseret}}{V_{oseret} \times MW_{nep}}} \right) \times \frac{MW_{amf}}{1000000} + kA_{osechooseret} \left(\frac{MA_{osecho}}{V_{osecho}} - \frac{MA_{oseret}}{V_{oseret}} \right)$$

$$- kA_{oseretvh} \left(\frac{MA_{oseret}}{V_{oseret} \times KA_{poseretvh}} - \frac{MA_{vh}}{V_{vh}} \right) - kA_{oseretteppret} \left(\frac{MA_{oseret}}{V_{oseret}} - \frac{MA_{eppret}}{V_{eppret}} \right) - QA_{oserets} \left(\frac{MA_{oseret}}{V_{oseret}} \right)$$

(Eq. 23)

MA_{osecho}: Mass of amfenac accumulated in the choroid (ora serrata to equator section)

MA_{oseret}: Mass of amfenac accumulated in the retina (ora serrata to equator section)

MA_{eppret}: Mass of amfenac accumulated in the retina (equator to posterior pole section)

MA_{vh}: Mass of amfenac accumulated in the vitreous humor compartment

V_{osecho}: Volume of the choroid (ora serrata to equator section) compartment

V_{oseret}: Volume of the retina (ora serrata to equator section) compartment

V_{eppret}: Volume of the retina (equator to posterior pole section) compartment

V_{vh}: Volume of the vitreous humor compartment

$kA_{osechooseret}$: Rate constant of amfenac transport from the choroid ora serrata to equator section) to the retina (ora serrata to equator section)

$kA_{oseretteppret}$: Rate constant of amfenac transport from the retina (ora serrata to equator section) to the retina (equator to posterior pole section)

$kA_{oseretvh}$: Rate constant of amfenac transport from the retina (ora serrata to equator section) to the vitreous humor

$KA_{poseretvh}$: Partition coefficient of amfenac between the retina (ora serrata to equator section) and the vitreous humor which is concentration in the retina (ora serrata to equator section) divided by the concentration in the vitreous humor

$QA_{oserets}$: Rate of amfenac systemic absorption from the retina (ora serrata to equator section)

V_{max}: Maximum velocity of amidase metabolism (generation of amfenac product)

K_{mi}: Nepafenac concentration at which velocity of amidase metabolism reaches half of the maximum velocity

Exp_{oseret}: Expression of amidase at the retina (ora serrata to equator section)

$$\frac{dMA_{eppret}}{dt} = \left(\frac{Exp_{eppret} \times V_{max} \times \frac{M_{eppret}}{V_{eppret} \times MW_{nep}}}{K_{mi} + \frac{M_{eppret}}{V_{eppret} \times MW_{nep}}}\right) \times \frac{MW_{amf}}{1000000} + kA_{eppchoeppret}\left(\frac{MA_{eppcho}}{V_{eppcho}} - \frac{MA_{eppret}}{V_{eppret}}\right) +$$

$$kA_{oseretteppret}\left(\frac{MA_{oseret}}{V_{oseret}} - \frac{MA_{eppret}}{V_{eppret}}\right) - kA_{eppretvh}\left(\frac{MA_{eppret}}{V_{eppret} \times KA_{peppretvh}} - \frac{MA_{vh}}{V_{vh}}\right) - QA_{epprets}\left(\frac{MA_{eppret}}{V_{eppret}}\right)$$

(**Eq. 24**)

MA_{eppcho}: Mass of amfenac accumulated in the choroid (equator to posterior pole section)

MA_{oseret}: Mass of amfenac accumulated in the retina (ora serrata to equator section)

MA_{eppret}: Mass of amfenac accumulated in the retina (equator to posterior pole section)

MA_{vh}: Mass of amfenac accumulated in the vitreous humor compartment

V_{eppcho}: Volume of the choroid (equator to posterior pole section) compartment

V_{oseret}: Volume of the retina (ora serrata to equator section) compartment

V_{eppret}: Volume of the retina (equator to posterior pole section) compartment

V_{vh}: Volume of the vitreous humor compartment

$kA_{eppchoeppret}$: Rate constant of amfenac transport from the choroid (equator to posterior pole section) to the retina (ora serrata to equator section)

$kA_{oseretteppret}$: Rate constant of amfenac transport from the retina (ora serrata to equator section) to the retina (equator to posterior pole section)

$kA_{eppretvh}$: Rate constant of amfenac transport from the retina (equator to posterior pole section) to the vitreous humor

$KA_{peppretvh}$: Partition coefficient of amfenac between the retina (equator to posterior pole section) and the vitreous humor which is concentration in the retina (equator to posterior pole section) divided by the concentration in the vitreous humor

$QA_{epprets}$: Rate of amfenac systemic absorption from the retina (equator to posterior pole section)

V_{max}: Maximum velocity of amidase metabolism (generation of amfenac product)

K_{mi}: Nepafenac concentration at which velocity of amidase metabolism reaches half of the maximum velocity

Exp_{eppret}: Expression of amidase at the retina (equator to posterior pole section)

The vitreous humor compartment

The vitreous humor is a semisolid gel structure that contains similar collagen to those of the cornea but a different percentage of water. It fills most of the space of the posterior section of the eye and helps to keep the underlying retina pressed against the choroid (Davson and Perkins., 2022). The vitreous humor is separated from the aqueous humor by the lens and ciliary body. The ocular compartments that interact with the vitreous humor are the aqueous humor, iris and ciliary body, and the retina (ore serrata to equator section and equator to posterior pole section). An inward liquid convection exists from the iris and ciliary body to vitreous humor and an outward liquid convection exists from the vitreous humor to the aqueous humor.

The change of nepafenac mass with time in the vitreous humor compartment is described by equation 25:

$$\frac{dM_{vh}}{dt} = k_{ahvh}\left(\frac{M_{ah}}{V_{ah}} - \frac{M_{vh}}{V_{vh}}\right) + k_{oseretvh}\left(\frac{M_{oseret}}{V_{oseret}\times K_{poseretvh}} - \frac{M_{vh}}{V_{vh}}\right) + k_{eppretvh}\left(\frac{M_{eppret}}{V_{eppret}\times K_{peppretvh}} - \frac{M_{vh}}{V_{vh}}\right) + k_{icbvh}\left(\frac{M_{icb}}{V_{icb}\times K_{pvhicb}} - \frac{M_{vh}}{V_{vh}}\right) - Q_{vhah}\left(\frac{M_{vh}}{V_{vh}}\right)$$

(**Eq. 25**)

M_{oseret}: Mass of nepafenac accumulated in the retina (ora serrata to equator section)

M_{eppret}: Mass of nepafenac accumulated in the retina (equator to posterior pole section)

M_{ah}: Mass of nepafenac accumulated in the aqueous humor compartment

M_{vh}: Mass of nepafenac accumulated in the vitreous humor compartment

M_{icb}: Mass of nepafenac accumulated in the iris and ciliary body compartment

V_{oseret}: Volume of the retina (ora serrata to equator section) compartment

V_{eppret}: Volume of the retina (equator to posterior pole section) compartment

V_{ah}: Volume of the aqueous humor compartment

V_{vh}: Volume of the vitreous humor compartment

V_{icb}: Volume of the iris and ciliary body compartment

k_{ahvh}: Rate constant of nepafenac transport from the aqueous humor to the vitreous humor

k_{icbvh}: Rate constant of nepafenac transport from the iris and ciliary to the vitreous humor

$k_{oseretvh}$: Rate constant of nepafenac transport from the retina (ora serrata to equator section) to the vitreous humor

$k_{eppretvh}$: Rate constant of nepafenac transport from the retina (equator to posterior pole section) to the vitreous humor

K_{picbvh}: Partition coefficient of nepafenac between the iris and ciliary body and the vitreous humor (concentration in iris and ciliary body divided by the concentration in the vitreous humor)

$K_{poseretvh}$: Partition coefficient of nepafenac between the retina (ora serrata to equator section) and the vitreous humor which is concentration in the retina (ora serrata to equator section) divided by the concentration in the vitreous humor

$K_{peppretvh}$: Partition coefficient of nepafenac between the retina (equator to posterior pole section) and the vitreous humor which is concentration in the retina (equator to posterior pole section) divided by the concentration in the vitreous humor

Q_{icbvh}: Rate of liquid convection from the iris and ciliary body to the vitreous humor

Q_{vhah}: Rate of liquid convection from the vitreous humor to the aqueous humor

The change of amfenac mass with time in the vitreous humor compartment is described by equation 26:

$$\frac{dMA_{vh}}{dt} = kA_{ahvh}\left(\frac{MA_{ah}}{V_{ah}} - \frac{MA_{vh}}{V_{vh}}\right) + kA_{oseretvh}\left(\frac{MA_{oseret}}{V_{oseret}\times KA_{poseretvh}} - \frac{MA_{vh}}{V_{vh}}\right) + kA_{eppretvh}\left(\frac{MA_{eppret}}{V_{eppret}\times KA_{peppretvh}} - \frac{MA_{vh}}{V_{vh}}\right) + kA_{icbvh}\left(\frac{MA_{icb}}{V_{icb}\times KA_{pvhicb}} - \frac{MA_{vh}}{V_{vh}}\right) - Q_{vhah}\left(\frac{MA_{vh}}{V_{vh}}\right)$$

(**Eq. 26**)

MA_{oseret}: Mass of amfenac accumulated in the retina (ora serrata to equator section)

MA_{eppret}: Mass of amfenac accumulated in the retina (equator to posterior pole section)

MA_{ah}: Mass of amfenac accumulated in the aqueous humor compartment

MA_{vh}: Mass of amfenac accumulated in the vitreous humor compartment

MA_{icb}: Mass of amfenac accumulated in the iris and ciliary body compartment

V_{oseret}: Volume of the retina (ora serrata to equator section) compartment

V_{eppret}: Volume of the retina (equator to posterior pole section) compartment

V_{ah}: Volume of the aqueous humor compartment

V_{vh}: Volume of the vitreous humor compartment

V_{icb}: Volume of the iris and ciliary body compartment

kA_{ahvh}: Rate constant of amfenac transport from the aqueous humor to the vitreous humor

kA_{icbvh}: Rate constant of amfenac transport from the iris and ciliary to the vitreous humor

$kA_{oseretvh}$: Rate constant of amfenac transport from the retina (ora serrata to equator section) to the vitreous humor

$kA_{eppretvh}$: Rate constant of amfenac transport from the retina (equator to posterior pole section) to the vitreous humor

K_{picbvh}: Partition coefficient of nepafenac between the iris and ciliary body and the vitreous humor (concentration in iris and ciliary body divided by the concentration in the vitreous humor)

$KA_{poseretvh}$: Partition coefficient of amfenac between the retina (ora serrata to equator section) and the vitreous humor which is concentration in the retina (ora serrata to equator section) divided by the concentration in the vitreous humor

$KA_{peppretvh}$: Partition coefficient of amfenac between the retina (equator to posterior pole section) and the vitreous humor which is concentration in the retina (equator to posterior pole section) divided by the concentration in the vitreous humor

Q_{icbvh}: Rate of liquid convection from the iris and ciliary body to the vitreous humor

Q_{vhah}: Rate of liquid convection from the vitreous humor to the aqueous humor

The systemic circulation compartment

Drugs that accumulate in vascularized ocular tissue compartments are subjected to systemic absorption. However, given that the systemic circulation compartment is not a therapeutic site of topically applied nepafenac suspension, systemic exposure of the drug is not of interest to the proposed model.

4.3 The precorneal component of the PBPK model

4.3.1 Overview of equations and parameters in the precorneal model

The pre-corneal model describes the drug-tear interaction that happens immediately after the drug is applied on the ocular surface and ends when the volume of the tear film drops back to that of the steady status. The drug-tear interaction includes four major dynamic processes undergoing on the ocular surface: dissolution of solid drug particles in the suspension; dilution of the drug caused by the tear flow; drainage of the drug to the nasal-lacrimal duct and drug absorption through the cornea, the conjunctiva and the sclera (limbus to ora serrata section).

In vivo drug dissolution rate can be described by either modification of the Hixon-Crowell equation (assuming spherical drug particles and uniformly distributed particles size) or *in vitro* drug dissolution data obtained from the pulsatile microdialysis (PMD) based drug releasing test. It is important to notify that the Hixon-Crowell equation can only help with the theoretical drug dissolution process based on standard surface area calculated by hypothetical particle size (this value can be further verified by testing the particle size distribution of both NEVANAC® and ILEVRO®) while crucial effect results from the existence of potential solubilizer and initial drug distribution in the oil/water phase (or bound with polymer) of the formulations can only be accurately reflected by the *in vitro* drug dissolution data.

The volume of the precorneal compartment (dependent on the tear film) drops from the maximum loading capacity of the conjunctival sac (40 μL) to the physiological volume of the tear film at steady status (7 μL), assuming that any liquid overfilled during the drug-

tear interaction process will spill out of the eye. The constant tear production rate is programmed to equal the sum of the zero-order tear evaporation and the base tear drainage (when no formulation is present in the eye) assuming that the volume of the tear film is consistent without turbulence. The transient drainage rate is modeled as declining in a first-order manner from a maximum (immediately after instilling a drop) to zero (signifying a return to the base drainage rate) during the resident period of the drug (dependent on the viscosity of the formulation).

The model assumes rates for tear production, tear evaporation, a base rate of drainage (when no formulation is present in the eye), and a transient drainage rate that reflects the extra drainage and runoff in the minutes after a drop is administered. The loss of the nepafenac from the precorneal compartment caused by the drainage is counted for both nepafenac that is dissolved (in the tears and aqueous phase of the formulation) and undissolved (as particles).

The change in the mass of undissolved nepafenac in the precorneal compartment with time is described by Equation 27:

$$\frac{dM_{pct}}{dt} = -k_{Dpc}\left(\frac{M_{pct}}{\frac{Dose}{2} - 33 \times C_s}\right) \times V \times \left(C_s - \frac{M}{\mathrm{V}}\right) - k_{pc}\left(\frac{M_{pct}}{\mathrm{V}}\right)$$

(**Eq. 27**)

M_{pct}: Total mass of nepafenac undissolved (over all particles)

M: Total mass of nepafenac dissolved in the precorneal compartment

k_{Dpc}: First-order rate constant of nepafenac particles dissolution

k_{pc}: First-order rate constant of nepafenac particle reduction caused by the drainage

V: Total volume of the pre-cornea compartment

C_s: Water solubility of nepafenac

Dose: 33µg for NEVANAC® 0.1% suspension and 99µg for ILEVRO® 0.3% suspension

The initial value of the total mass of the undissolved nepafenac is calculated from the dose and the initial concentration of nepafenac dissolved in the aqueous phase is set to the drug solubility in water. The initial value of the number of particles is calculated by the total mass of the undissolved nepafenac, the density of drug particles, the radius of each drug particle (assuming a uniform particle size for the first model), and the particle surface area is calculated by the r radius of each drug particle. The compartments that interact with tear film are the chemical drug depot, corneal, conjunctiva, and sclera (limbus to ora serrata section). The changes in the total mass of the undissolved nepafenac and the number of nepafenac particles in the tear film compartment are described by Eq. 28:

$$\frac{dM}{dt} = k_{Dpc}\left(\frac{M_{pct}}{\frac{Dose}{2} - 33\times C_s}\right) \times V \times \left(C_s - \frac{M}{\mathrm{V}}\right) - k_{td}\left(\frac{M}{\mathrm{V}} - \frac{M_d}{V_d \times K_{pdt}}\right) - k_{tc}\left(\frac{M_{diss}}{V_t} - \frac{M_c}{V_c \times K_{ptc}}\right) -$$

$$k_{tcon}\left(\frac{M}{\mathrm{V}} - \frac{M_{con}}{V_{con}\times K_{ptcon}}\right) - k_{tlossc}\left(\frac{M}{\mathrm{V}} - \frac{M_{lossc}}{V_{lossc}\times K_{ptlossc}}\right) - Q_{out}\left(\frac{M}{\mathrm{V}}\right) \quad \textbf{(Eq. 28)}$$

Here, Q_{out} is the rate of tear drainage (µL/min)at which the tear layer drains from the precorneal region, and the tear layer volume V is the total of the steady state tear volume plus any administered formulation volume that has not cleared out of the ocular region. These are given by Eq. 29 and 30 as

$$Q_{out} = Q_{tf} + 33\alpha\, e^{-at} \quad \textbf{(Eq. 29)}$$

$$V = 7 + 33\, e^{-at} \quad \textbf{(Eq. 30)}$$

M_{pct}: Total mass of nepafenac undissolved (over all particles)

M: Total mass of nepafenac dissolved in the tear film compartment

M_d: Total mass of nepafenac in the chemical depot compartment

M_c: Total mass of nepafenac in the cornea compartment

M_{con}: Total mass of nepafenac in the conjunctiva compartment

M_{lossc} : Total mass of nepafenac in the sclera (limbus to ora serrata section) compartment

V: Total volume of the tear film compartment

V_d: Total volume of the chemical drug depot compartment

V_c: Total volume of the cornea compartment

V_{con}: Total volume of the conjunctiva compartment

V_{lossc}: Total volume of the sclera (limbus to ora serrata section) compartment

k_D: First-order rate constant of nepafenac dissolution

k_{td}: Rate constant of nepafenac transport from tear film to the chemical depot

k_{tc}: Rate constant of nepafenac transport from the tear film to the cornea

k_{tcon}: Rate constant of nepafenac transport from the tear film to the conjunctiva

k_{tlossc}: Rate constant of nepafenac transport from the tear film to the sclera (limbus to ora serrata section)

K_{pdt}: Partition coefficient of nepafenac between the chemical drug depot and the tear film (solubility in the chemical drug depot divided by the solubility in the tear layer)

K_{ptc}: Partition coefficient of nepafenac between tear film and the chemical depot (concentration in the tear film divided by the concentration in the cornea)

K_{ptcon}: Partition coefficient of nepafenac between the tear film and the conjunctiva (concentration in the tear film divided by the concentration in the conjunctiva)

$K_{ptlossc}$: Partition coefficient of nepafenac between the tear film and the sclera (limbus to ora serrata section) which is the concentration in the tear film divided by the concentration in the sclera (limbus to ora serrata section)

Q_{out}: Total tear drainage rate, which is the sum of a base rate plus a transient rate

Q_{tf} : Tear base tear drainage rate (just before and sufficiently long time after administering a drop)

C_s: Water solubility of nepafenac

t: Time after drug administration

Dose: 33µg for NEVANAC® 0.1% suspension and 99µg for ILEVRO® 0.3% suspension

Change in the tear film compartment volume is described by Equation 30:

$$\frac{dV}{dt} = Q_{tf} - (Q_{out} + Q_{ev}) \quad \textbf{(Eq. 30)}$$

V: Total volume of the tear film

Q_{out}: Total tear drainage rate, which is the sum of a base rate plus a transient rate

Q_{tf} : Tear base tear drainage rate (just before and sufficiently long time after administering a drop)

Q_{ev}: Tear evaporation rate

Change in the mass of nepafenac in mass with time in the chemical depot compartment with time is described by Equation 31:

$$\frac{dM_d}{dt} = k_{td}\left(\frac{M}{V} - \frac{M_d}{V_d \times K_{pdt}}\right) \quad \textbf{(Eq. 31)}$$

M: Total mass of nepafenac dissolved in the tear film compartment

M_d: Total mass of the nepafenac in the chemical depot compartment

V: Total volume of the tear film compartment

V_d: Total volume of the chemical drug depot compartment

k_{td}: Rate constant of nepafenac transport from the chemical drug depot to tear film

K_{pdt}: Partition coefficient of nepafenac between the chemical drug depot and the tear film (concentration in the chemical drug depot divided by the concentration in the tear film)

C_s: Water solubility of nepafenac

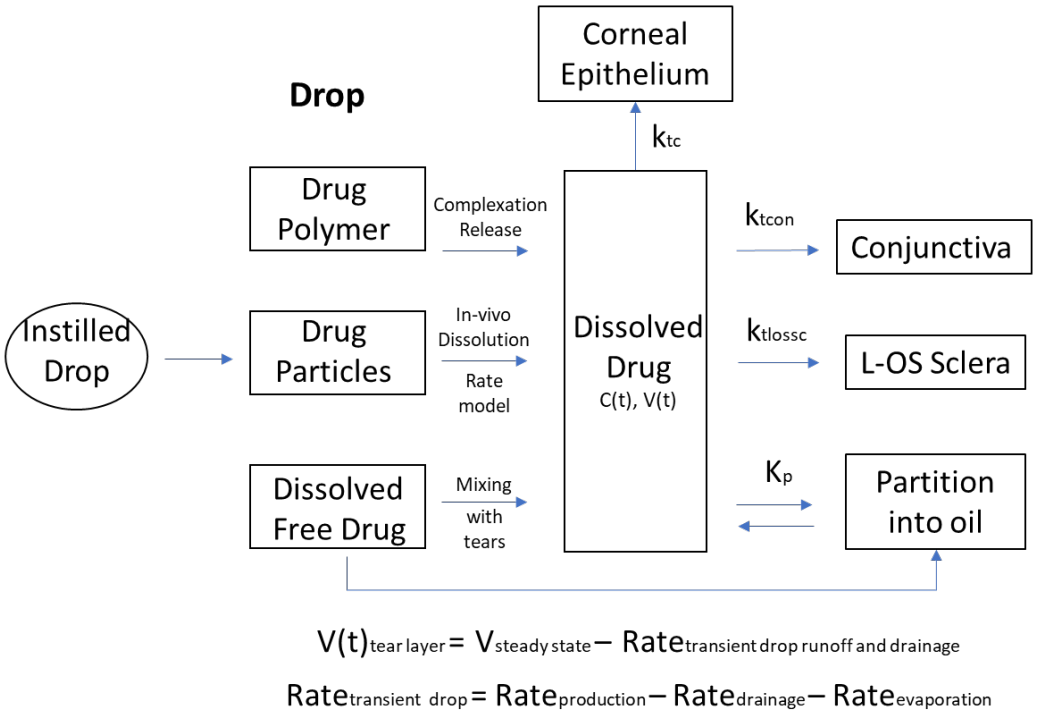

Figure 4-3. Diagram of the precorneal compartment.

4.4 In vitro data as input for the PBPK model

4.4.1 Brief description of PMD

Microdialysis has been applied as a standard method for *in vivo* analysis of drug concentration. The original setup (referred to as CFMD) utilizes a probe comprising a permeable section of porous tubing (the probe window) that is connected to two segments of impermeable tubing, serving as an inlet and an outlet. A schematic diagram of a is shown in Figure 4-4.

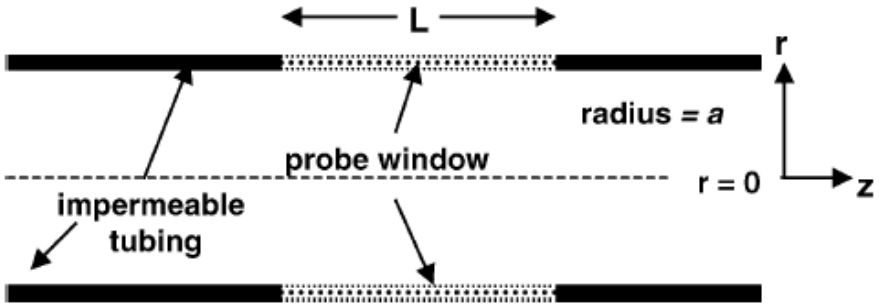

Figure 4-4. Schematic diagram of a microdialysis probe.

The inlet tubing is connected to a syringe pump that feeds a flowing liquid (the dialysate) through the probe window at a known constant flow rate and the outlet feeds into a vial for sample collection. The probe setup is immersed in a larger volume containing the drug (the donor medium), and the dialysate initially contains no drug. As the dialysate passes through the probe window, it accumulates drug molecules that diffuse through the window membrane pores in a manner that depends on the flow rate, the geometry of the probe window (length and volume), the drug concentration in the donor medium, and the composition of the donor medium and dialysate.

Pulsatile microdialysis (PMD) is a sampling method that utilized the CFMD setup, but with varying flow rates so each sample collected is the result of collection at a different flow pattern. In this method, the dialysate is pumped through the probe window at a high flow rate (flush rate), subsequently allowed to stop and rest at the window for a short period (the resting time), and then flushed out at the same flush rate and collect for assay. A sufficient amount of dialysate is flushed after resting so all of the dialysate that was at rest in the window is collected as part of the sample. The flush rate is chosen to be fast

enough so the elements of dialysate flowing through the window without resting spend very little time in the window and accumulate little drug, so the great majority of the drug in a PMD sample is accumulated by the portion of the dialysate that was allowed to reside at rest in the probe window (Kabir et al., 2004).

4.4.2 Data obtained from PMD experiments

PMD was used for two *in vitro* characterizations. 1) Measure the nepafenac distribution in the suspension, specifically evaluating the mass of nepafenac that is initially dissolved in the aqueous phase. Existing dissolution models have assumed that the concentration of the drug dissolved in the aqueous phase of a suspension formulation is equal to its solubility (Le Merdy et al., 2019), but this may not be true due to the presence of excipients and other formulation-specific factors. 2) Perform *in vitro* release tests (IVRTs) to measure the rate at which nepafenac shifts into the aqueous phase as its dissolved form (its dissolution and release) caused by events occurring in the ocular region, including dilution by tears, drug absorption, and drug partitioning into the chemical depot. The PMD measurements were done using non-sink (low-volume) receiver conditions, making them more biorelevant than previous experimental methods (Lu et al., 1993)

These *in vitro* characterization data were used to model the *in vivo* nepafenac dissolution and release in the PBPK model. Only the drug that is dissolved in the aqueous phase can be absorbed by ocular tissues of partition into chemical depts, so the initial drug distribution and subsequent dissolution from undissolved particles or release from the bound state in possible drug-excipient complexes critically impact the drug absorption *in*

vivo. The *in vivo* dissolution/release component of the PBPK model was based on PMD IVRT data, which was the most physiologically relevant *in vitro* data available, to describe dissolution/release into non-sink, low volume, thin layer receivers with limited agitation and tear exchange.

NEVANAC® and ILEVRO® undiluted formulations as well as various dilutions with artificial tears were used for PMD-based IVRTs to determine the drug dissolution/release profiles. Samples were collected for quantitative analysis at different time points for a period that is longer than the anticipated ocular residence time of the formulation (for instance, 20 minutes). The *in vitro* data reflected different formulation properties, including viscosity, the initial drug distribution in the aqueous phase, and potential drug-polymer interaction together with their effect on the nepafenac dissolution and release data during the ocular residence time, and were used to model *in vivo* dissolution and release.

The initial drug distribution in the formulations during storage, specifically to assess the fraction of the nepafenac that is dissolved and free vs. in suspended, undissolved particles or bound to excipients in the formulations, is important given the insight of ocular suspension manufacturing: whether the dose or the initial aqueous concentration is the determining factor to determine the ocular bioavailability of nepafenac.

4.4.4 Analysis of PMD data for the fraction of nepafenac initially dissolved in the aqueous phase and for nepafenac dissolution

Summary of Physical Pharmaceutica LLC data

Using in-house proprietary probes, PMD was performed on an aqueous nepafenac solution (18.17 μ/mL) at 23 °C. The PMD used a proprietary modification of the method reported by Bellantone (2012) using a flow rate of 20 μL/min.

The data are shown in Figure 4-5 for F_R vs. t_R, where F_R is the concentration in the PMD sample divided by the donor concentration (18.17 μg/mL) and t_R is the resting time.

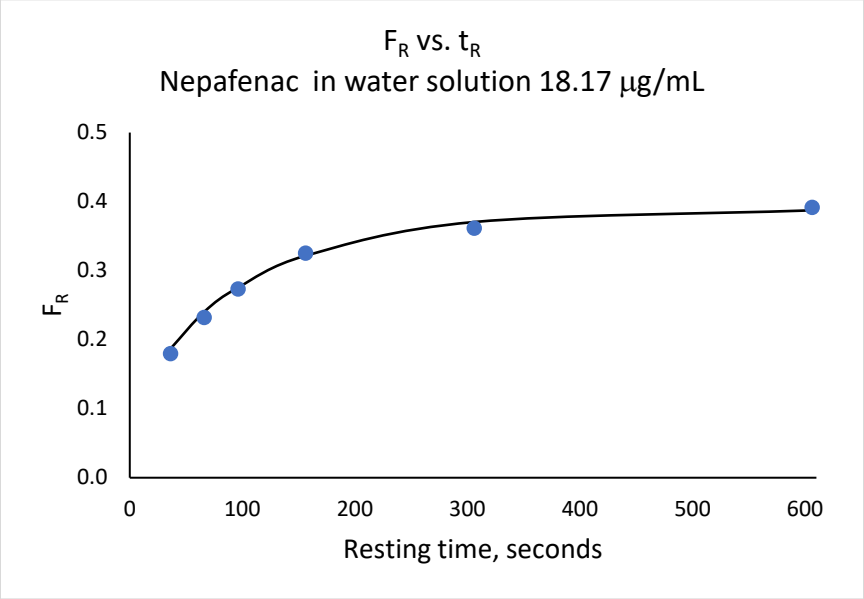

Figure 4-5. Analysis of nepafenac/PMD parameters: F_R vs. t_R plot for nepafenac solution

From the data, the diffusion coefficient in an aqueous medium is D = 7.7 x 10^{-6} cm^2/s (experimental at 23 °C) and D ~ 1 x 10^{-5} cm^2/s (estimated using a Physical Pharmaceutica

algorithm). The PMD probe properties were the window volume V_W = 2.04 μL and the fractional recovery for 30-second t_R sampling was F_R = 0.187.

These results were then used in dissolution sampling by introducing aliquots of each formulation into small volumes of water (as a dissolution medium), then monitoring the dissolved nepafenac in the dissolution medium using a variation of the method reported by Shah et al. (2014), with a flow rate of 20 μL/min and a resting time t_R = 30 seconds.

The nepafenac distribution (fraction of the total nepafenac in the formulation that is initially dissolved in the aqueous phase of the suspension) for formulations was obtained by performing PMD on pure water, then spiking in a volume of formulation in a formulation-to-water ratio of 1:100 (nominally). Typical results are shown for nepafenac 0.3% suspension in Figure 4-6

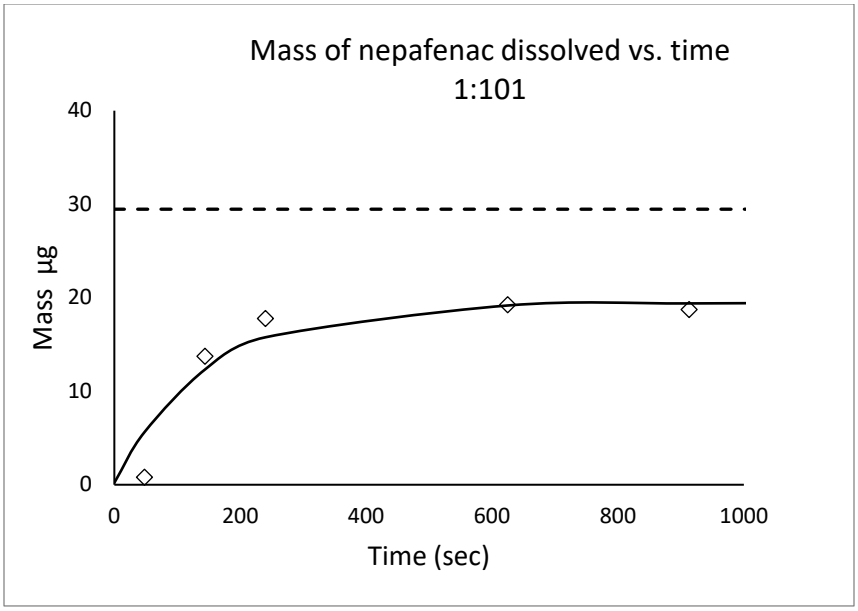

Figure 4-6. Determination of initial fraction of nepafenac dissolved in suspension aqueous phase.

The dashed line represents the theoretical maximum dissolved in the dissolution medium for an aliquot of 0.3% nepafenac suspension (3,000 μg/mL times the aliquot volume in mL), assuming all of the suspension could hypothetically dissolve. The diamonds represent the experimental mass dissolved in the dissolution medium, and the solid line represents a fit of the equation

$$M_{dissolved} = M_0 e^{-\beta t} + M_1\left(1 - e^{-\beta t}\right) \qquad \text{Eq. 4-1}$$

where M_0 is the mass of nepafenac dissolved in the aqueous phase of the suspension aliquot $M_0 = C_S V_{aliquot}$ where $C_S \sim 21.5$ μg/mL, and $M_1 = VC_S$ is the maximum mass of nepafenac that can dissolve in the dissolution medium during the dissolution experiment. The fraction that can dissolve in the experimental timeframe is $M_1 / VC_{suspension}$, where $C_{suspension}$ = 3000 μg/mL for 0.3% and 1000 μg/mL for 0.1% nepafenac suspensions, respectively, and V is the total dissolution medium volume (~ 4 mL in these experiments), and β is a rate constant with units of sec^{-1}.

Eq. 4-1 is the solution to the equation

$$\frac{dM}{dt} = \beta V\left(C_s - \frac{M}{V}\right) \qquad M = M_0 \text{ when } t = 0 \qquad \textbf{Eq. 4-2}$$

Eq. 4-2 is similar to Eq. 28 but omits the factor Mpct/32.01 (the undissolved nepafenac mass at any time divided by the initial undissolved mass). Since there is no loss of formulation due to tear drainage, Mpct/32.29 = 1. It should be noted that the value of 32.29 μg is specific to the 0.1% suspension, as the initially undissolved mass of

nepafenac delivered in a drop is taken as 33 μL x (1000 μg/mL – 0.0215 μg/mL). For nepafenac 0.3% suspension, the initially undissolved mass in the administered drop would be taken as 98.29 μg = 33 μL x (3000 μg/mL – 0.0215 μg/mL) with the ensuing factor of Mpct/98.29 (which also equals one during the *in vitro* dissolution experiments).

The nepafenac dissolutions in low-volume dissolution media (far from sink conditions, in which only a small fraction of the total drug can dissolve in the dissolution medium) were obtained by performing PMD on pure water, then spiking in a volume of formulation in a formulation-to-water ratio of 1:6 nominally. Typical results are shown for nepafenac 0.3% suspension in Figure 4-7.

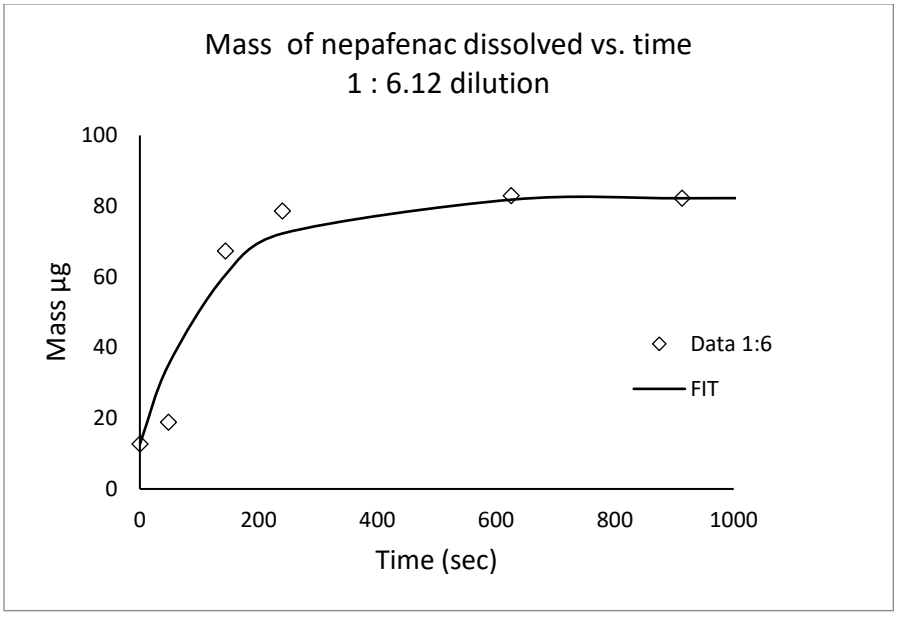

Figure 4-7. Nepafenac dissolution data used to simulate *in vivo* drug dissolution from the nepafenac suspensions.

The fit of Eq. 4-1 to the data in Figure 4-7 yielded an estimate of $\beta \sim 0.00808$ sec^{-1} (~0.485 min^{-1}). The *in vitro* PMD dissolution results can be used to simulate the *in vivo*

dissolution (mass of nepafenac dissolved in the tear layer from the formulation per time) by setting replacing βV with kDpc×V(t), leading to

$$\left.\frac{dM}{dt}\right|_{in\ vivo} = \text{kDpc} \times V(t)\left(C_s - \frac{M}{V(t)}\right) \qquad \text{Eq. 4-3}$$

where k is taken from the PMD data fits described above, but V(t) represents the tear layer volume, which changes with time. Thus, the dissolution rate constant is replaced by a product that varies with time. (In this model, the tear layer volume V is in μL.)

Eq. 4-3 has important implications for the simulated *in vivo* dissolution of any formulation because it implies that the formulation viscosity (via the parameter alpha) has two effects on the formulation-tear layer interaction. A higher viscosity not only creates a longer residence time for the formulation due to slower drainage, but it also increases the dissolution rate product kV by reducing V more slowly.

4.5 Viscosity and estimated *in vivo* formulation clearance and tear layer volume recovery

The transient drug drainage rate (Q_{out}) which reflects the tear clearance and the drug's residence time is determined by the intrinsic viscosity of the original formulations. Considering that ILEVRO® has an elevated viscosity compared to that of the NEVANAC®,

The transient drug drainage rate of ILEVRO® decreases, in this case, indicating a longer residence time (time needed for the volume of tear film to drop from the maximum level to the steady state level) compared to that of the NEVANAC®. Similarly, the transient

drug drainage rate increases, indicating a shorter residence time, when the viscosity of original formulations is determined to be low or diluted formulations are being applied in the simulation. The viscosity of the formulations only changes the first-order rate constant in the transient drug drainage rate while tear base tear drainage rate (Q_{tf}) is not to be affected by the formulation properties.

CHAPTER 5. USING THE PBPK MODEL AS A SIMULATOR

5.1 Description of the R computer code and implementation of the solvers

The overall ocular PBPK model includes, including the precorneal section, was programmed in the R programming language (version 4.1.0) using R-Studio version 1.4.1106, and the differential equations were integrated programing language using the R deSolve package. The major components of the computer program include a data input section, a value adjustment section, the Ocular PBPK functions, an ODE (ordinary differential equations) solver, and a data output and summary section.

The data input section defined all of the variables and parameters included in the overall ocular PBPK model. For time-dependent variables (time is the only independent variable in this model) their initial value at time zero was given in the data input section. For time-constant parameters, typical values (determined by calculation and literature review) were also provided in the data input section.

Although values of parameters are constant during the same simulation, cases vary the value of one or more parameters for multiple simulations (e.g. for a sensitivities analysis). Therefore, a value adjustment section is designed in the program based on this special demand. The value adjustment section distinguishes the typical value defined in the data input section from the current values of parameters that will be used in the new simulation. The adjusted value instead of the typical value was then identified by the parameter caller of the ODE solver and then passed to all of the equations included in the ocular PBPK function.

The ocular PBPK function serves as a major part of this program describing all physical and physiological processes during the release of drug molecules from the original formulation at the ocular surface, loss caused by the drainage and systemic absorption, travel through all ocular tissue compartments and bioactivation results from local enzyme metabolism. The dynamic processes that happen in each of the precorneal or ocular tissue compartments were represented by one differential equation (listed exclusively in chapter 4). This ocular PBPK function is called by the ODE solver for each time simulation.

The ODE solver consists of five parts: the objective function, variables and their initial values used in the function, parameters and their current values used in the function, the independent variable in the function (time), and the method used for the iterative calculation. A fixed-step 4th-order Runge-Kutta method (rk4) was used in this project.

The output of each simulation is generated in one R data frame, integrated with a record of all parameters and their values used in the presented simulation. The output R data frame can be easily written into a .xlsx file for further data checking and calculations.

5.2 Input data and output results to plot or analyze

5.2.1 Physiological and physiochemical data

Therapeutic effect and period at target ocular tissues are affected by different physiological and physiochemical factors. In the precorneal model, equations, and parameters are incorporated to reflect tear turnover properties (tear generation rate, tear drainage rate, tear evaporation rate) and formulation properties (initial amount of

dissolved drug, drug particle dissolution rate, drug particle drainage rate, and dissolved drug drainage rate).

It is important to notice that the value of certain parameters is determined by other factors and therefore they are considered to be indicators of crucial properties. For example, the first-order drug drainage rate is directly related to the velocity of nasal-lacrimal drainage. Moreover, the velocity of nasal-lacrimal drainage will then be decided by the viscosity of the original formulation. In this case, even if there are no parameters that directly indicate a viscosity property of the formulation, it can be reflected by the first-order drug drainage rate constant.

In ocular tissue compartments, here are first-order drug transport rate constant and partition coefficient-related factors to reflect the velocity and extent of drug distribution between neighbor tissue compartments. Meanwhile, there are rate constants for liquid convection (these are not affected by the type of drug molecules and partitioning effects) and systemic absorption (different values for nepafenac vs. amfenac). Last but most importantly Michaelis-Menten parameters (K_{mi}, $V_{max,}$ and local enzyme expression) reflect the enzyme metabolism of nepafenac molecules as bioactivation of the prodrug and generation of amfenac molecules as the active metabolite.

5.2.2 *In vitro* data

The drug release rate from the original formulation and drug distribution (aqueous phase/oil phase/polymer complexed) properties were determined by pulsatile microdialysis (PMD)-based *in vitro* drug release test of NEVANAC® (0.1% nepafenac

suspension) and ILEVRO® (0.3% nepafenac suspension). Theoretically, assuming the suspension is a uniformly distributed system of spherical particles with common size, solid particle distribution could be described by the Hixon-Crowell equation with the introduction of particle size and density parameters. However, considering the complex interactions between suspended drug molecules and polymer matrix and the existence of potential solubilizer in the original formulations, it is more reasonable to use *in vitro* experimental data as the input of the ocular PBPK model for a better estimate of the drug release process at the ocular surface.

5.2.3 Output data

The result of each run of the simulation was written in an EXCEL® spreadsheet for further analysis. There are three major sections in the output: 1) the mass of nepafenac (μg) and mass of amfenac (μg) accumulated in each compartment over time; 2) the parameter values used in the simulations, including the rate constants (μL/s), partition coefficients (no units), compartment volumes (μL), and the enzyme parameters K_{mi} (μM) and V_{max} (μM/min). Unit conversions (mass and μ-moles, minutes and seconds, etc.) were done within the R-program code as needed. Examples include the nepafenac loss (μg) from the ocular surface region due to nasal-lacrimal drainage over time; the mass of nepafenac absorption (μg) through the cornea, conjunctiva, and sclera on the ocular surface over time; the mass of nepafenac metabolized (μg) over time; the mass of nepafenac (μg) picked up by systemic absorption from the vascularized tissue compartments; the mass of amfenac (μg) produced by metabolism over time; and the mass of amfenac (μg) in the various compartments over time. These numbers facilitate

the mass balance check in the model verification, while also providing data needed to understand the pharmacokinetic characteristics of nepafenac and amfenac with changes in the various physical or physiological parameters. The last section in the output spreadsheet is a list of the parameters and their values that were used in the presented simulations. That information was included for the convenience to carry on sensitivities analysis and to identify possible errors in the program by spotting unphysical values of the nepafenac or amfenac masses calculated during the simulations.

An extra tab of calculations and plots was added to each output file of the sensitivities analysis to visualize the impact of changing parameters on certain results of interest (e.g. drug concentration at therapeutical sites, on-set and off-set time points, and percentage of drug metabolized). Details of data analysis are discussed in section 5.5.3.

5.4 Verification of the program

5.4.1 Mass balance requirement

The mass balance was checked throughout the output spreadsheet to verify that 1) there was no mismatch caused by missing or extra terms in the equations describing pharmacokinetic behavior in the model, 2) there was no error of parameter definition (e.g. name and unit) and value pass within the program, and 3) the result of each simulation run was tracible and reproducible.

Three different parts of mass balance were checked during the model verification. The first one is the overall model balance in which the dose administrated (μg) was proved equal to the sum of nepafenac in the tear (Mpct + M), nepafenac in the chemical depot (Md), nepafenac drained to nasal-lacrimal duct and nepafenac absorbed at the ocular

surface (Ma) at any time of the simulation. The second one is drug absorption (μM) balance in which nepafenac absorbed at the ocular surface (Ma) over time was proved equal to the sum of nepafenac and amfenac accumulated in all ocular tissue compartments over time and nepafenac and amfenac picked up by systemic absorption (MS + MAS). The last one is drug metabolism balance in which the amount of nepafenac molecules metabolized (ME, ug converted to molarity) overtime was proved equal to the sum of amfenac molecules accumulated in all of the ocular tissues overtime and amfenac picked up by systemic absorption (MAS, ug converted to molarity) over time. Calculations in the mass balance check were carried on in the same EXCEL spreadsheet of simulation output. New columns were added for each term in the balance check and EXCEL functions were applied for data conversion.

5.4.2 Sensitivity Analysis

Objectives of the sensitivity analysis

The parameters used in the model represent or reflect a property or process in the formulation or ocular physiology such as first-order drug transport constants, drug partition coefficients, and Michaelis-Menten parameters. Given a set of values for the parameters and an initial dose of nepafenac, values of the nepafenac and amfenac masses in each compartment vs. time were calculated. Of particular interest were the amfenac levels vs. time in the compartments involved in the therapeutic response, and the period in which these amfenac levels were at the therapeutic levels.

While 104 parameters were used in the model, it was anticipated that the amfenac mass versus time profiles in compartments of interest would be relatively insensitive to

changes in the value used in the simulation for most of the parameters. For those parameters, any physiologically reasonable parameter value would suffice for the model simulation. On the other hand, changes in the values of other parameters might significantly affect the amfenac profiles. These are referred to as “sensitive” parameters and require specifying their values as accurately as possible. If the value of a sensitive parameter cannot be determined with sufficient accuracy, then the simulations can be performed using a reasonable range of values (low/high) for each such sensitive parameter.

To determine which parameters were sensitive, each parameter was tested for individual sensitivities (a sensitivity analysis) to determine the impact of changes in each on the following. 1) The amfenac concentration profiles at therapeutical sites. 2) The time during which the amfenac was within the therapeutic window at the therapeutic sites. In the sensitivity analysis, this was assessed by reviewing changes, in the duration of time for which the mass of amfenac in a compartment was above half of its maximum value for that simulation. 3). The impact on nepafenac bioavailability in the eye (percentage of drug absorption/dose) and amfenac bioavailability (% of nepafenac metabolism).

In the sensitivity analysis, a “baseline” set of parameter values was assumed. The sensitivity of each parameter was assessed by individually changing its value (0.1, 1.0, and 10 times the respective baseline value) while holding the others equal to the baseline values. The baseline values were carefully determined from the literature to be physiologically “reasonable” if not exact, using chemical data such as log P solubility data, published physiological data, enzyme kinetic data for nepafenac, etc. The one exception was for the Michaelis-Menten parameters. From the simulation results and data

published by Chastain et al. (2016) and Ke et al. (2000), the nepafenac concentration (μM) was much smaller than the K_{mi} in all compartments and at all times. Thus, in the enzyme kinetics equation, which follows the general form (expressing all units in concentration instead of converting from mass) of $Rate = \frac{Expression \times V_{\max} \times C}{K_{mi} + C}$, since $K_{mi} >> C$, this simplifies to $Rate = \frac{Expression \times V_{\max} \times C}{K_{mi}}$.

Thus, the rate of amfenac production is approximately proportional to the ratio $Expression \times V_{\max} / K_{mi}$. The *Expression* and V_{max} always appear in the same combination (multiplied), so they can be reduced to a single parameter that will be denoted as V_{max}, which might vary between compartments as a result of different amidase *Expression* that may occur in different compartments. This is important because, while the values of V_{max} and K_{mi} may not be exactly known, it is possible to pick one value of K_{mi} and simply vary the value of V_{max} in the sensitivity analysis. (A physiological range of ratios can be determined from nepafenac metabolism data published by Ke, et al.)

Table 5-1. Parameters in Sensitivities Analysis

Drug Transport Rate Constants		**Partition Factors**		**Michaelis-Menten Parameters**
Nepafenac	*Amfenac*	*Nepafenac*	*Amfenac*	*Both*
kDpc		Kpdt		Kmi
kpc		Kptc		Vmax
ktd		Kptcon		
ktc		Kptlossc		
ktcon		Kpcah	KApcah	
ktlossc		Kpahicb	KApahicb	
kcah	kAcah	Kpahosecho	KApahosecho	

kconlossc	kAconlossc	Kposeretvh	KAposeretvh	
kahicb	kAahicb	Kpeppretvh	KApeppretvh	
kahvh	kAahvh			
kahosecho	kAahosecho			
kicbosecho	kAicbosecho			
klosscosesc	kAlosscosesc			
kosescosecho	kAosescosecho			
kosesceppsc	kAosesceppsc			
keppsceppcho	kAeppsceppcho			
kosechopseret	kAosechopseret			
kosechoeppcho	kAosechoeppcho			
koseretеppret	kAoseretеppret			
keppchpeppret	kAeppchpeppret			
koreretvh	kAoreretvh			
keppretvh	kAeppretvh			

Method of sensitivities analysis

Three steps were taken for a sensitivities analysis of each parameter selected. In the first step, typical values of each parameter were determined, based on physical principles calculations or references from the literature. In the second step, a range was set for the selected parameter and run a simulation using the lower limit, the typical value, and the higher limit respectively resulting in three different sets of outputs saved in separate EXCEL files. Outputs of each parameter were combined into the same EXCEL spreadsheet. One calculation tab was added to each of the spreadsheets to 1) calculate the slope of the maximum drug levels and time to reach this level (T_{max}) changed with low/mid/high parameter values, 2) calculate the fraction of nepafenac absorbed on the ocular surface (the bioavailability), 3) calculate fractions of nepafenac metabolized during the simulation time, and 5) calculate therapeutic periods (on-set time minus off-set time) and their change with different parameter values.

Sensitivities analysis results

The tear clearance parameters alpha and ktd, Kmi and Vmax were identified to be the critical parameters among all of the selected parameters in the sensitivities analysis while kAosesceppsc, kAosechoeppcho, and kAoseretеppret were identified as the least relevant parameters. Here, the result of the Vmax is shown as an example to illustrate the calculation and results of interest in the sensitivities analysis.

Table 5-2. Sensitivities Analysis Calculation of V_{max}

Range of Vmax (ug/min)			
0.0025			
0.025			
0.25			
	MAicb	*MAeppcho*	*MAeppret*
Delta M_max (ug)	5.49E-04	2.92E-04	2.02E-04
M_max (highest/lowest)	3768%	4614%	3617%
Delta Tmax (min)	200.00	100.00	80.00
Tmax (highest/lowest)	145%	138%	129%
Fraction of Ocular Absorption			
	MAicb	*MAeppcho*	*MAeppret*
0.0025	0.02%	0.01%	0.01%
0.025	0.22%	0.10%	0.08%
0.25	0.93%	0.49%	0.34%
Bioavailability(Fraction of Dose Absorbed)	**Total**	**Dissolved**	
0.0025	0.189%	6.112%	
0.025	0.189%	6.112%	
0.25	0.189%	6.114%	
Fraction of Nepafenac Metabolized			
0.0025	1.34%		
0.025	11.02%		
0.25	37.45%		
Therapeutic Period (Dosing Interval)	*MAicb*	*MAeppcho*	*MAeppret*
Time On-Set 0.0025	210.00	135.00	160.00
Time Off-Set 0.0025	2360.00	1740.00	2120.00
Interval 0.0025	2150.00	1605.00	1960.00
Time On-Set 0.025	200.00	130.00	155.00
Time Off-Set 0.025	2140.00	1420.00	1700.00

Interval 0.025	1940.00	1290.00	1545.00
Time On-Set 0.25	160.00	110.00	135.00
Time Off-Set 0.25	1480.00	680.00	780.00
Interval 0.25	1320.00	570.00	645.00

Table 5-2 results depict sensitivities of Vmax that were calculated and examined following the five steps.

1) The maximum amount of amfenac accumulated in three target sites (icb, eppose, and eppret) changed by 36 to 46 times when Vmax was increased from 0.0025 to 0.25, indicating that Vmax has a considerable impact on drug delivered to therapeutic sites. The time needed to reach the maximum amount of amfenac accumulated in three target sites (icb, eppose, and eppret) changed from 80 minutes to 200 minutes when Vmax was increased from 0.0025 to 0.25, indicating that increasing Vmax accelerates the drug delivery to therapeutic sites.

2) The fraction of amfenac accumulated in three target sites (icb, eppose, and eppret) to the total amount of drug absorbed at the ocular surface changed by 34 to 49 times, indicating that Vmax is a crucial factor to increase the efficacy of nepafenac prodrug bioactivation after they are absorbed into the ocular tissues.

3) The bioavailability which is the fraction of drug absorbed to the total amount of dose in the formulation or dissolved drug in the tear was almost the same despite the increase of Vmax, indicating that Vmax has a negligible effect on drug absorption or drug drainage at the ocular surface.

4) The fraction of nepafenac prodrug metabolized jumped from 1.34% to 37.45% when Vmax was increased from 0.0025 to 0.25, indicating that Vmax is a major and crucial factor in the conversion of prodrug to the active metabolism in the ocular tissues.

5) The dosing intervals or periods when the amfenac concentration level stays within its therapeutic window were calculated using the time at which the concentration first entered the therapeutic window and the time at which it fell below the therapeutic window. Doing intervals in three target sites (icb, eppose, and eppret) all decreased sharply when Vmax was increased from 0.0025 to 0.25, an indication that even though a higher enzyme activity benefits the drug conversion in ocular tissues, it requires a more frequent dosing strategy to keep the drug's effect in patients.

CHAPTER 6. HOW THE PARAMETER VALUES WERE CHOSEN

From the sensitivity analysis, several parameters were found to be significant concerning the amfenac concentrations in tissue compartments that were thought to elicit therapeutic effects. In this chapter, the results of varying these parameters, while holding other parameter values constant, are presented.

The approach was as follows. First, determine the values for the "fixed" parameters. Second, determine the range of values used for the sensitive parameters. Third, determine a specific therapeutic level for the amfenac. Fourth, perform the simulations with the various parameter values, and identify the time interval for which the amfenac concentrations are above that level. These are discussed in detail below.

6.1 Parameters in ocular tissue compartments

Parameters in ocular tissue compartments can be divided into two major groups: first-order drug transfer rate constant and portion factor of the drug (nepafenac or amfenac) between neighbor (aqueous/lipophilic) tissue compartments.

The first-order drug transfer rate constants were calculated based on a physical understanding of typical drug molecules' permeability across a hydrated physiological membrane, which typically falls in a fairly narrow range around a value of ~$5x10^{-4}$ cm/min (Le Merdy et al, 2019). Specifically, Ke et al. (2000) reported a value obtained from nepafenac *in vitro* permeation across freshly excised cornea taken from NZA (New Zealand Albino) rabbits of $k = 7.3 \times 10^{-04}$ min^{-1}. Assuming the interaction surface area A of neighboring ocular tissues is similar to the ocular surface area of ~1 cm^2 (Tsubota and

Nakamori, 1995] in the equation $\frac{dM_i}{dt} = PA(C_1 - C_2)$, the first-order drug transport rate constant is $k \sim AP \sim 5\text{x}10^{-4}$ cm^3/min = $5\text{x}10^{-4}$ mL/min, or 0.5μL/min when the volume units are changed from mL to μL. In a physiological environment, this first-order rate constant can be varied due to the lipophilicities gap of different drug molecules, Therefore, in the simulation, the first-order drug transfer rate constants were adjusted within the range of 0.05-0.5 to represent the difference in drug molecules (nepafenac and amfenac in this study). Importantly, for all parameters, the amfenac profiles were not highly sensitive to variations in the rate constants over this range, so the value of 0.5 μL/min was used for the ocular rate constants unless other noted.

The partitioning effect of drug molecules is affected by two factors: a). the intrinsic lipophilicity of drug molecules and b). the relative hydrophilicity/lipophilicity of neighbor tissue compartments. For example, the iris and ciliary body is a highly lipophilic tissue in the anterior chamber of the eye. It is surrounded by aqueous humor which is a highly aqueous component flowing like water. The partition factor of nepafenac molecules between the iris and ciliary body and aqueous (Kpahicb) was set to 100, consistent with the reference log P (octanol/water) of 2.08 for nepafenac. For amfenac molecules, considering the lipophilicity of amfenac is less than that of nepafenac (due to the replacement of the amide group by the carboxyl group), the partition coefficient of amfenac between the iris and ciliary body and aqueous (KApahicb) was set to be 10. In the simulation, partition factor values were adjusted within the range of 10 to 500 to represent the relative affinity of the drug in neighbor ocular tissues.

6.2 Precorneal parameters

In the pre-corneal model, the values of the parameters were determined by physical test results or physiochemical principles. The important parameters were the effects of the formulation drainage (characterized by alpha), the nepafenac partitioning between the chemical depot and the tear layer (characterized by Kpct), the initial dissolved nepafenac distribution in the formulations, and the nepafenac dissolution and release behaviors characterized by the rate (kDPC) and extent of dissolution or release of undissolved or complexed nepafenac in the formulation (characterized by Mpct). For example, the solid particles dissolve rate constant (**kDpc**) of 0.5 µg/min was calculated based on PMD *in vitro* drug release test data for NEVANAC® and ILEVRO® (original formulation and serial dilutions).

6.2.1 Formulation clearance and ocular residence time (alpha)

The first-order drug drainage rate constant (alpha) was calculated based on hypothetical resident times (times taken for tear volume to drop back to 7µl after drug administration). The resident time is affected by the viscosity of the original formulations. Therefore, the first-order drug drainage rate constant (alpha) was adjusted to represent the difference in behavior due to viscosity property differences between NEVANAC and ILEVRO. The viscosity agent used in NEVANAC is poloxamer 974P (FDA NEVANAC Label), which displays a reduction in viscosity when exposed to the sodium chloride found in tears [Handbook of Pharm Excipients]. The ILEVRO® formulation utilizes a patented combination of polymers consisting of carbomer 974P with guar gum and carboxymethylcellulose (FDA ILEVRO Label) that resists the decrease in viscosity due to exposure to sodium chloride (Chowhan et al., 2014). Thus, ILEVRO is purported to

display a significantly longer ocular residence time than NEVANAC (Chastain et al., 2016) (Jones and Neville, 2013). Experimental data are not available for the residence time behaviors of the two formulations, it is expected from experience in general that a typical suspension ocular residence time would range from a few minutes (low viscosity) to 45 minutes or longer (higher persistent viscosity). Thus, the approach was taken to perform simulations with a physiologically reasonable range of values for alpha, as discussed below.

The ocular residence time can be characterized in two ways, either by considering the time it takes for the formulation volume to be cleared or by considering the time it takes for the dissolved nepafenac in the tear layer to be cleared.

Since the administered drop volume of the formulation was taken as 33 μL and the tear layer volume at steady state was taken as 7 μL, the formulation volume clearance time represents the time for the total tear layer volume to drop from 40 μL to 8 μL. (Because the tear layer volume approaches the steady state volume asymptotically, 8 μL was chosen since the remaining drop to 7 μL would take very long and not reflect the physical clearance behavior.)

The mass of nepafenac initially dissolved in the tear layer was taken as the amount delivered by a 33 μL drop of formulation, which was ~ 0.7 μg in all cases, as shown in the PMD data. The dissolved mass was subsequently reduced because of partitioning from the tear layer into the chemical depot, although this was partially offset by the transfer of nepafenac into the dissolved form in the tear layer from the formulation by dissolution or release from complexes with the polymer system).

It is important to point out that, for a given choice of alpha, the dissolved mass versus time profiles did not exactly match the tear volume versus time profiles. Thus, the ocular residence time is not uniquely defined. Studies in the literature have focused more on the volume versus time profiles, but the fates of the nepafenac and amfenac depend on the dissolved mass and concentration of nepafenac in the tear layer. In this model, the values of alpha were chosen based on reasonable estimates of formulation clearance and tear layer volume versus time profiles but were varied over a range that would include all likely physical scenarios.

For reference, the ocular residence time of NEVANAC® [by volume or mass] was taken as ~7.5 minutes, which corresponded to a value of alpha = 0.6 min^{-1} based on the calculations in the PBPK program. calculations. For comparison, the ocular residence time of ILEVRO was taken as 45 minutes, corresponding to alpha = 0.1 min^{-1}. Because the exact behavior *in vivo* is not exactly known or modeled, the range of alpha used in the simulations was expanded to 0.05 – 0.9 min^{-1} to represent a representative range of estimated or assumed formulation property effects.

6.2.2 Partitioning and transfer rates between the tear layer and the chemical depot

The parameter Kpdt represents the partition coefficient of nepafenac molecules between the chemical depot and the tear layer (concentration in the chemical depot over the concentration in the tear layer). The chemical depot is a thin layer of oil secreted by Meibomian glands on the eyelids. It is highly lipophilic. Therefore, we can refer to the log P (octanol/water) value of nepafenac 2.08 (Chemaxon, REWF) for its partitioning effect between the tear layer and the chemical depot. In the simulation, the Kpdt value was

adjusted within the range of 10 to 650 to represent the relative lipophilicity of the chemical depot against the tear layer. This is consistent with the partitioning of ibuprofen (another nonsteroidal anti-inflammatory drug with similar molecular weight) in oil, for which the oil/water partition coefficients range from ~ 5000 to 15000 (log Ko/w ~ 3.6 to 4.2) based on an ibuprofen solubility of ~22 μg/mL in water (Roni and Jalil, 2011).

The rate of transfer of the drug between the tear layer and the chemical depot is characterized by the rate constant ktd. This transfer is expected to be very rapid because the tear layer and chemical depot are in direct contact (no physical barrier or membrane is separating them, and both are very thin. , and 3) the diffusion coefficients are relatively large. These are discussed as follows.

6.2.3 Nepafenac release and distribution in the formulation from PMD

One of the shortcomings of previous ocular PBPK studies is that the *in vivo* drug release from the formulation to the tear layer was not properly characterized. Most typically, dissolution models based on the Hixson-Crowell or similar model or other class were used to simulate the drug particle dissolution into the available tears, based on data for which particles of the pure drug were allowed to dissolve into high volumes of stirred receiver media. These data are not relevant to the ocular dissolution of drugs with poor aqueous solubility because 1) the dissolution studies were done for pure drug particles instead of for the drug from a formulation, and 2) the dissolutions were done using large receiver volumes (so the receiver medium concentration is negligible compared to the solubility of the drug in the receiver) instead of the very small tear layer volumes that are relevant to ocular dissolution.

In this study, the drug distribution and release data were obtained using pulsatile microdialysis (PMD). The data and analyses for obtaining the relevant parameters to

6.3 The Michaelis-Menten parameters for enzyme kinetics

The local amidase expression at specific ocular tissues (Exp_i), maximum amidase-mediated hydrolysis reaction rate (Vmax) and nepafenac concentration when amidase-mediated hydrolysis reaction reached half of its highest rate (Kmi) are parameters applied to describe nepafenac prodrug metabolism in the proposed ocular PBPK model. The values of such parameters were calculated based on published nepafenac in-vitro hydrolysis data by the human cornea and iris/ciliary body (Ke et al., 2000).

Ke's paper reported amidase-mediated hydrolysis reaction rates in the cornea (per mg of tissue wet mass) of 26 ± 7 pM/min/mg and 107 ± 47 pMm/min/mg for nepafenac substrate concentrations of 8.9 μM and 111 μM, respectively. Taking an assumed cornea volume of 50 μL and approximating its density as 1 g/cm^3 (1 mg/μL), the reaction rate converted to 1.30×10^{-3} μM /min (26 pM/min/mg of the wet mass of tissue × 50 μL × 1 mg/μL = 1300 pM/min = 1.30×10^{-3} μM /min) and 5.35×10^{-3} μM /min by a similar calculation.

Based on the Michaelis-Menten equation $V = \frac{Vmax}{1+Kmi[S]}$ where [S] is the nepafenac concentration, a double-reciprocal plot of $1/V$ vs. 1/[S] was constructed according to

$$\frac{1}{V} = \frac{1}{Vmax} + \frac{Kmi}{Vmax} \times \frac{1}{[S]}$$

The slope of the straight line connected by two points indicated the value of Km / Vmax and the y-intercept of the plot indicated a value of 1 / Vmax. From the plot, values were calculated of Vmax = 7.30×10^{-3} μM/min and Kmi = 41.38 μM in the cornea compartment. Following the same method, values Vmax = 0.13 μM /min and Kmi = 1.42×10^{3} μM were calculated for the iris/ciliary body compartment.

It was thought that Kmi should be relatively consistent for the same type of enzyme no matter where were located. However, the calculation results suggested a significant difference in Kmi between the cornea and iris/ciliary body. While the specific reason for this observation was not clear, values of Kmi = 1.0×10^{2} μM Vmax = 2.5×10^{-2} μM/min were taken for use in the PBPK model. The values of the expression were then adjusted so the maximum amfenac concentrations in the various compartments were consistent with those reported by Chastain et al. (2016). (The values of V reported by Ke et al. reflect the product of $V_{max} \times Exp_i$ in the proposed model.)

CHAPTER 7. THE EFFECTS OF FORMULATION PARAMETERS ON THE DOSING INTERVAL

7.1 Impact of formulation properties and parameters on the simulated precorneal interactions

7.1.1 Impact of formulation viscosity on tear layer volume

The parameter alpha was chosen to characterize the loss of extra tear layer volume associated with the administered drop of suspension (33 μL) and the return from the initial volume with the drop to the steady state tear layer volume (from 40 μL to 7 μL). As specified by Eq. 30, alpha characterizes the drop volume recovery half-life (i.e., the time to clear half of the remaining drop volume) as 0.693 / alpha. The calculated effects of alpha on the tear volume depend only on the tear rate production and evaporation rate, which are constant. The calculated tear volumes versus time profiles for various alpha = 0.1 min^{-1} to 0.6 min^{-1} (corresponding to drop volume recovery half-lives of ~ 7 min to 1.15 minutes, respectively) are shown in Figure 7-1.

When alpha is 0.6, it took approximately 1.5 minutes for the volume of tear film to drop from its maximum 40μl to half. Even though the tear drainage equation is not strictly first order, the drop from 40 to 7 μL (representing the loss of the volume from the initial drop plus existing tear layer volume to the steady state volume) is first order with a half-life of 0.693/alpha. Thus, it is possible to characterize the timeframe for the loss of the formulation volume using a factor of five half-lives

the half-life for that decrease using five times the $\mathbf{t_{1/2}}$ which is 7.5 minutes in this case. When alpha was decreased from 0.6 to 0.1, it took approximately 9 minutes for the

volume of tear film to drop from its maximum 40µl to the half (again, not strictly first order but very close). The estimated elimination time was 45 minutes in this case. We can conclude that the resident time of the drug has an inversely proportional relationship with the alpha (as it can be deducted from the equation). What is left to be known is the relationship between formulation viscosity and alpha (it is expected to be positive but does not have to be linear). If that is cleared by *in vitro* test, then we can easily establish the numeric relationship between formulation viscosity and the drug's resident time on the ocular surface.

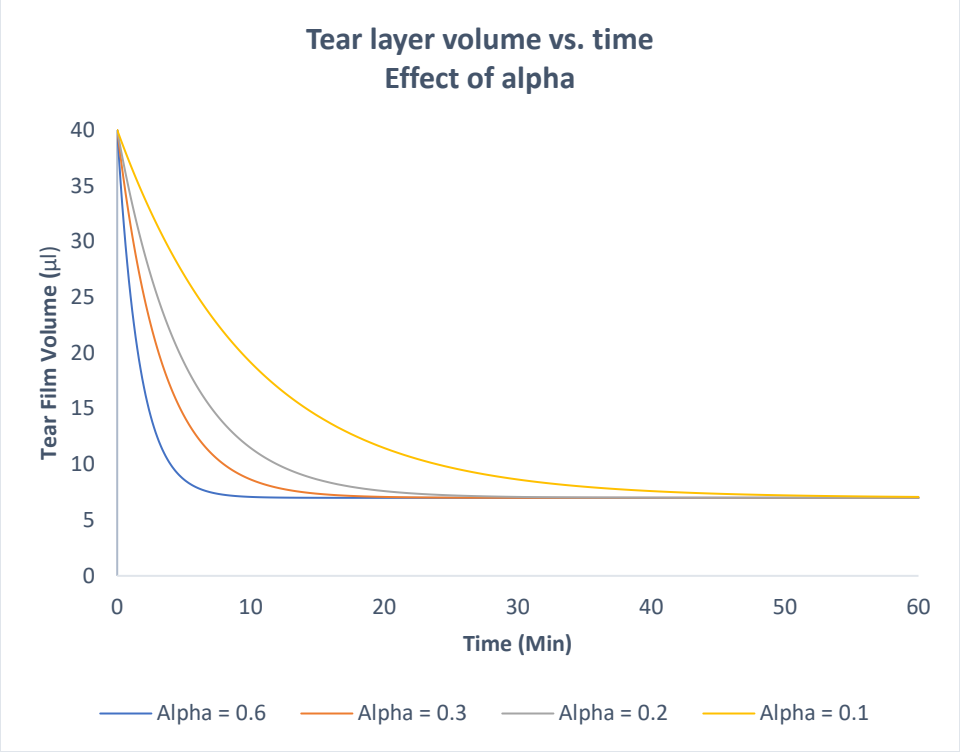

Figure 7-1. Tear layer volume versus time: effects of alpha.

7.1.2 Impact of formulation clearance on the nepafenac dissolved drug in the tear layer

Given that liquid in the tear film was removed rapidly by the tear drainage, the amount of drug dissolved in the tear film (**M**) also dropped very fast within the first 10-20 minutes after administration. The profile of the drug dissolved in the tear film (**M**) is comparable to that of the tear volume, indicating that the tear layer volume level or tear drainage rate is a limiting factor for how much nepafenac is dissolved in the tear layer.

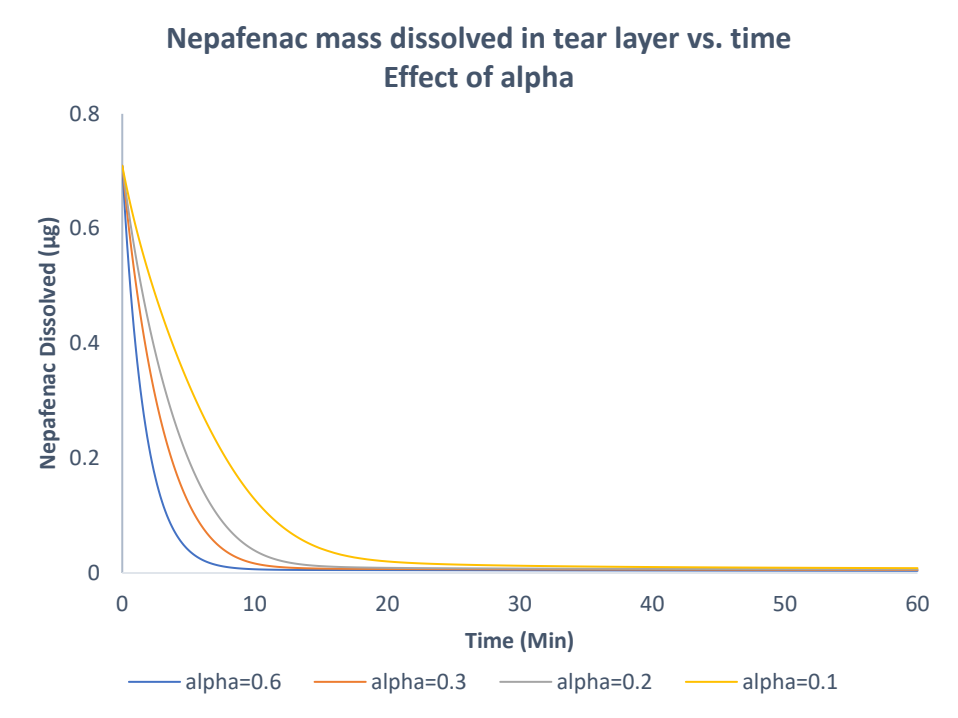

Figure 7-2. Nepafenac mass dissolved in the tear layer versus time: effect of alpha.

7.1.3 Impact of formulation viscosity on drug's absorption on the ocular surface for a single dose

It was seen from the simulations that the nepafenac absorption increased as alpha was decreased, which is consistent with the physical expectations that slower clearance of the formulation from the ocular surface region results in more absorption. When alpha was decreased from 0.3 to 0.1, the calculated absorption of nepafenac absorption at the ocular surface increased from 0.584% to 0.918% of the total dose particles in the suspension formulation. For this comparison, the nepafenac absorption was taken as the maximum value of Ma (at late times) where Ma = Mc + Mcon + Mlossc)

If calculated by the percentage of the nepafenac that is dissolved in the tear layer, the nepafenac absorption jumped from 40.42% to 63.61%. These data indicate that increasing the resident time of the formulation could significantly increase bioavailability in ocular tissues. With the relationship between formulation viscosity and alpha being cleared, we can further state that increasing the formulation viscosity helps boost up drug's bioavailability in ocular tissues. A similar trend was observed in the simulation result of multiple doses.

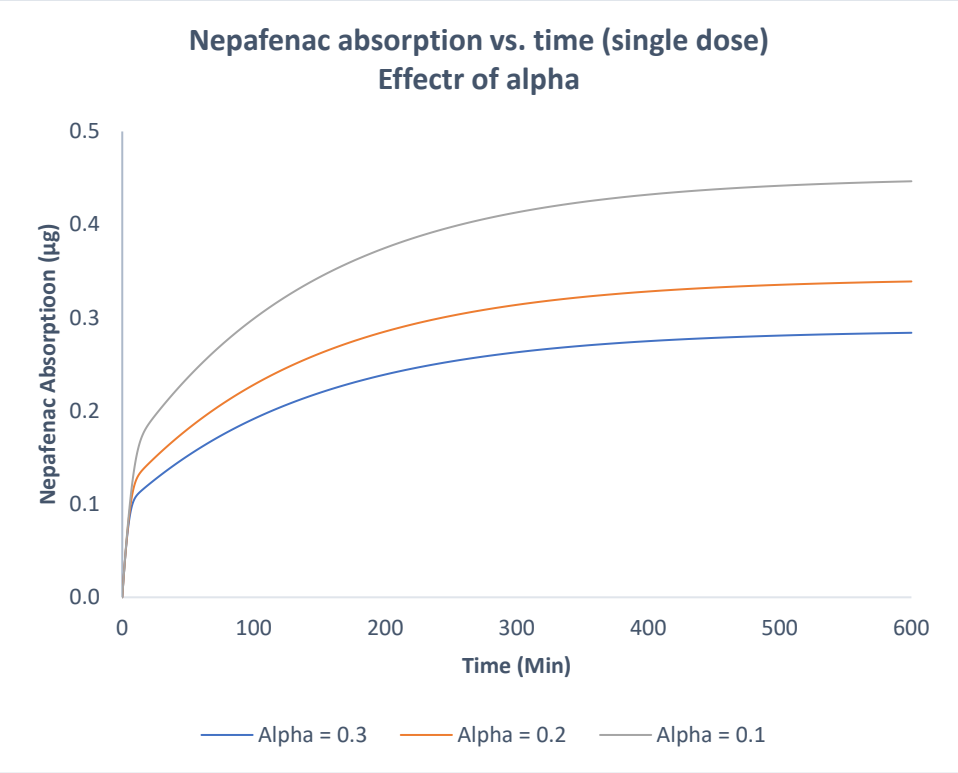

Figure 7-3. Nepafenac absorption versus time: effect of alpha.

7.1.6 The effect of the total dose in the suspension on the nepafenac absorption

The PMD-based *in vitro* drug release test indicated that only about half of the undissolved nepafenac in the formulations can be dissolved in a timeframe relevant to the ocular residence time, with the other half undissolved. Further, the half that can dissolve will only do so if the receiver (tear layer) volume is large enough so the dissolved amount of nepafenac does not exceed the solubility in the tear layer, which was assumed to be ~ 21.5 µg/mL. This has two implications. 1) The simulated *in vivo* drug dissolution/release was based on the dissolvable mass of nepafenac in the formulation (comprised of solid particles and possibly nepafenac complexed with formulation excipients), not the total nepafenac content or "Dose" in the formulations. 2) As discussed in Section 4.4.4, the

dissolution rate "constant" actually is not constant when simulating dissolution *in vivo*, but instead is a variable parameter that varies with the tear volume as kDpc × V(t), where the tear layer volume V(t) varies with time due to formulation drainage. Thus, the dissolution or release of the nepafenac from the formulation depends on the difference in solubility vs. the tear layer dissolved concentration and the rate at which the tear layer volume changes (characterized by the parameter alpha).

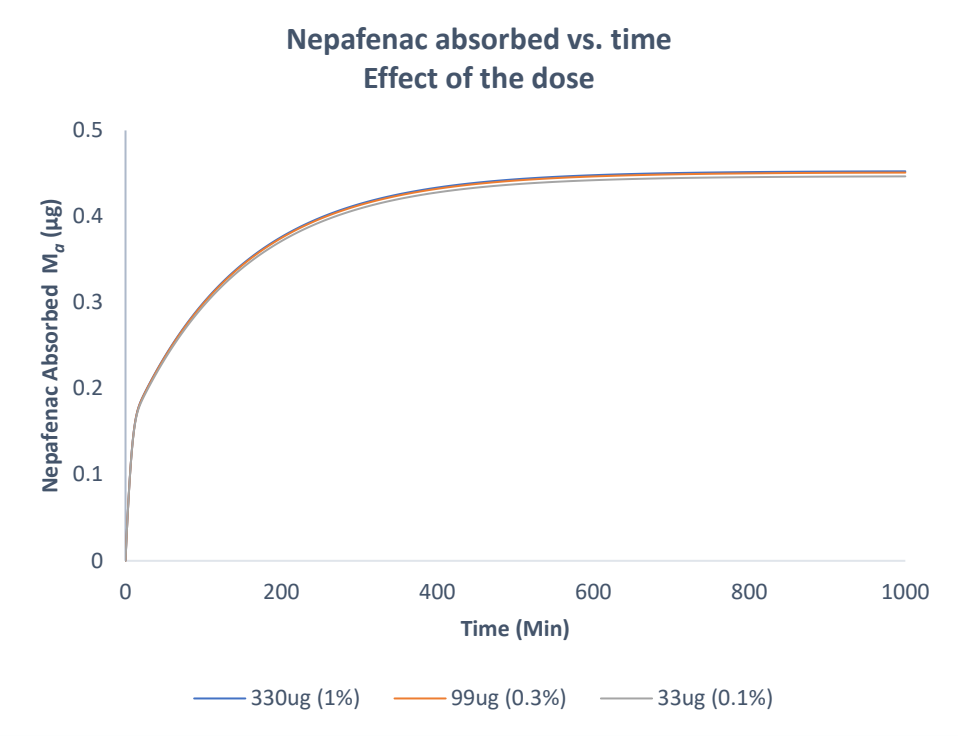

Figure 7-4. Nepafenac absorption versus time: effect of total dose in the suspension.

Alpha = 0.3 in the simulations.

The simulation results showed that neither drug absorption at the ocular surface nor drug concentration at the therapeutic site changed significantly with the dose of the

formulation increased by 3 or 10 times from 0.1%. The observation indicates a crucial point that effort in elevating doses of the ophthalmic suspension, while it might revoke concern about systemic toxicity, would not help with drug concentration at the therapeutic sites in the eyes.

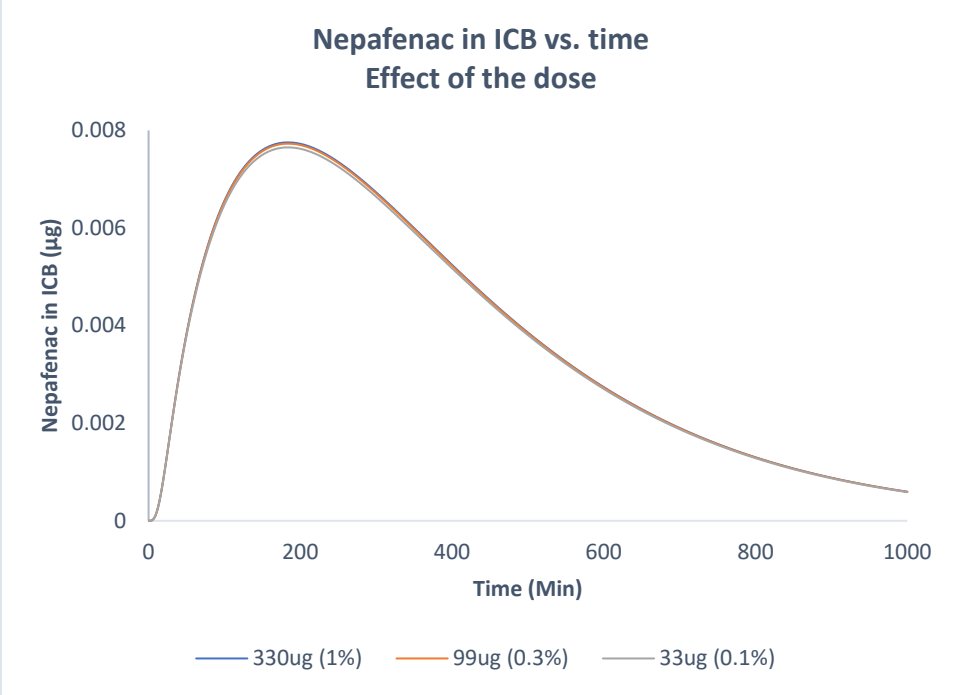

Figure 7-5. Mass of nepafenac in the ICB versus time: effect of the total dose. Alpha = 0.3 in the simulations.

7.1.4 Dosing interval changed by the viscosity and dose? (dosing interval calculated based on Cicb vs high/mid/low viscosity and dose)

As discussed previously, the period during which the amfenac concentration stays above its estimated or assumed effective level at therapeutical sites increased with higher alpha values, indicating that higher viscosity of the formulations might help with the

prolongation of doing interval. Change of doses in the formulation has a negligible effect on the dosing interval.

7.1.5 Effects of the dissolution rate on the nepafenac absorption

For simulations in which the tear layer drainage is rapid (for instance, alpha = 0.9 min^{-1}), the nepafenac dissolution rate *in vivo* has only a minor effect on the nepafenac bioavailability. This is because the tear layer liquid would be removed very quickly (75% of liquid loss within the first 20 minutes) so there is not enough time for the undissolved nepafenac in the suspension to dissolve in the tear layer to a significant degree. However, if the drug has already been dissolved in the suspension before it was applied to the ocular surface, the results are very different. (This effect of the initial drug distribution in the formulation is discussed in the next bullet point.)

7.1.6 Effect of nepafenac distribution in the suspension on nepafenac absorption

The apparent solubility of nepafenac in the aqueous phase of the formulations affects its distribution in the original formulation. In other words, it changes the proportion of the drug that is initially dissolved in the aqueous phase when the suspension is administered to the eye. That leads to a sharp change in the drug absorption at the ocular surface. The simulation results suggested that when the apparent aqueous solubility of nepafenac in the original formulation increased from 0.0215 μg (the experimental value from the PMD testing) to 0.215 μg and 1 μg, the proportion of drug dissolved in the original formulation (ILEVRO® 0.3% nepafenac suspension in this case) increased from 1.43% to 14.3% and 66.7%. Both the drug absorbed within the first half hour and the maximum drug absorbed overall increased by 20-fold and 60-fold, respectively, as a result. This observation

indicates that increasing the dissolved concentration of nepafenac in the administered suspension can dramatically boost the drug's bioavailability to ocular tissues.

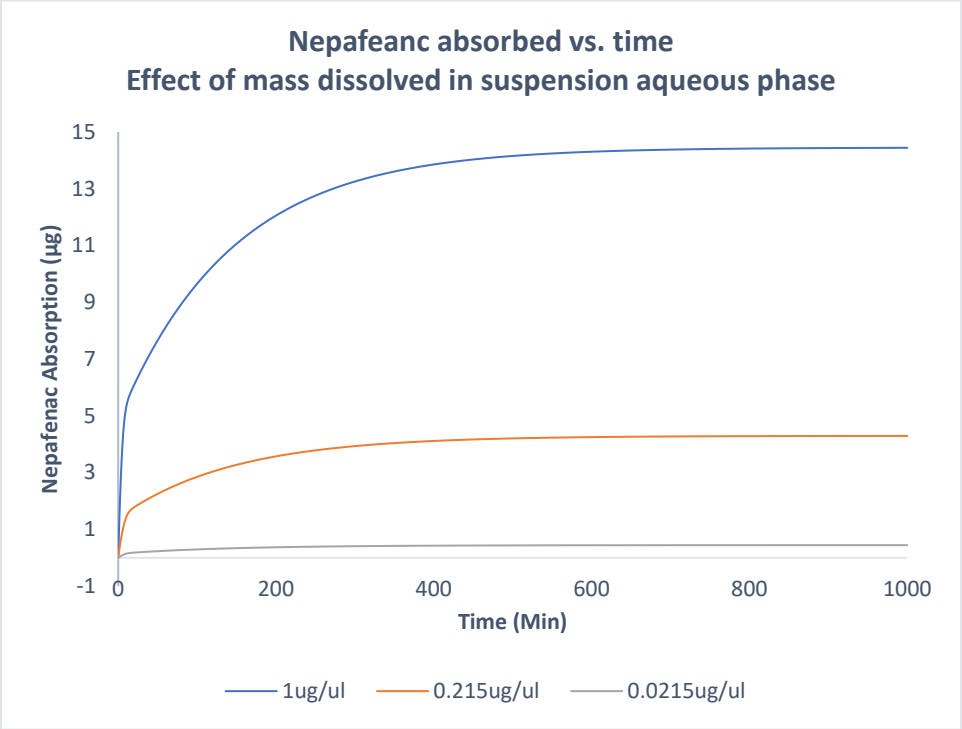

Figure 7-6. Mass of nepafenac absorbed versus time: effect of the mass initially dissolved in the suspension aqueous phase.

The NEVANAC was simulated for dosing every 8 hours (alpha = 0.6) and the ILEVRO was simulated for dosing every 24 hours (alpha = 0.1.

7.2 Effect of the chemical depot (and its importance on drug's bioavailability in ocular tissues)

One of the novel features introduced in this PBPK model is the chemical depot. This is postulated to primarily reflect the existence of the meibomian oily layer (0.5-1 µL volume) that sits on the surface of a thin layer of tears (~ 7 µL volume) on the ocular

surface. It has long been thought that the primary function of the meibomian layer was to slow the evaporation of tears from the ocular surface. However, this study indicates that it also plays an important role in the nepafenac disposition.

The simulations showed that its presence has a significant impact on the absorption of nepafenac. In addition, the simulations indicate that the chemical depot likely plays an important role in the ocular disposition of lipophilic drugs in general but is likely much less impactful on the disposition of more hydrophilic drugs. Since ophthalmic suspensions and emulsions are utilized to accommodate drugs with poor aqueous solubility, the introduction of the chemical depot concept may be an important consideration in modeling the ocular disposition of lipophilic drugs, and perhaps play a role in future formulation efforts.

7.2.1 The percentage of nepafenac stored in the chemical depot versus the total absorption.

In the case of ILEVRO® (0.3% nepafenac suspension), when the chemical depot is fully functional (ktd=50µl/min, Kpdt=500), nepafenac accumulated in the chemical depot (**Md**) reached its maximum of around 0.6µg with alpha equal to 0.1. That indicates 1.22% of total dissolvable solid drug particles and 84.6% of dissolved drug in the original formulation. Without the storage effect of the chemical depot, most of the solid drug particles and the drug dissolved in the formulation will be lost and not absorbed due to the aggressive drainage of the tear layer caused by irritation of particles in the suspension. Therefore, the chemical depot helps to save a significant amount of nepafenac and enhanced its absorption at the ocular surface.

7.2.2 Nepafenac absorption in the hypothetical absence of the chemical depot

It was seen that the chemical depot significantly enhanced the absorption of nepafenac. From simulation results done for the theoretical case of no chemical depot, it was seen that the drug absorption through the cornea, conjunctiva and sclera in the theoretical absence of the chemical depot was faster during the first 100 minutes after administration than with the chemical depot included, and reached its maximum level at around 30 mins. However, due to the drainage of the tear layer, the lack of a chemical depot resulted in the drug absorption essentially stopping after about 30 minutes.

In comparison, when the chemical depot was included in the simulation, the drug absorption was slower during the first ~ 90 minutes after administration than in its absence due to the competition between partitioning into the lipophilic chemical depot and absorption at the ocular surfaces. However, as the dissolved nepafenac concentration in the tear layer declined due to absorption and loss due to tear layer drainage, the drug accumulated in the chemical depot started to release back into the tear layer, from which some of the nepafenac was absorbed and some was lost due to drainage. Because of the rapid and high degree of nepafenac partitioning into the chemical depot, the net effect of the depot was to cause the nepafenac absorption to continue much longer than the 30 minutes shown in the absence of the depot and to a significantly greater extent. This interesting observation partially answered one of the questions of this study-- why nepafenac suspension performs a longer therapeutic effect than other popular topical applied ophthalmic NSAIDs?

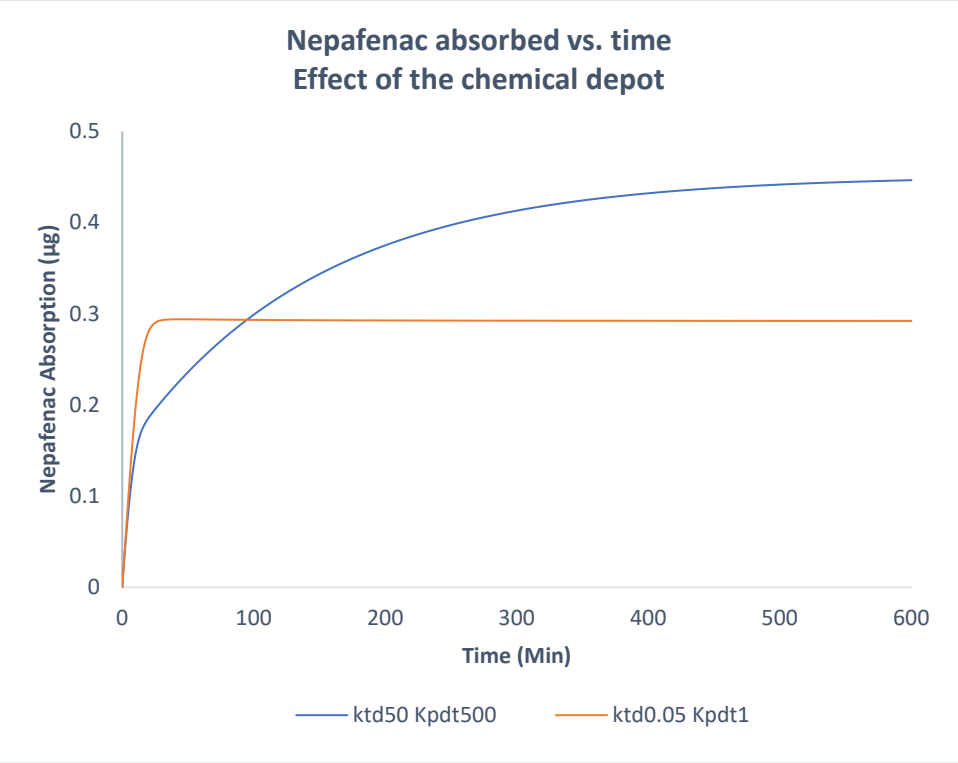

Figure 7-7. Effect of the chemical depot presence on nepafenac absorption

The chemical depot effect was shut off in the simulation by setting Kpdt = 1 (chemical depot/water partition coefficient = 1) and ktd = 0.05 (slow exchange between the tear layer and the chemical depot).

7.2.3 Effect of drug lipophilicity on simulated chemical depot effects

As an amide analog of amfenac, nepafenac molecules are intrinsically more lipophilic and that might add to the long-term boost effect of the chemical depot on the ocular surface. To prove this hypothesis simulations were done with high and low partition coefficient (Kpdt) values to investigate the difference in the boost effect of chemical depot given to hydrophilic or lipophilic drugs.

From the simulation results we can see that for high lipophilicity, the chemical depot was able to store more than six times more of a lipophilic drug than a drug that is not highly

lipophilic. This result indicates that the more lipophilic drug is, the more benefit it could get from the existence of a chemical depot on the ocular surface.

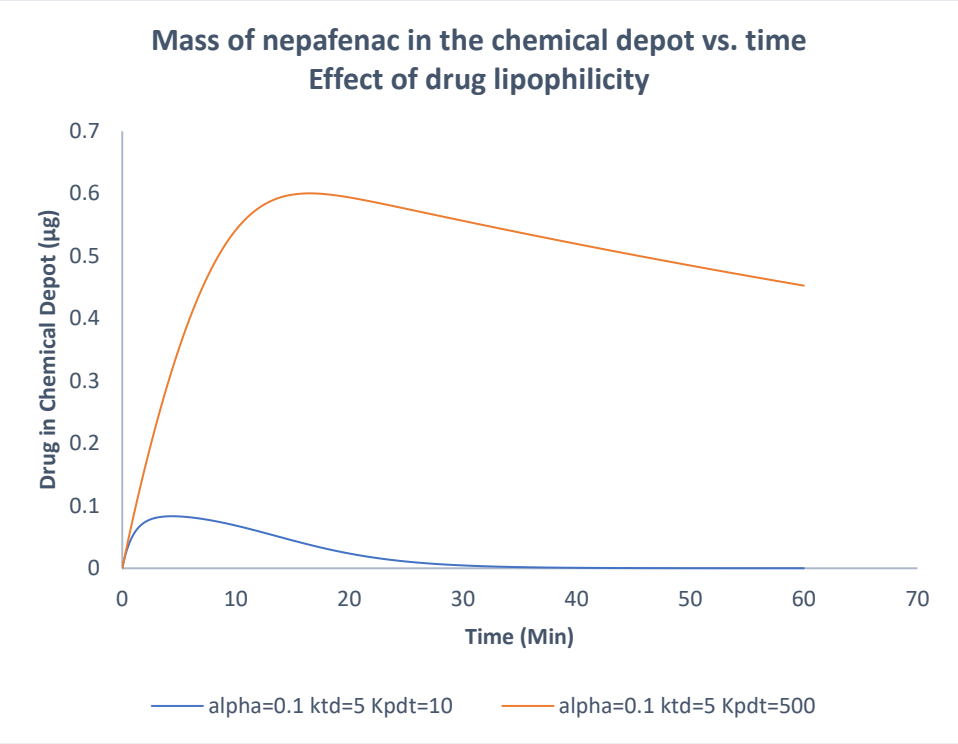

Figure 7-8. Mass of nepafenac in the chemical depot versus time: effect of drug lipophilicity.

Simulations were done for a more lipophilic drug (oil/water coefficient Kpdt = 500) and a less lipophilic drug (Kpdt = 10).

This observation had implications regarding the nepafenac absorption through the cornea, conjunctiva, or sclera surface. For a hypothetical drug with lower lipophilicity, the absorption profile approached the profile calculated when the chemical depot was omitted from the model (shown in Figure 7-7). This shows that the boost effect of the

chemical depot on drug absorption would be very limited if the drug molecule is hydrophilic, and is most important for lipophilic drugs.

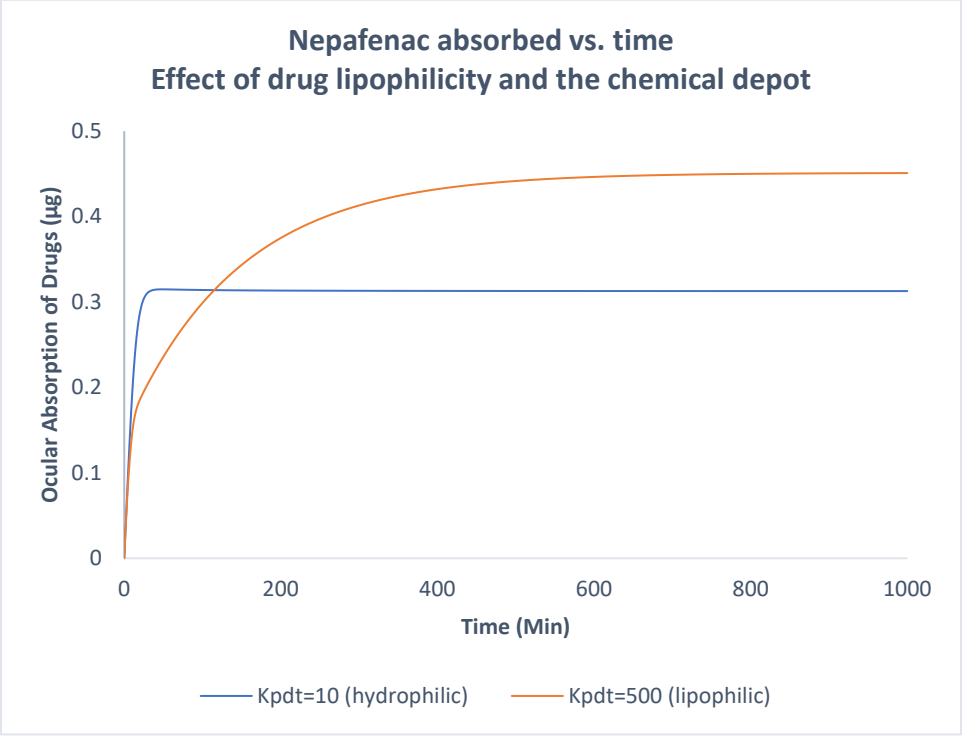

Figure 7-9. Mass of nepafenac absorbed versus hypothetical drug lipophilicities. The oil/water partition coefficients were the same as used to simulate Figure 7-8.

7.3 Parameter and dosing frequency effects on the tissue amfenac levels

In the simulations below, amfenac levels were simulated for multiple dosing. This was done because the amfenac levels showed residual amounts after 8 hours, and even after 24 hours for the more viscous formulations.

Based on the results in Section 7.1, the formulation property that exerts the greatest influence on the dosing frequency was the ocular residence time, as characterized by the parameter alpha. (The drug distribution, particularly the mass of nepafenac initially dissolved in the aqueous phase of the suspension, is theoretically also highly impactful. However, its effect is not considered in the simulations because NEVANAC and ILEVRO show nearly identical dissolved drug concentrations of ~ 21.5 μg/mL in the aqueous phase of the suspensions.)

7.2.1 Impact of formulation clearance on the amfenac concentrations

As noted previously, the formulation clearance from the ocular surface region is physically reflected by its viscosity. The clearance, in turn, is mathematically characterized by the parameter alpha. Thus, it is of interest to explore the effects of alpha and the formulation clearance on the amfenac tissue levels.

For the simulation results of multiple doses every 8 hours, we can see that amfenac concentration at the iris and ciliary body reached its maximum at similar times with different alpha values. However, the maximum amfenac concentration at the iris and ciliary body increased from around 900 nM to around 1900 nM when alpha was decreased from 0.6 to 0.1.

For comparison purposes, it was assumed that the amfenac is effective for pain relief in the iris and ciliary body (ICB) when its compartment concentration exceeds ~600 nM. While this value is arbitrary, the value of alpha = 0.6 is likely reasonably representative of the formulation clearance. (As noted previously, there were no experimental data on the NEVANAC formulation clearance. However, for a vehicle that loses viscosity rapidly

when exposed to sodium chloride in tears, it is known that the clearance can occur in less than 10 minutes.)

Figure 7-10 shows the effect of alpha on the amfenac concentrations in the ICB for simulated multiple dosing (every 8 hours) of NEVANAC. For simulations using alpha = ≤ 0.3 min^{-1}, the amfenac reached an effective tissue level after the second dose and stayed well above the minimum concentration required during the rest of the dosing days in the simulation. When alpha = 0.6 min^{-1} the amfenac concentrations remain above the threshold concentration after the third dose, but require a dosing strategy of 8 hours or more frequently. If alpha < 0.6 min^{-1}, even every 8-hour dosing resulted in subtherapeutic amfenac levels in the ICB (not shown).

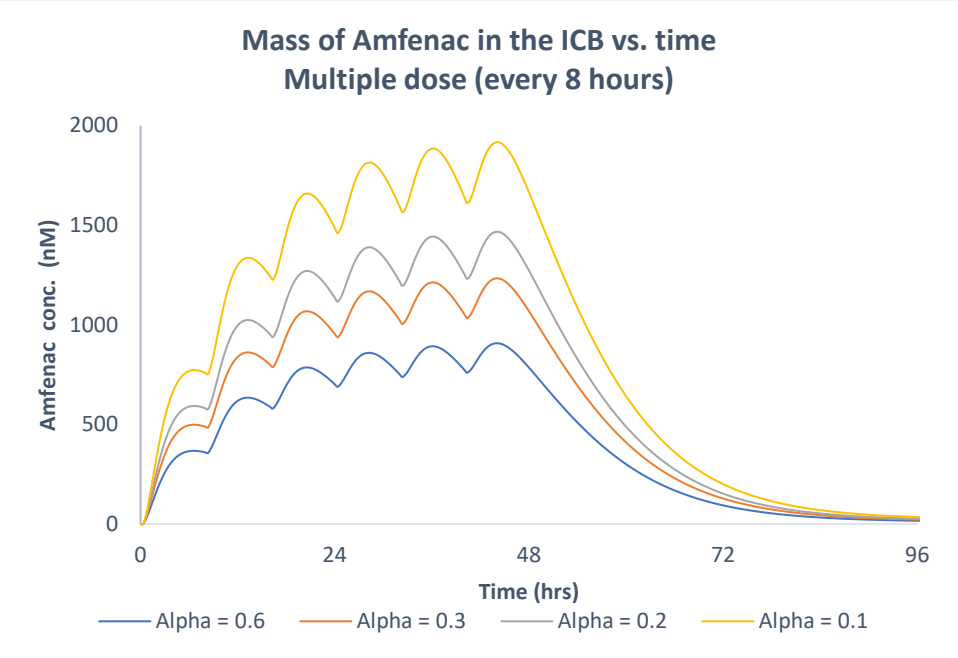

Figure 7-10. Amfenac concentration in the ICB versus time for dosing every 8 hours: effect of alpha.

Figure 7-11 shows a comparison of the same NEVANAC simulation (alpha = 0.6 min^{-1}) and a representative ILEVRO simulation (alpha = 0.05 min^{-1}). Although the formulations contain different total doses, the masses of nepafenac dissolved in the aqueous phase of the suspensions were taken as the same (21.5 µg/mL). However, as discussed in Section 7.1.6, the total dose has little effect on the absorbed nepafenac (and the amfenac profiles). Thus, the most important difference in the formulations was the slower clearance of the ILEVRO from the ocular region, reflecting the more persistent viscosity of ILEVRO and a lower value of alpha.

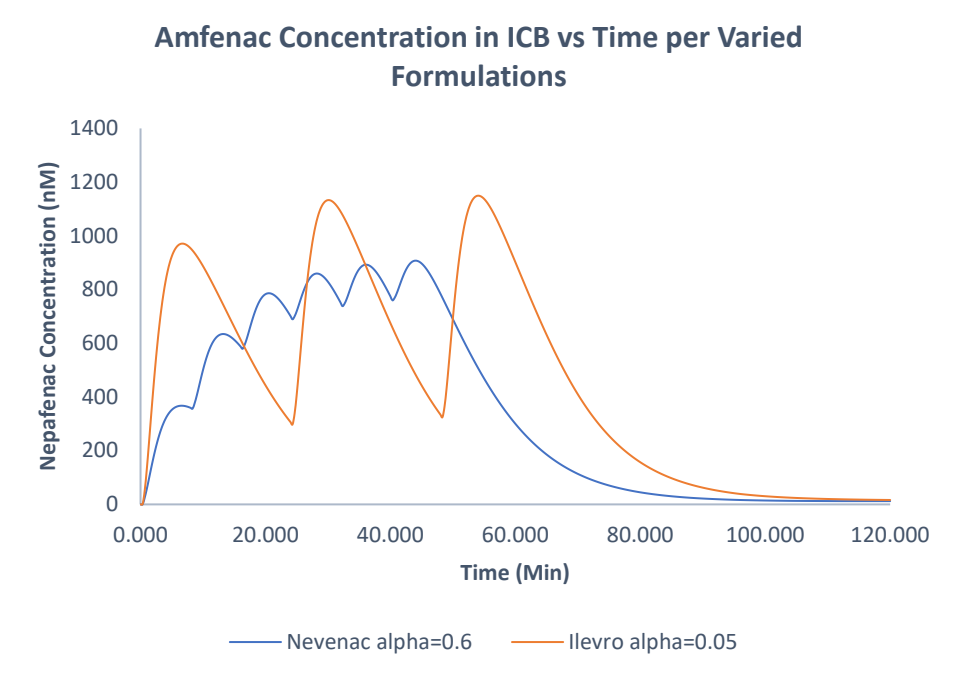

Figure 7-11. Amfenac concentration in the ICB versus time: comparison of NEVANAC and ILEVRO simulations.

The NEVANAC was simulated for dosing every 8 hours (alpha = 0.6) and the ILEVRO was simulated for dosing every 24 hours (alpha = 0.05).

Figure 7-12. Amfenac concentration in the ICB vs. time: comparison of NEVANAC and ILEVRO simulations.

The NEVANAC was simulated for dosing every 8 hours (alpha = 0.6) and the ILEVRO was simulated for dosing every 24 hours (alpha = 0.05).

Figure 7-13. Amfenac concentration in the ICB vs. time: comparison of NEVANAC and ILEVRO simulations.

The NEVANAC was simulated for dosing every 8 hours (alpha = 0.6) and the ILEVRO was simulated for dosing every 24 hours (alpha = 0.05).

CHAPTER 8. OBSERVATIONS AND DISCUSSION

8.1 Pros and cons of lipophilic prodrug (manufacturing, drug release, drug's ADME, percentage of prodrug activated)

Nepafenac is a lipophilic prodrug. It is an amide analogy of carboxyl acid NSAIDs amfenac. In traditional drug manufacturing understanding, it is desired to make drug molecules more hydrophilic to increase their water solubility. Amide prodrug might not be a good option in this case. However, with the development of suspension technology, the problem of poor aqueous solubility for a drug can be solved by other methods such as adding polymeric solubilizers, surfactants, etc. . From then on, the focus of manufacturing idea shifted from increasing the drug's water solubility to facilitate absorption into tissues. This idea especially applies to the manufacturing of topical ophthalmic drugs. Researchers already stated in published papers that nepafenac has a superior permeability compared to other popular NSAIDs (non-steroidal anti-inflammatory drugs) ophthalmic suspensions such as diclofenac (Ke et al. 2000).

In this study, the novel precorneal model further investigated regarding anticipated absorption profile differences between lipophilic and hydrophilic drugs on the ocular surface. The simulation results suggested that the existence of an oil layer secreted by the meibomian glands, which lie on the upper and lower eyelids, serves as a chemical drug depot. This chemical depot takes up the drug much like a sponge and protects against drug loss from the ocular region by tear drainage and formulation clearance. One of the interesting observations is this depot effect majorly results from the relatively high partitioning tendency of lipophilic drug molecules to enter the chemical depot (oil layer). In other words, the more lipophilic drug molecules are, the more benefit they get for a

boosted bioavailability in ocular tissues. Instead, hydrophilic drug molecules were not benefited from this chemical mechanism. This observation further justifies the rationale behind why should we bother to make a lipophilic prodrug like nepafenac.

8.2 The model suggests ways to increase a drug's ocular bioavailability

Increasing drug bioavailability has been one of the major concerns in drug development and manufacturing. In the case of ophthalmic suspension, taking NEVANEC (0.1% nepafenac suspension) and ILEVRO® (0.3% nepafenac suspension) as examples, it was seen that a drug's bioavailability in ocular tissues could be increased in at least two ways, specifically increasing the fraction of the dose dissolved in the aqueous phase of the formulation and slowing the formulation clearance from the ocular region (by increasing the suspension viscosity or resistance to drop in viscosity *in vivo* due to tear interactions). This answers, at least partially, the question of which formulation factors are considered dominant in deciding a drug's ocular bioavailability.

Based on the deduction of physical principles and different formulations using the novel PBPK model, several points were identified points that might be instructive to drug development and manufacturing: 1) Increasing the total dose without changing any other properties of formulation minimally affects the drug's absorption. 2) Increasing formulation viscosity helps the drug to stay longer on the ocular surface, offering higher chances for dissolved drug molecules to be absorbed from either tissue surfaces (cornea, conjunctiva, and sclera) or, in the case of lipophilic drugs, being stored in the chemical depot and add to the total absorption in longer terms. 3) Dissolving more of the drug in the aqueous phase of the suspension is a key way to increase bioavailability. Once the

drug suspension is administered to the eye, any liquid in the tear film starts to be lost rapidly due to aggressive tear layer drainage. The short residence time of the drug allows only very limited amounts (if any) of solid particles in the suspension to dissolve. In practice, it can be assumed that any of the drug that was not dissolved in the formulation or formulated to be in a highly accessible form (such as complexed with polymer excipients) before drug administration will probably never get any chance to be absorbed into ocular tissues. 4) Lipophilic prodrugs benefit from the presence of the lipophilic chemical depot, which acts to store the drug and protect it from formulation clearance. In addition, lipophilic drugs are more able to partition into lipoidal tissues, which can increase physiological membrane permeability. That helps with a drug's overall bioavailability in ocular tissues and specifically increases drug distribution to therapeutical sites at the posterior section of the eyes such as the choroid and retina.

8.3 How to reduce the dosing frequency without losing the therapeutic effect

Prolongation of dosing intervals and reduction in dosing frequency requires that the drug concentrations at therapeutic sites stay above threshold levels for a longer period. The discussions above show that increasing formulation viscosity, causing more of the drug to be dissolved in the aqueous phase of the formulation, and making a drug molecule more lipophilic (as a prodrug, for instance) are three impactful ways to increase a drug's availability at therapeutical sites. Simulation results from the proposed ocular PBPK model are also supported by clinical data which suggest a better therapeutical effect and longer effective period of nepafenac at choroid and retina compared to other popular NSAIDs ophthalmic suspensions (Gamache et al, 2000).

8.4 Pros and cons of using the PBPK model to inform drug and formulation development

Different from the traditional PK/PD model, the PBPK modeling is based on a deeper understanding of physiological details information from tissue's locations, lipophilicities, volumes, and enzyme expressions to their relationship with others. That knowledge requires extensive evidence from clinical study results, which could be hard to acquire in some cases. Besides, during the development and testing of the PBPK model, a researcher needs to focus on not only numerical rationales but also physiological accuracy which is of less importance in traditional PK/PD studies. In industry, the PBPK modeling method arises unprecedented interest and enthusiasm, even though PBPK modeling is currently not considered the first choice for most drug development projects due to its complicated verification process. In another word, there are always easier and more efficient options to answer the pursuing question and therefore PBPK model would only be applied if very specific details (such as drug-drug interactions) are needed. However, the field is developing rapidly and has been identified as a priority for FDA-based research initiatives.

8.5 Knowledge and crucial conceptions required for researchers using the PBPK model

The PBPK model is a very powerful tool for drug development and regulation if used appropriately. For an emerging research method especially in ophthalmic suspension development, scientists who are interested in developing knowledge and experience in

(but not limited to) certain areas might be benefited from PBPK model developing and handling works:

Sensitivities in math: Modeling studies require not only the computational ability but also sensitivity to a change of numbers. This sensitivity is developed with both a mathematical understanding of equations and life experience. Experienced researchers can anticipate the trend of simulation results without exclusive calculations. This ability is very helpful in finding dominant factors in model structure and spotting trends and errors in the mess of large-scale simulation results. It also makes one's observation of his/her own life interesting. Optimistically, more pharmaceutical scientists will develop these skills in the future.

Basic understanding of anatomy and physiology: Anatomy and physiology are areas that most graduate curricula in pharmaceutics do not emphasize. However, a PBPK study can hardly proceed without a sufficient understanding of human body structure and physiological processes. For example, in the cataract surgery-related ocular inflammation, before going for the model development we might want to know what caused the inflammation and pain. where is the target site of the drug? How was the drug delivered to the site and how long could the therapeutical effect last for a single/multiple dose strategy? To answer those questions, we need to realize the basic structure of the human eye (which is way more complicated than you thought), the major tissues in the eye, their functions and locations, dynamic processes that happen in the eye (tear turnover, aqueous humor turnover, liquid convection between tissues, etc.) and their relationship with pathological symptoms. While an individual scientist or modeler might not have all of this knowledge before the study, a study of the literature study and

communication with other experienced researchers can provide much useful knowledge that is put into a cohesive framework by the PBPK model.

Pharmacokinetic and pharmacodynamic principles: PK/PD is not a new topic for students in pharmaceutical-related majors. The challenge in PBPK modeling majorly lies in the increase of model (and equations) complexity and data granularities from simulation results. It is worth mentioning that the existence of commercial PBPK software, such as Simnulink® and GastroPlus® might provide certain conveniences in a question-directed project. However, for a graduate student who wants to develop their understanding of the dynamic process, equation derivative, compartment relationship, and other factors that affect a drug's PK/PD properties, click-and-run "canned" and run software might not be the best option for their goals.

8.6 How can the current model can be improved and what it might be used for?

The established PBPK model has been proven to be mathematically functional and flexible in equations and parameter manipulations. However, due to the limit of *in vitro* experimental results and clinical data, many parameter values in the model were determined by physical principles and literature review. Even though the proposed hypothesis was proved by the simulation results using the current model, according *in vitro*/*in vivo* experimental data would be helpful to further support our observations.

More than that, as an open resource based on the R programming language. Our established model could serve as a template for any human or animal-related PBPK study for different indications and drug entities. That encourages further modification and

improvement of the current version of the model with emerging clinical data and fancy topics.

CHAPTER 9. SUMMARY AND CONCLUSIONS

The major objective of this study came from the interesting question that increasing the dose of nepafenac ophthalmic suspension results in a proportional extension of the drug dosing interval or frequency. Hypotheses were proposed for potential reasons. First, the dosing interval of nepafenac ophthalmic suspension might be affected by the formulation viscosity. It was expected that formulation with higher viscosity stays longer at the ocular surface, allowing more time for the solid particles to get dissolved. Second, nepafenac bioavailability is changed by the existence of a chemical depot on the ocular surface. The chemical depot consists of a thin oil layer secreted by the Meibomian gland to prevent tear evaporation. Nepafenac, considering its higher lipophilicity compared to other carboxyl acid NSAIDs, was expected to be sponged into the chemical depot during excessive tear drainage and released to the tear layer gradually, causing a suspended-releasing effect.

An Ocular PBPK model was established using R programming language to simulate the reasonable effect of formulation factors and other physiological properties on the nepafenac total absorption (bioavailability in tissues) and concentration of active metabolite at therapeutical sites in iris and ciliary body, choroid, and retina. The established model includes a precorneal section to monitor the drug-tear interaction on the ocular surface. Rapid tear turnover and the sponge-like effect of a chemical depot on the ocular surface were both reflected by equations in the pre-corneal section. The ocular tissues section referred to a developed Ocular Compartmental Absorption and Transition model in the GastroPlus® (Le Merdy, et al 2019), especially on tissue locations and dynamic drug transfers. Tissues of the sclera, choroid, and retina were separated into

multiple compartments to identify a proposed periocular pathway of nepafenac drug distribution (Chastain et al, 2016).

A mass balance check on the nepafenac was done as part of the verification of the PBPK model. Typical parameter values in the model were determined by physical principle-based calculations and a literature review that included clinical data and animal studies. The sensitivities of parameters were tested by varying the values of each parameter within a reasonable range and comparing simulation results.

The model was used for different simulations to prove our hypothesis (can be true or false) in this study and to provide knowledge of interest. The results suggested the following.

- Tear drainage rate has a significant effect on the nepafenac total absorption on the ocular surface.

- The mass of nepafenac absorbed at the ocular surface highly depends on how much of the drug was initially dissolved in the aqueous phase of the original suspension formulation, as opposed to what must be dissolved or released *in vivo* during the drug-tear interaction.

- The existence of the chemical depot on the ocular surface slows down the drug absorption at the first 20-40 minutes but it increased total drug absorption during a longer period. This facilitation effect only applies to lipophilic drugs such as nepafenac and not to hydrophilic drugs.

- Simply increasing the dose in the original suspension does not lead to significantly higher drug bioavailability in ocular tissues.

- Administering ILEVRO every 24 hours results in a similar therapeutical period (a period during which amfenac concentration at ICB, choroid, and retina stays above the minimum effective level) with NEVANAC® every 8 hours, this observation is consistent with the label of Alcon's drug label. The major factor that caused this result was that the viscosity of ILEVRO ® was increased compared to that of NEVANAC®.

- A higher concentration of nepafenac prodrug and the active metabolite amfenac was obtained through our simulation compared to Chastain's rabbit data. This observation could suggest that the proposed periocular distribution is not the dominant pathway of nepafenac. However, given that the total amount of drug delivered to the posterior chamber is very small, any reasonable experiment execution or quantitative analysis error could cause large relative variations in the data. Therefore, further *in vivo* studies are necessary to investigate the distribution properties of nepafenac in the ocular environment.

The model established in this study was proved to be functional for investigating the relationship between formulation properties and nepafenac ophthalmic suspension dosing interval. The inclusion of dynamic drug-tear interaction and chemical depot mechanism in the novel precorneal model was testified to be a determining factor of drug absorption and a big improvement of existing ocular PBPK models. With successful application in this study, however, the established ocular PBPK model has much potential for further

improvement in the future. Parameter values in the model can be verified by new clinical data. Permeability and partition factor can be adjected for drugs with different lipophilicities. Enzyme expression and affinity with drug substrate can be obtained from *in vitro* tests. A very important point is the precorneal model can be further related to PMD or other advance *in vitro* drug release test results for a better estimate of drug dissolution and absorption on the ocular surface.

This study also provides meaningful insight for ophthalmic suspension manufacturing in how to improve a drug's bioavailability in ocular tissues. Simulation from our proposed model suggested that instead of raising the dose, manufacturers should consider how to improve the drug's solubility in the formulation and how to increase the viscosity of the suspension without irritating or damaging the ocular surface. Studies on adding solubilizers or reducing drug particles (e.g. manufacturing of polymer complexed nanoparticles) to increase solubility could become a direction for future formulation studies.

REFERENCES

Agrahari V, Mandal A, Agrahari V, Trinh HM, Joseph M, Ray A, Hadji H, Mitra R, Pal D, Mitra AK. A comprehensive insight on ocular pharmacokinetics. Drug Deliv Transl Res. 2016 Dec;6(6):735-754.

Awwad S, Day RM, Khaw PT, Brocchini S, Fadda HM. Sustained release ophthalmic dexamethasone: *In vitro in vivo* correlations derived from the PK-Eye. Int J Pharm. 2017 Apr 30;522(1-2):119-127.

Awwad S, Lockwood A, Brocchini S, Khaw PT. The PK-Eye: A Novel In Vitro Ocular Flow Model for Use in Preclinical Drug Development. J Pharm Sci. 2015 Oct;104(10):3330-42.

Barar J, Asadi M, Mortazavi-Tabatabaei SA, Omidi Y. Ocular Drug Delivery; Impact of *in vitro* Cell Culture Models. J Ophthalmic Vis Res. 2009 Oct;4(4):238-52.

Bellantone RA. Method for Use of Microdialysis. U.S. Patent 8,333,107, Dec. 2012.

Bellantone RA, Shah KB, Patel PG, Kaplan M, Xu X, Li V, Newman B, Abul Kaisar M. Cyclosporine release and distribution in ophthalmic emulsions determined by pulsatile microdialysis. Int J Pharm. 2022 Mar 5;615:121521.

Bussing D, K Shah D. Development of a physiologically-based pharmacokinetic model for ocular disposition of monoclonal antibodies in rabbits. J Pharmacokinet Pharmacodyn. 2020 Dec;47(6):597-612.

Butovich IA. Lipidomics of human Meibomian gland secretions: Chemistry, biophysics, and physiological role of Meibomian lipids. Prog Lipid Res. 2011 Jul;50(3):278-301.

Campbell M, Humphries P. The blood-retina barrier: tight junctions and barrier modulation. Adv Exp Med Biol. 2012;763:70-84.

Carslaw HS, Jaeger JC. Conduction of Heat in Solids, Second Edition. Clarendon Press, 1959, p. 104.

Chastain JE, Sanders ME, Curtis MA, Chemuturi NV, Gadd ME, Kapin MA, Markwardt KL, Dahlin DC. Distribution of topical ocular nepafenac and its active metabolite amfenac to the posterior segment of the eye. Exp Eye Res. 2016 Apr;145:58-67.

Chockalingam A, Xu L, Stewart S, Le Merdy M, Tsakalozou E, Fan J, Patel V, Rouse R. Protocol for evaluation of topical ophthalmic drug products in different compartments of fresh eye tissues in a rabbit model. J Pharmacol Toxicol Methods. 2019 Mar-Apr;96:9-14.

Choi SH, Lionberger RA. Clinical, pharmacokinetic, and *in vitro* studies to support bioequivalence of ophthalmic drug products. AAPS J. 2016;18(4):1032–8

Chowhan MA, Ghosh M, Asharian B, Han WW. US Patent 8,921,337, Dec. 2014.

Coca-Prados M. The blood-aqueous barrier in health and disease. J Glaucoma. 2014 Oct-Nov;23(8 Suppl 1):S36-8.

Davidson HJ, Kuonen VJ. The tear film and ocular mucins. Vet Ophthalmol. 2004 Mar-Apr;7(2):71-7.

Davson, Hugh and Perkins, Edward S.. "human eye". Encyclopedia Britannica, 20 Oct. 2022, https://www.britannica.com/science/human-eye. Accessed 27 October 2022.

Davson, Hugh and Perkins, Edward S.. "human eye". Encyclopedia Britannica, 20 Oct. 2022, https://www.britannica.com/science/human-eye. Accessed 27 October 2022.

Deng F, Ranta VP, Kidron H, Urtti A. General Pharmacokinetic Model for Topically Administered Ocular Drug Dosage Forms. Pharm Res. 2016 Nov;33(11):2680-90

Entezari M, Karimi S, Ramezani A, Nikkhah H, Fekri Y, Kheiri B. Choroidal Thickness in Healthy Subjects. J Ophthalmic Vis Res. 2018 Jan-Mar;13(1):39-43.

FDA Label for ILVERO. Available online at https://www.accessdata.fda.gov/drugsatfda_docs/label/2012/203491s001lbl.pdf.

FDA Label for NEVANAC. Available online at https://www.accessdata.fda.gov/drugsatfda_docs/label/2011/021862s008lbl.pdf

Gamache DA, Graff G, Brady MT, Spellman JM, Yanni JM. Nepafenac, a unique nonsteroidal prodrug with potential utility in the treatment of trauma-induced ocular inflammation: I. Assessment of anti-inflammatory efficacy. Inflammation. 2000 Aug;24(4):357-70.

Gaynes BI, Onyekwuluje A. Topical ophthalmic NSAIDs: a discussion with focus on nepafenac ophthalmic suspension. Clin Ophthalmol. 2008 Jun;2(2):355-68.

Geroski DH, Edelhauser HF. Transscleral drug delivery for posterior segment disease. Adv Drug Deliv Rev. 2001 Oct 31;52(1):37-48.

Goel M, Picciani RG, Lee RK, Bhattacharya SK. Aqueous humor dynamics: a review. Open Ophthalmol J. 2010 Sep 3;4:52-9.

https://www.accessdata.fda.gov/drugsatfda_docs/nda/2012/203491Orig1s000CrossR.pdf Accessed on 07Oct2022

Hu DN, Simon JD, Sarna T. Role of ocular melanin in ophthalmic physiology and pathology. Photochem Photobiol. 2008 May-Jun;84(3):639-44.

Hui HW, Robinson JR. Effect of particle dissolution rate on ocular drug bioavailability. J Pharm Sci. 1986 Mar;75(3):280–7.

Jones BM, Neville MW. Nepafenac: an ophthalmic nonsteroidal anti-inflammatory drug for pain after cataract surgery. Ann Pharmacother. 2013 Jun;47(6):892-6.

Jordán J, Ruíz-Moreno JM. Advances in the understanding of retinal drug disposition and the role of blood-ocular barrier transporters. Expert Opin Drug Metab Toxicol. 2013 Sep;9(9):1181-92.

Ke TL, Graff G, Spellman JM, Yanni JM. Nepafenac, a unique nonsteroidal prodrug with potential utility in the treatment of trauma-induced ocular inflammation: II. In vitro

bioactivation and permeation of external ocular barriers. Inflammation. 2000 Aug;24(4):371-84.

Kida T, Kozai S, Takahashi H, Isaka M, Tokushige H, Sakamoto T. Pharmacokinetics and efficacy of topically applied nonsteroidal anti-inflammatory drugs in retinochoroidal tissues in rabbits. PLoS One. 2014 May 5;9(5):e96481.

Kimko H, Pinheiro J. Model-based clinical drug development in the past, present and future: a commentary. Br J Clin Pharmacol. 2015 Jan;79(1):108-16.

Knop E, Knop N. Anatomy and immunology of the ocular surface. Chem Immunol Allergy. 2007;92:36-49.

Lane SS. Nepafenac: a unique nonsteroidal prodrug. Int Ophthalmol Clin. 2006 Fall;46(4):13-20.

Le Merdy M, AlQaraghuli F, Tan ML, Walenga R, Babiskin A, Zhao L, Lukacova V. Clinical Ocular Exposure Extrapolation for Ophthalmic Solutions Using PBPK Modeling and Simulation. Pharm Res. 2022 Sep 23.

Le Merdy M, Fan J, Bolger MB, Lukacova V, Spires J, Tsakalozou E, et al. Application of mechanistic ocular absorption modeling and simulation to understand the impact of formulation properties on ophthalmic bioavailability in rabbits: a case study using dexamethasone suspension. AAPS J. 2019 May 20;21(4):65.

Le Merdy M, Tan ML, Babiskin A, Zhao L. Physiologically Based Pharmacokinetic Model to Support Ophthalmic Suspension Product Development. AAPS J. 2020 Jan 6;22(2):26.

Lehrer RI, Xu G, Abduragimov A, Dinh NN, Qu XD, Martin D, Glasgow BJ. Lipophilin, a novel heterodimeric protein of human tears. FEBS Lett. 1998 Aug 7;432(3):163-7.

Lindstrom R, Kim T. Ocular permeation and inhibition of retinal inflammation: an examination of data and expert opinion on the clinical utility of nepafenac. Curr Med Res Opin. 2006 Feb;22(2):397-404.

Liu L, Liu X. Roles of Drug Transporters in Blood-Retinal Barrier. Adv Exp Med Biol. 2019;1141:467-504.

Lorenzo-Veiga B, Diaz-Rodriguez P, Alvarez-Lorenzo C, Loftsson T, Sigurdsson HH. In Vitro and Ex Vivo Evaluation of Nepafenac-Based Cyclodextrin Microparticles for Treatment of Eye Inflammation. Nanomaterials (Basel). 2020 Apr 9;10(4):709.

Lu AT, Frisella ME, Johnson KC. Dissolution modeling: factors affecting the dissolution rates of polydisperse powders. Pharm Res. 1993 Sep;10(9):1308-14

Mannermaa E, Vellonen KS, Urtti A. Drug transport in corneal epithelium and blood-retina barrier: emerging role of transporters in ocular pharmacokinetics. Adv Drug Deliv Rev. 2006 Nov 15;58(11):1136-63.

Maurice DM. Drug delivery to the posterior segment from drops. Surv Ophthalmol. 2002 Aug;47 Suppl 1:S41-52.

Missel PJ, Sarangapani R. Physiologically based ocular pharmacokinetic modeling using computational methods. Drug Discov Today. 2019 Aug;24(8):1551-1563.

Mudie DM, Murray K, Hoad CL, Pritchard SE, Garnett MC, Amidon GL, Gowland PA, Spiller RC, Amidon GE, Marciani L. Quantification of gastrointestinal liquid volumes and distribution following a 240 mL dose of water in the fasted state. Mol Pharm. 2014 Sep 2;11(9):3039-47.

Nardi M, Lobo C, Bereczki A, Cano J, Zagato E, Potts S, Sullins G, Notivol R. Analgesic and anti-inflammatory effectiveness of nepafenac 0.1% for cataract surgery. Clin Ophthalmol. 2007 Dec;1(4):527-33

Parrott N, Hainzl D, Scheubel E, Krimmer S, Boetsch C, Guerini E, Martin-Facklam M. Physiologically based absorption modelling to predict the impact of drug properties on pharmacokinetics of bitopertin. AAPS J. 2014 Sep;16(5):1077-84.

Perkins ES. Prostaglandins and the eye. Adv Ophthalmol. 1975;29:2-21. PMID: 113023

Perkins, Edward S. and Davson, Hugh. "human eye". Encyclopedia Britannica, 1 Dec. 2021, https://www.britannica.com/science/human-eye. Accessed 19 October 2022. Assessed on 19Oct2022

Ramsay E, Del Amo EM, Toropainen E, Tengvall-Unadike U, Ranta VP, Urtti A, Ruponen M. Corneal and conjunctival drug permeability: Systematic comparison and pharmacokinetic impact in the eye. Eur J Pharm Sci. 2018 Jul 1;119:83-89.

Reinstein DZ, Archer TJ, Gobbe M, Silverman RH, Coleman DJ. Epithelial thickness in the normal cornea: three-dimensional display with Artemis very high-frequency digital ultrasound. J Refract Surg. 2008 Jun;24(6):571-81.

Reinstein DZ, Gobbe M, Archer TJ, Silverman RH, Coleman DJ. Epithelial, stromal, and total corneal thickness in keratoconus: three-dimensional display with artemis very-high frequency digital ultrasound. J Refract Surg. 2010 Apr;26(4):259-71.

Roni MA and Jalil, R. Comparative Study of Ibuprofen Solubility in Synthetic and Nagtrual Lipid Vehicles. Dhaka Univ. J. Pharm. Sci. 10(1): 65-66, 2011.

Rothwell RT, Meira DM, Oliveira MA, Ribeiro LF, Fonseca SL. Evaluation of Choroidal Thickness and Volume during the Third Trimester of Pregnancy using Enhanced Depth Imaging Optical Coherence Tomography: A Pilot Study. J Clin Diagn Res. 2015 Aug;9(8): NC08-11.

Sager JE, Yu J, Ragueneau-Majlessi I, Isoherranen N. Physiologically based pharmacokinetic (PBPK) modeling and simulation approaches: a systematic review of published models, applications, and model verification. Drug Metab Dispos. 2015;43(11):1823–37.

Schoenwald RD, Stewart P. Effect of particle size on ophthalmic bioavailability of dexamethasone suspensions in rabbits. J Pharm Sci. 1980 Apr;69(4):391-4.

Shell JW. Pharmacokinetics of topically applied ophthalmic drugs. Surv Ophthalmol. 1982 Jan-Feb;26(4):207-18.

Sheppard JD, Cockrum PC, Justice A, Jasek MC. In Vivo Pharmacokinetics of Bromfenac Ophthalmic Solution 0.075%, Bromfenac Ophthalmic Solution 0.07%, and Nepafenac/Amfenac Ophthalmic Suspension 0.3% in Rabbits. Ophthalmol Ther. 2018 Jun;7(1):157-165.

Siepmann J, Siepmann F. Mathematical modeling of drug dissolution. Int J Pharm. 2013 Aug 30;453(1):12-24.

Shah KB, Patel PG, Khairuzzaman AKM, Bellantone RA. An improved method for the characterization of supersaturation and precipitation of poorly soluble drugs using the pulsatile dialysis technique. Int. J. Pharm. 468, 64-74 (2014).

Silverman RH, Lizzi FL, Ursea BG, Rondeau MJ, Eldeen NB, Kaliscz A, Lloyd HO, Coleman DJ. High-resolution ultrasonic imaging and characterization of the ciliary body. Invest Ophthalmol Vis Sci. 2001 Apr;42(5):885-94.

Smith DW, Lee CJ, Gardiner BS. No flow through the vitreous humor: How strong is the evidence? Prog Retin Eye Res. 2020 Feb 6:100845.

Sridhar MS. Anatomy of cornea and ocular surface. Indian J Ophthalmol. 2018 Feb;66(2):190-194.

Stader F, Penny MA, Siccardi M, Marzolini C. A comprehensive framework for physiologically based pharmacokinetic modelling in Matlab®. CPT Pharmacometrics Syst Pharmacol. 2019 Feb 18;8(7):444–59.

Stay MS, Xu J, Randolph TW, Barocas VH. Computer simulation of convective and diffusive transport of controlled-release drugs in the vitreous humor. Pharm Res. 2003 Jan;20(1):96-102.

Sun Y, Smith LEH. Retinal Vasculature in Development and Diseases. Annu Rev Vis Sci. 2018 Sep 15;4:101-122.

Takahashi K, Saishin Y, Saishin Y, Mori K, Ando A, Yamamoto S, Oshima Y, Nambu H, Melia MB, Bingaman DP, Campochiaro PA. Topical nepafenac inhibits ocular neovascularization. Invest Ophthalmol Vis Sci. 2003 Jan;44(1):409-15.

Tsakalozou E, Babiskin A, Zhao L. Physiologically-based pharmacokinetic modeling to support bioequivalence and approval of generic products: A case for diclofenac sodium topical gel, 1. CPT Pharmacometrics Syst Pharmacol. 2021 May;10(5):399-411.

Tsubota K, Nakamori K (1995). Effects of Ocular Surface Area and Blink Rate on Tear Dynamics. Arch, Ophthalmol. 113: 155-158.

Varela-Fernández R, Díaz-Tomé V, Luaces-Rodríguez A, Conde-Penedo A, García-Otero X, Luzardo-Álvarez A, Fernández-Ferreiro A, Otero-Espinar FJ. Drug Delivery to the Posterior Segment of the Eye: Biopharmaceutic and Pharmacokinetic Considerations. Pharmaceutics. 2020 Mar 16;12(3):269.

Varela-Fernández R, Díaz-Tomé V, Luaces-Rodríguez A, Conde-Penedo A, García-Otero X, Luzardo-Álvarez A, Fernández-Ferreiro A, Otero-Espinar FJ. Drug Delivery to the Posterior Segment of the Eye: Biopharmaceutic and Pharmacokinetic Considerations. Pharmaceutics. 2020 Mar 16;12(3):269.

Walters T, Raizman M, Ernest P, Gayton J, Lehmann R. In vivo pharmacokinetics and *in vitro* pharmacodynamics of nepafenac, amfenac, ketorolac, and bromfenac. J Cataract Refract Surg. 2007 Sep;33(9):1539-45.

Willoughby, C.E., Ponzin, D., Ferrari, S., Lobo, A., Landau, K. and Omidi, Y. (2010), Anatomy and physiology of the human eye: effects of mucopolysaccharidoses disease on structure and function – a review. Clinical & Experimental Ophthalmology, 38: 2-11.

Yamamura K, Sasaki H, Nakashima M, Ichikawa M, Mukai T, Nishida K, Nakamura J. Characterization of ocular pharmacokinetics of beta-blockers using a diffusion model after instillation. Pharm Res. 1999 Oct;16(10):1596-601.

Yang S, Zhou J, Li D. Functions and Diseases of the Retinal Pigment Epithelium. Front Pharmacol. 2021 Jul 28;12:727870.

Yanni SE, Clark ML, Yang R, Bingaman DP, Penn JS. The effects of nepafenac and amfenac on retinal angiogenesis. Brain Res Bull. 2010 Feb 15;81(2-3):310-9.

Zhang Y, Wildsoet CF. RPE and Choroid Mechanisms Underlying Ocular Growth and Myopia. Prog Mol Biol Transl Sci. 2015;134:221-40.

GLOSSARY OF TERMS

Variables	**(values change with time during simulation)**
M	Total mass (μg) of dissolved nepafenac in the drug-tear mixture
Ma	Total mass (μg) of nepafenac absorbed at the ocular surface (Ma = Mc + Mcon + Mlossc)
MAah	Total mass (μg) of amfenac in the aqueous humor
Mac	Total mass (μg) of amfenac in the cornea
Macon	Total mass (μg) of amfenac in the conjunctiva
MAeppcho	Total mass (μg) of amfenac in the choroid (equator to posterior pole)
MAeppret	Total mass (μg) of amfenac in the retina (equator to posterior pole)
MAeppsc	Total mass (μg) of amfenac in the sclera (equator to posterior pole)
Mah	Total mass (μg) of nepafenac in the aqueous humor
MAicb	Total mass (μg) of amfenac in the iris and ciliary body
MAlossc	Total mass (μg) of amfenac in sclera (limbus to ora serrata)
MAosecho	Total mass (μg) of amfenac in the choroid (ora serrata to equator)
MAoseret	Total mass (μg) of amfenac in the retina (ora serrata to equator)
MAosesc	Total mass (μg) of amfenac in the sclera (ora serrata to equator)
MAS	Total mass (μg) of amfenac in the plasma via systemic absorption
MAvh	Total mass (μg) of amfenac in the vitreous humor
Mc	Total mass (μg) of nepafenac in the cornea
Mcon	Total mass (μg) of nepafenac in the conjunctiva
Md	Total mass (μg) of nepafenac in the chemical depot
ME	Total mass (μg) of nepafenac metabolized
Meppcho	Total mass (μg) of nepafenac in the choroid (equator to posterior pole)
Meppret	Total mass (μg) of nepafenac in the retina (equator to posterior pole)
Meppsc	Total mass (μg) of nepafenac in the sclera (equator to posterior pole)
Micb	Total mass (μg) of nepafenac in the iris and ciliary body
ML	Total mass (μg) of nepafenac lost at the ocular surface (particles and dissolved drug via drainage)
Mlossc	Total mass (μg) of nepafenac in sclera (limbus to ora serrata)
Mosecho	Total mass (μg) of nepafenac in the choroid (ora serrata to equator)
Moseret	Total mass (μg) of nepafenac in the retina (ora serrata to equator)
Mosesc	Total mass (μg) of nepafenac in the sclera (ora serrata to equator)
Mpct	Total mass (μg) of nepafenac solid particles in the drug-tear mixture
MS	Total mass (μg) of nepafenac lost the plasma via systemic absorption

Mvh	Total mass (μg) of nepafenac in the vitreous humor
V_∞	Volume of drug-tear layer mixture (μL)

Parameters (values are fixed during a simulation)

alpha	Rate constant for formulation tear layer volume clearance (μin^{-1})
Cs	Solubility in (μg/mL) of nepafenac in formulation aqueous phase (21.5 μg/mL or 0.0215 μg/μL)
Expc	Expression of amidase (μM) in cornea
Expcon	Expression of amidase (μM) in conjunctiva
Expeppcho	Expression of amidase (μM) in choroid (equator to posterior pole)
Expeppret	Expression of amidase (μM) in retina (equator to posterior pole)
Expicb	Expression of amidase (μM) in iris and ciliary body
Exposecho	Expression of amidase (μM) in choroid (ora serrata to equator)
Exposeret	Expression of amidase (μM) in retina (ora serrata to equator)
Exposesc	Expression of amidase (μM) in sclera (ora serrata to equator)
kAahicb	Rate constant (μL/min) of amfenac drug from aqueous humor to iris and ciliary body
kAahosecho	Rate constant (μL/min) of amfenac drug from aqueous humor to choroid (ora serrata to equator)
kAahvh	Rate constant (μL/min) of amfenac drug from aqueous humor to vitreous humor
kAcah	Rate constant (μL/min) of amfenac drug from cornea to aqueous humor
kAconlossc	Rate constant (μL/min) of amfenac drug from conjunctiva to sclera (limbus to ora serrata)
kAeppchoeppret	Rate constant (μL/min) of amfenac drug from choroid (equator to posterior pole) to retina (equator to posterior pole)
kAeppretvh	Rate constant (μL/min) of amfenac drug from retina (equator to posterior pole) to vitreous humor
kAeppsceppcho	Rate constant (μL/min) of amfenac drug from sclera (equator to posterior pole) to choroid (equator to posterior pole)
kahicb	Rate constant (μL/min) of nepafenac drug from aqueous humor to iris and ciliary body
kahosecho	Rate constant (μL/min) of nepafenac drug from aqueous humor to choroid (ora serrata to equator)
kahvh	Rate constant (μL/min) of nepafenac drug from aqueous humor to vitreous humor
kAicbosecho	Rate constant (μL/min) of amfenac drug from iris and ciliary body to choroid (ora serrata to equator)
kAicbvh	Rate constant (μL/min) of amfenac drug from iris and ciliary body to vitreous humor

kAlosscosesc	Rate constant (μL/min) of amfenac drug from sclera (Limbus to ora serrata) to sclera (ora serrata to equator)
kAosechoeppcho	Rate constant (μL/min) of amfenac drug from choroid (ora serrata to equator) to choroid (equator to posterior pole)
kAosechooseret	Rate constant (μL/min) of amfenac drug from choroid (ora serrata to equator) to retina (ora serrata to equator)
kAoseretеppret	Rate constant (μL/min) of amfenac drug from retina (ora serrata to equator) to retina (equator to posterior pole)
kAoseretvh	Rate constant (μL/min) of amfenac drug from retina (ora serrata to equator) to vitreous humor
kAosesceppsc	Rate constant (μL/min) of amfenac drug from sclera (ora serrata to equator) to sclera (equator to posterior pole)
kAosescosecho	Rate constant (μL/min) of amfenac drug from sclera (Ora serrata) to choroid (ora serrata to equator)
KApahicb	Partition coefficient of amfenac- iris and ciliary body to aqueous humor
KApahosecho	Partition coefficient of amfenac- choroid (ora serrata to equator) to aqueous humor
KApcah	Partition coefficient of amfenac- cornea to aqueous humor
KApeppretvh	Partition coefficient of amfenac- retina (equator to posterior pole) to vitreous humor
KApicbvh	Partition coefficient of amfenac between iris and ciliary body to vitreous humor
KAposeretvh	Partition coefficient of amfenac- retina (ora serrata to equator) to vitreous humor
kcah	Rate constant (μL/min) of nepafenac drug from cornea to aqueous humor
kconlossc	Rate constant (μL/min) of nepafenac drug from conjunctiva to sclera (limbus to ora serrata)
kDpc	Rate constant (μL/min) of nepafenac from formulation to tear layer
keppchoeppret	Rate constant (μL/min) of nepafenac drug from choroid (equator to posterior pole) to retina (equator to posterior pole)
keppretvh	Rate constant (μL/min) of nepafenac drug from retina (equator to posterior pole) to vitreous humor
keppsceppcho	Rate constant (μL/min) of nepafenac drug from sclera (equator to posterior pole) to choroid (equator to posterior pole)
kicbosecho	Rate constant (μL/min) of nepafenac drug from iris and ciliary body to choroid (ora serrata to equator)
kicbvh	Rate constant (μL/min) of nepafenac drug from iris and ciliary body to vitreous humor
klosscosesc	Rate constant (μL/min) of nepafenac drug from sclera (limbus to ora serrata) to sclera (ora serrata to equator)
Kmi	Nepafenac substrate concentration in (μM) when rate of the amidase-mediated hydrolysis reaction reaches half of its maximum rate

kosechoeppcho	Rate constant (μL/min) of nepafenac drug from choroid (ora serrata to equator) to choroid (equator to posterior pole)
kosechooseret	Rate constant (μL/min) of nepafenac drug from choroid (Ora Serrata to Equator) to retina (ora serrata to equator)
koseretеppret	Rate constant (μL/min) of nepafenac drug from retina (ora serrata to equator) to retina (equator to posterior pole)
koseretvh	Rate constant (μL/min) of nepafenac drug from retina (ora serrata to equator) to vitreous humor
kosesceppsc	Rate constant (μL/min) of nepafenac drug from sclera (ora serrata to equator) to sclera (equator to posterior pole)
kosescosecho	Rate constant (μL/min) of nepafenac drug from sclera (ora serrata to equator) to choroid (ora serrata to equator)
Kpahicb	Partition coefficient of nepafenac between aqueous humor and iris and ciliary body
Kpahosecho	Partition coefficient of nepafenac between aqueous humor and choroid (ora serrata to equator)
kpc	Rate constant First order drainage rate constant of dissolved nepafenac)
Kpcah	Partition coefficient of nepafenac- cornea to aqueous humor
Kpdt	Partition coefficient of nepafenac- chemical depot to tear
Kpeppretvh	Partition coefficient of nepafenac- retina (equator to posterior pole) to vitreous humor
Kpicbvh	Partition coefficient of nepafenac- iris and ciliary body to vitreous humor
Kposeretvh	Partition coefficient of nepafenac- retina (ora serrata to equator) to vitreous humor
Kptc	Partition coefficient of nepafenac- cornea to tear
Kptcon	Partition coefficient of nepafenac- conjunctiva to tear
Kptlossc	Partition coefficient of nepafenac- sclera (limbus to ora serrata) to tear
ktc	Rate constant (μL/min) of nepafenac drug from tear to cornea
ktcon	Rate constant (μL/min) of nepafenac drug from tear to conjunctiva
ktd	Rate constant (μL/min) of nepafenac drug from tear to chemical depot
ktlossc	Rate constant (μL/min) of nepafenac drug from tear to sclera (limbus to ora serrata)
MWamf	Molecular weight of amfenac
MWnep	Molecular weight of nepafenac
QAahs	Rate of systemic absorption of amfenac from aqueous humor in (μL/min)
QAcons	Rate of systemic absorption of amfenac from conjunctiva in (μL/min)
QAeppchos	Rate of systemic absorption of nepafenac from choroid (equator to posterior pole)

QAepprets	Rate of systemic absorption of amfenac from retina (equator to posterior pole) in (μL/min)
Qahosecho	Rate of liquid convection from aqueous humor to choroid (ora serrata to equator) in (μL/min)
Qahs	Rate of systemic absorption of nepafenac from aqueous humor in (μL/min)
QAlosscs	Rate of systemic absorption of amfenac from sclera (limbus to ora serrata) in (μL/min)
QAosechos	Rate of systemic absorption of amfenac from choroid (ora serrata to equator) in (μL/min)
QAoserets	Rate of systemic absorption of amfenac from retina (ora serrata to equator) in (μL/min)
Qcah	Rate of liquid convection from cornea to aqueous humor in (μL/min)
Qcons	Rate of systemic absorption of nepafenac from conjunctiva in (μL/min)
Qeppchos	Rate of systemic absorption of nepafenac from choroid (equator to posterior pole) in (μL/min)
Qepprets	Rate of systemic absorption of nepafenac from retina (equator to posterior pole) in (μL/min)
Qev	Total tear evaporation rate in (μL/min)
Qin	Total tear generation rate in (μL/min)
Qlosscs	Rate of systemic absorption of nepafenac from sclera (limbus to ora serrata) in (μL/min)
Qosechos	Rate of systemic absorption of nepafenac from choroid (ora serrata to equator) in (μL/min)
Qoserets	Rate of systemic absorption of nepafenac from retina (ora serrata to equator) in (μL/min)
Qtf	Steady-state tear drainage rate in (μL/min)
Qvhah	Rate of liquid convection from vitreous humor to aqueous humor in (μL/min)
Vah	Volume of aqueous humor (μL)
Vc	Volume of cornea (μL)
Vcon	Volume of conjunctiva (μL)
Vd	Volume of chemical depot (μL)
Veppcho	Volume of choroid (equator to posterior pole) (μL)
Veppret	Volume of retina (equator to posterior pole) (μL)
Veppsc	Volume of sclera (equator to posterior pole) (μL)
Vicb	Volume of iris and ciliary body (μL)
Vlossc	Volume of sclera (limbus to ora serrata) (μL)
Vmax	Maximum reaction rate of the amidase metabolism (μM/min/μM)
Vosecho	Volume of choroid (ora serrata to equator) (μL)

Voseret	Volume of retina (ora serrata to equator) (μL)
Vosesc	Volume of sclera (ora serrata to equator) (μL)
Vvh	Volume of vitreous humor (μL)

RESUME

XU SUN

17 Audley St North Brunswick NJ 08902 917-530-9866 xu.sun@my.liu.edu

Ph.D. in Pharmaceutics Science with a specialization in PK/PD and physiological-based modeling and simulations. Doctoral research focused on bioavailability assessment of complex ophthalmic suspensions based on PBPK (physiologically based pharmacokinetic) model programmed by R language. Skilled with pharmacometrics modeling analysis using NONMEM and R. More than two years of GA experience in an analytical laboratory under good manufacturing practice (GMP).

QUALIFICATIONS

- Experienced in dataset curation and data analysis with R
- Experienced in model development and diagnostic using NONMEM
- Experienced in PBPK model development and evaluation using ordinary differential equation solver in R
- 2.5+ years of laboratory research experience (pharmaceutical analysis)
- Hand-on and trouble-shooting/problem-solving skills
- Excellent communication skills and capability of multitasking.
- Skilled in scientific writing and professional presenting

WORK EXPERIENCE

Boehringer Ingelheim, Ridgefield, CT

Pharmacometrics Internship May 2022-Aug 2022

Performance of high-quality pharmacometrics analysis on a project level essential for internal decision making

- Ensured timely delivery of clinical database exploratory analyses to support modeling strategy
  - Data visualization
  - Database curation and analysis dataset development
- Developed modeling strategy and contributed to clinical trials design
  - Feasibility check and importation of analysis dataset
  - Longitudinal model development
  - Model comparison and justification based on diagnostic test results and interpretation

Physical Pharmaceutica, Orangeburg, NY

Internship Apr 2021-Sep 2021

- Engaged in generic cyclosporine ophthalmic emulsion development under GMP
  - Performed in-vitro drug-releasing test based on a novel pulsatile microdialysis technique
  - Tested particle size distribution (PSD) and zeta-potential of complex ophthalmic formulation using advanced Zetasizer Nano

Lachman Laboratory, Long Island University, Brooklyn, NY

Quantitative Analyst, US Food and Drug Administration Analysis Project Mar 2018-Feb 2020

- Carried out drug dissolution tests on cutting-edge Fiber-Optical instrument
- Performed drug content uniformity test on HPLC-UV system
- Developed assay method based on USP compound monograph
- Participated in systemic training on standard operating procedures (SOPs) and good manufacturing practice (GMP)

RESEARCH EXPERIENCE

Long Island University, Brooklyn, NY

Doctorate Dissertation Project Aug 2017-Jan 2023

- Performed PBPK modeling analysis of nepafenac ophthalmic suspensions
  - Constructed a novel pre-corneal model to account for physical properties differences in formulations and tear-drug interaction in the conjunctival sac
  - Modeled ocular PBPK with enzymatic conversion of the pro-drug and active metabolite
  - Constructed ocular tissue compartments, wrote and solved system of differential equations with constraints
  - Evaluated model and equations using R and PK-Sim®

EDUCATION

Long Island University, LIU Pharmacy, Brooklyn, NY

- **Ph.D.** Concentration in Pharmaceutics Aug 2017- Jan 2023
- Courses: PBPK Modeling and Simulation, Pharmacokinetics, Pharmacogenomics, Drug Metabolism, Polymer Science, Dosage Form Design, Solid State Characters, Pharmaceutical Analysis, Biostatistics, Physical Pharmacy, Industrial Pharmacy, Pharmaceutical Regulatory

University of Illinois, College of Agricultural and Bioengineering, Urbana-Champaign, IL

- **M.S.** Concentration in Technical Systems Management Aug 2014 - May 2016
  Illinois Professional Science Master
- Courses: Nano-Biological Engineering, Plant Biochemistry

China Agricultural University, Beijing, CHINA

- **B.S.** in Horticultural Sciences Aug 2010 - May 2014
- Courses: Molecular Biology, Organic Chemistry, Biochemistry
- Honors and Awards: CAU Excellent Undergraduate's Research Paper

REFERENCE

Available upon request